IMPROVED INSTRUMENTATION AND SOME INVESTIGATIONS IN WIDELINE N. M. R.

K. J. WILSON

THESIS SUBMITTED IN PARTIAL FULFILMENT OF THE
REQUIREMENTS FOR THE AWARD OF THE DEGREE OF
DOCTOR OF PHILOSOPHY

DEPARTMENT OF PHYSICS
COCHIN UNIVERSITY OF SCIENCE AND TECHNOLOGY
COCHIN 682 022

1990

CERTIFICATE

Certified that the research work presented in this thesis is based on the original work done by Mr. K.J.Wilson under my guidance in the Department of Physics, Cochin University of Science and Technology, and has not been included in any other thesis submitted previously for the award of any degree.

Cochin 682 022
Feb.1, 1990

Prof.(Dr.) C.P.Girijavallabhan
Supervising Teacher

PREFACE

Wideline Nuclear Magnetic Resonance (NMR) has been extensively used as a very sensitive tool for probing the various phenomena in the solid state. As the effectiveness of the method mostly depends on the sensitivity and perfectness of the electronic instrumentation adopted for the NMR spectrometer design, great importance and care have to be devoted towards the different aspects of the instrumentation involved. The present thesis elucidates an altogether novel and innovative approach to instrumentation for wideline NMR aimed at achieving enhanced performance of the spectrometer. The thesis presents a detailed report of the work done by the author in this field during the past five years in the Department of Physics, Cochin University of Science and Technology.

Instead of adopting conventional methods, improved circuit designs using state-of-the-art solid state components have been adopted whenever possible in the different stages of spectrometer fabrication. The spectrometer thus designed, with improved instrumental capabilities has then been successfully utilised for carrying investigations of different types. The major achievements of these research work, which are outlined in this thesis, are the following:

(1) Design and fabrication of an improved high current stabilizer for the electromagnet, that totally eliminates the need of a seperate current sensing unit.

(2) Realisation of a perfectly linear electronic magnetic field sweep generator, utilising an improved IC bootstrap ramp generating circuit.

(3) Introduction of an innovative MOSFET based Robinson oscillator for NMR detection, that is not only very simple to fabricate but also possesses vastly improved sensitivity.

(4) Explanation for the anomalous features present in the proton resonance signal from ammonium chromate.

(5) Application of the NMR technique for the dynamic estimation of amount of water molecules absorbed by zeolites.

(6) Application of NMR method for the accurate estimation of oil content in dried coconut ('copra').

The thesis contains eight chapters, which are self-contained with seperate abstracts and references. The first chapter gives a general introduction to the subject of Nuclear Magnetic Resonance. A comprehensive description of the theoretical basis of NMR is given, which includes discussions about resonance condition, macroscopic magnetisation, magnetic susceptibilities and the relaxation processes. The chapter also mentions the two branches of NMR. At the end of the chapter the major applications of NMR are highlighted.

Chapter II gives a concise theoretical survey of Wideline NMR. A description of NMR absorption spectrum for rigid structures and the method of moments are outlined. The topics of structural determination from NMR absorption spectrum, molecular motion in solids and the important applications of wideline NMR also form the subject of the same chapter.

In chapter III the basic requirements of a wideline NMR spectrometer are described. The functions of the sub-assemblies and requirements of the various sub-systems of the spectrometer like electromagnet assembly, field modulation system, field sweep unit and r.f.oscillator-detector are discussed. The chapter also gives the importance of phase sensitive detection in the recording of NMR signals. The important conditions for the observation of NMR absorption are then mentioned, followed by a brief description of a typical wideline NMR spectrometer set up.

An improved high current stabilizing circuit, that completely eliminates the need for a seperate current sensing unit, forms the focal theme of chapter IV. Besides, the chapter also presents a novel current sensing technique as well as an innovative reference voltage selector design, that is free from some of the inherent drawbacks of conventional multi-turn potentiometer circuit.

Chapter V is devoted to a discussion of the improved instrumental capability achieved in the field of magnetic field sweeping. The first part of the chapter mentions the earlier field sweep methods and their shortcomings. The design and fabrication of an electronic magnetic field sweep system working as a seperate unit is discussed next. The chapter then describes the improved field sweep unit that generates almost perfectly linear field sweeps.

Chapter VI begins with a description of the earlier NMR detectors. The principle and functioning of marginal oscillator-detectors and Robinson oscillator detectors are then given. The chapter then presents an improved MOSFET based Robinson oscillator circuit, capable of working at r.f.levels down to 1mV and providing thereby highly satisfactory recording of broadline proton signals from solids even at room temperature.

In chapter VII some investigations carried out in liquids, for the purpose of standardising the newly fabricated wideline NMR spectrometer set up, are described. Proton resonance signals from different liquids and F^{19} resonance signal from hydroflouric acid are given. Some studies of proton resonance linewidth versus concentration of different paramagnet impurities also form the content of this chapter.

The investigations carried out in different solids using the newly fabricated wideline NMR spectrometer are reported in the concluding chapter. The peak-to-peak strength of the proton resonance signal from zeolites is shown to represent a true measure of the amount of proton containing molecules absorbed by them. The chapter also reports that the strength of the proton resonance signal from dried coconut ('copra') gives an accurate measure of its oil content. Besides, a satisfactory explanation for the anomalous features present in the proton resonance signal from polycrystalline ammonium chromate is also presented. A discussion of the results of these investigations are given at the end of chapter VIII.

Part of the work contained in this thesis has been published/accepted for publication in reputed jouranls or presented in symposia in the form of the following research papers:

1. "A simple technique for current sensing in high current magnets used in NMR experiments"; Proceedings of Solid State Physics symposium; vol.28 C, p.327 (1985)

2. "An improved stabilization circuit for high current magnets used in NMR experiments"; International Journal of Electronics (UK); vol.63, no.1, p.105-107 (1987)

3."An improved linear magnetic field sweep generating technique for wideline NMR experiments"; Proceedings of Solid State Physics symposium; vol.30 C, p.445 (1987)

4. "A linear electronic magnetic field sweep generator for wideline NMR experiments"; Journal of the Instrument Society of India; vol.18, p.265-267 (1988)

5. "A simple linear magnetic field sweep generator for magnetic resonance experiments"; Journal of Physics E: Scientific Instruments (UK); vol.22, p.131-132 (1989)

6. "An improved MOSFET based Robinson oscillator for NMR detection"; Measurement Science and Technology (UK); (In press)

CONTENTS

Chapter I

INTRODUCTION TO
NUCLEAR MAGNETIC RESONANCE

Abstract

This introductory chapter begins by highlighting the importance of the choice of the problem and then gives an insight to the field of magnetic resonance, with special emphasis on Nuclear Magnetic Resonance (NMR). The two early spectacular discoveries of NMR have been briefly mentioned. The expression for resonance condition as obtained from a simple quantum mechanical viewpoint is also given. The relevance of macroscopic magnetisation as well as magnetic susceptibilities, their dependence on different parameters and the two different branches of NMR have been outlined. At the end of the chapter the major application of NMR have been mentioned, with special reference to NMR imaging.

1.1 : Introduction

Since its discovery in the mid 1940's, NMR spectroscopy has progressed and expanded at such a rapid pace that it has found important applications in almost all branches of science. Especially the past twenty years have seen phenomenal developments in the methodology and application of NMR to biophysics, physics and chemistry. Magnetic Resonance Imaging (MRI) has already got established as a potential diagnostic tool in the field of medicine. Several other inventions have also sprung up in the field like multi-dimensional FT NMR, multiple quantum NMR etc. These advances had been mainly the result of major improvements in instrumental capabilities like improvements in super-conducting magnet technology, computer techniques, multi-nuclear capability, spectrometer design for FT NMR, realisation of higher magnetic field strengths and sensitivities for proton and other nuclei etc. Thus the instrumentation part plays a key role in further developments in the field. With this consideration the present thesis work has been carried out mainly from an instrumentational viewpoint so that the novel NMR spectrometers being fabricated may give much improved performance than earlier ones and hence will permit more sensitive and accurate investigations.

1.2 : Magnetic Resonance spectroscopy

Magnetic resonance is a phenomenon exhibited by systems that possess both magnetic moments and angular momentum. One of the reasons for the impact of magnetic reasonance on physics is its ability to give information about processes at the atomic level.

The term 'resonance' implies that we are in tune with a natural frequency of the magnetic system; in this case it corresponds to the frequency of gyroscopic precession of the magnetic moment in an external static magnetic field. Because of the analogy between the characteristic frequencies of atomic spectra, and because the magnetic resonance frequencies fall typically in the radio-frequency region (for nuclear spins) or microwave region (for electron spin) the terms radio-frequency and microwave spectros-

copy are often used to mention the different branches of magnetic resonance spectroscopy [1].

1.2.1 : Nuclear Magnetic Resonance (NMR) comes under the radiofrequency branch of magnetic resonance spectroscopy. NMR spectroscopy studies the behaviour of those atomic nuclei which have magnetic moments arising from their 'spin', in the prescence of applied magnetic fields. The applied field is responsible for creating energy levels for nucleus, between which transitions may be caused to occur by absorption of suitable electromagnetic radiation.

In the case of NMR, the resonance corresponds to the gyroscopic precession of the nuclear magnetic moment in an external magnetic field. The rate of the precessional motion is proportional to the strenght of the magnetic field, and usually lies in the region of radio-frequencies. By 'tuning' to the resonance frequency of precession information can be obtained characterizing the nuclear magnetic moment, its motions and environments.

1.2.2 : Electron Spin Resonance (ESR) deals with the study of magnetic resonance spectra of those species having one or more unpaired electrons. The method takes advantage of the spin of the electron and its magnetic moment to reveal a wealth of information.

Being a stronger magnet and much lighter than a proton, the electron precesses much more rapidly in a given magnetic field; the frequency of precession being in the microwave region. Hence ESR falls under the microwave branch of magnetic resonance spectroscopy.

ESR has been used for detection and identification of paramagnetic materials like free radicals, impurity centres etc., for determination of electronic structure, for studies of interaction between molecules and for measurements of nuclear spins and moments [2,3].

1.3 : NMR - the two discoveries

Nuclear magnetic resonance in bulk matter was discovered independently by Purcell, Torrey and Pound at Harvard and by Bloch, Hansen and Packard at Stanford towards the end of 1945. The Purcell group conceived magnetic resonance in terms of transitions between quantum states while the Bloch group visualized magnetic moments being reoriented with respect to a magnetic field [4].

The kernel of the 'resonance absorption' approach to NMR by Purcell's group is as follows: "If a diamagnetic solid containing nuclei of spin I and magnetic moment μ is placed in a steady magnetic field H, there will be 2I + 1 Zeeman levels seperated in energy by $\Delta W = \mu H / I$. Application of a radio-frequency magnetic field perpendicular to H induces transitions between adjacent levels when the frequency is near the resonant value $v = \Delta W / h$" [5,6].

The 'magnetic induction' approach to NMR by the Stanford physcists, on the other hand, is based on the following consideration: "The nuclear magnetic moments of a substance in a strong magnetic field H_z would be expected to give rise to a small magnetic polarization, provided thermal equilibrium be established. A superimposed oscillating field H_x in the x direction will produce a change in orientation of the polarization with

a component perpendicular to the strong field" [7,8].

The two methods, viz resonance absorption and nuclear induction are essentially equivalent. In both experiments, the sample is subjected to a weak magnetic field oscillating at right angles to a strong constant magnetic field. However, for Purcell the oscillating field "induces transitions" while for Bloch it produces "a change in orientation". The nuclear induction approach has associated with it vivid imagery, and it can be conceptualized in classical terms. For this reason, it is particularly useful when discussing dynamical or transient effects [9]. The resonance absorption approach, on the other hand, brings with it the formal appeal of quantum mechanics and the powerful methods of spectroscopy.

In the present thesis the resonance absorption approach has been adopted to reproduce the expression for the resonance condition from a simple quantum mechanical viewpoint as well as to explain the single coil NMR detection method employed in this work.

1.4 : Resonance condition

Nuclear magnetic resonance is applicable to only those nuclei having a non-zero resultant spin angular momentum [10]. Nuclei with an odd number of protons and an even number of neutrons (and vice versa) will have a net nuclear spin. These are the nuclei of access to NMR.

Intrinsic nuclear spin corresponds to quantized angular momentum. The largest measurable component of this angular momentum is $I\hbar$, where I is integral or half integral and $\hbar$ is Planks constant devided by 2π. The spin angular momentum vector can then be written as

$$\vec{S} = \vec{I}\ \hbar \ \text{--------} (1.1)$$

Since the nucleus is a distribution of charge, the nuclei having a net spin will have a magnetic moment associated with them in accordance with the classical electromagnet theory. Assuming that the magnetic moment μ is co-linear and proportional to the angular momentum:

$$\mu = \gamma\ \hbar\ I \ \text{------} (1.2) \ ,$$

Where γ is the gyromagnetic ratio (the ratio between magnetic and mechanical moments). The value of γ varies from one nucleus to another depending on the mass and character of the nucleus. It is this specificity of γ to particular nuclei which gives NMR its ability to look at a specific atomic species in a complex system.

If the spin is placed in a static magnetic field H_0, then there is an energy of interaction given by the Hamiltonian,

$$\mathcal{H} = -\vec{H_0} \bullet \vec{\mu} \text{-----} (1.3)$$

Taking $\vec{H_0}$ to be in the z-direction and using equation (1.2)

$$\mathcal{H} = -\gamma \hbar H_0 I_z ------ (1.4)$$

Equation (1.3) and (1.4) are called Zeeman Hamiltonians and the operator I_z has eigen values

$$m = +I, I-1 ,........., -I$$

This situation corresponds to the fact that the spin is quantized such that it can take only certain discrete positions with respect to the field, corresponding to the discrete energies. The spin system in the field $\vec{H}_0$ thus has the energy levels

$$E_m = <m \mid \mathcal{H} \mid m> = -\gamma \hbar H_0 m ------(1.5)$$

In magnetic systems the selection rules allow only transitions between levels such that m =±1. Thus to cause transitions or "resonate" between levels one must supply a characteristic energy

$$\Delta E = -\gamma \hbar H_0 -------- (1.6)$$

One way to cause resonant transitions between such levels is to irradiate this system with photons of electro-magnetic energy at an angular frequency ω_0, such that

$$\hbar \omega_0 = \Delta E = -\gamma \hbar H_0 ----- (1.7)$$

Or $$\omega_0 = -\gamma H_0 -------- (1.8)$$

Equation (1.8) is the so-called resonance condition and relates the resonant frequency to the static field.

Because of the quantum nature of nuclear spins, the application of a magnetic field produces characteristic energy levels (or energy reservoirs) E_m. Transitions between these levels involve a characteristic frequency given by ω_0 , where ω_0 is an angular frequency interval equal to $2\pi f_0$ (where f_0 is expressed in cycles/second or Hertz). Equation (1.8) gives the resonant frequency for a particular species in a given magnetic field.

1.5 : Macroscopic Magnetisation

Unlike an X-ray photon of 10^5 eV, the photon involved in NMR is many orders of magnitude smaller, typically of the order of 10^{-7} eV [11]. Though it may be possible to detect a single X-ray photon at a given energy it is totally impossible to detect the photon from a single nuclear transition. Consequently, the signals that are detected by NMR must involve large number of nuclei. Unfortunately, even with large number of nuclei involved, there are still some other difficulties. The NMR energy is many orders of magnitude below those energies in a sample corresponding to molecular rotations, vibrations, etc. In short, the NMR energy is below thermal ambience (at room temperature).

Consider a collection of spin 1/2 nuclei (such as protons) in a field H_0. Suppose also they are in thermal equilibrium with their surroundings (or so-called lattice). Since there are only two possible states for I =1/2, the magnetic moments can point only in one of two directions. Some of the spins will lie parallel to the field (m = + 1/2) and some will lie anti-parallel (m = -1/2). Because of thermal motions there will be many transitions

between the two and though there is a small energetic advantage to a state pointing parallel to the field, the thermal motions will "stir" the ensemble violently. Hence there will be only a slight excess of spins pointing parallel to the field that can participate in resonant absorption.

This is the signal-to-noise (S/N) ratio difficulty inherent in NMR. The energy of a spin transition is extremely small. Further, because the energy is below thermal noise levels, even a large collection of N spins will not provide N times this energy because there is actually only a slight population difference due to thermal stirring.

To get an understanding of the number of spins pointing parallel and those pointing anti-parallel to the field, consider the collection of spin 1/2 nuclei to be in thermal equilibrium with the lattice. Assuming Boltzmann statistics and a dynamic equilibrium,

$$N_p/N_a = \exp\left[(E_p - E_a)/kT\right] \quad\text{------- (1.9)}$$

Using equation (1.6):

$$N_p/N_a = \exp\left[(\gamma \hbar H_0)/kT\right] \approx 1 + (\gamma \hbar H_0)/kT \quad\text{------ (1.10)} \quad,$$

Where k is Boltzmann's constant and T is the temperature of the lattice. The parameter kT represents a thermal energy, and for room temperature $kT > \gamma \hbar H_0$. Typically, the last term on the RHS of equation (1.10) has magnitude of 10^{-4} to 10^{-6} [11]. Clearly then, the net magnetization that we can expect from such a system is only a small fraction of the total number of spins. For example in the case of H^1, in a steady magnetic induction of one Tesla and at room temperature, the excess number of spins pointing parallel to the field is only about 7 per million.

Consider the magnetisation from an ensemble of spins such that
　　　　N(m) is the total number of spins in the state m, where
　　　　　m may take any of (2I+1) values and
　　　　　N is the total number of spins

Then, at equilibrium, using equation (1.5)
$$N(m) \approx [N/(2N+1)][1+(\gamma \hbar H_0 m)/kT] \quad\text{-------- (1.11)}$$

and $\quad N = \sum_{m=-I}^{I} N(m) \quad\text{------- (1.12)}$

The magnetisation is the weighed sum
$$M = \sum_{m=-I}^{I} N(m)\, \gamma \hbar\, m \quad\text{------ (1.13)}$$

$\therefore \quad M \approx [(N\gamma^2 \hbar^2 B_0)/(2I+1)kT] \sum_{m=-I}^{I} m^2 \quad\text{----- (1.14)}$

or $\quad \vec{M} \approx [(N\gamma^2 \hbar^2 I(I+1)/3kT]\vec{H}_0 \quad\text{------ (1.15)}$

This result is known as Curie's law and is the classical equivalent of

$$\vec{M} = \chi\vec{H}_0 \quad\text{------- (1.16)}$$

This result shows that the magnetisation of a collection of spins in thermal

equilibrium is proportional to the number of spins, the gyromagnetic ratio squared and the strength of the field. It is also the reason why proton is the most observable of naturally occuring nuclei. Proton has the highest γ and in general occurs with high concentration in different samples (as in water).

1.6 : Magnetic susceptibilities

As mentioned before an assembly of nuclear magnets in a steady magnetic field absorbs power from a suitably applied radio-frequency field. From a macroscopic point of view this absorption may be described by means of the imaginary part χ'' of the complex nuclear magnetic susceptibility [12], which are given below:

$$\chi' = [(1/2)\chi_0\omega_0 T_2][(\omega_0-\omega)T_2] / [(1+(\omega_0-\omega)^2T_2^2+\gamma^2H_1^2T_1T_2] ----- (1.17) \text{ and}$$

$$\chi'' = [(1/2)\chi_0\omega_0 T_2] / [1+(\omega_0-\omega)^2T_2^2+\gamma^2H_1^2T_1T_2] ------- (1.18) ,$$

Where χ_0 $\longrightarrow$ static magnetic susceptibility of the system
ω_0 $\longrightarrow$ Larmor angular frequency
ω $\longrightarrow$ angular frequency of r.f.field
T_2 $\longrightarrow$ spin-spin interaction time of the sample
T_1 $\longrightarrow$ spin-lattice relaxation time
γ $\longrightarrow$ gyromagnetic ratio of nuclear magnets
and H_1 $\longrightarrow$ strength of r.f. field

The term $\gamma^2H_1^2T_1T_2$ determines the degree of saturation. If H_1 is small enough to avoid appreciable saturation, namely when $\gamma^2H_1^2T_1T_1 << 1$, the bulk susceptibilities reduces to the form

$$\chi' = [(1/2)\chi_0\omega_0 T_2][(\omega_0-\omega)T_2] / [1+(\omega_0-\omega)^2T_2^2] --------- (1.19)$$

$$\text{and} \quad \chi'' = [(1/2)\chi_0\omega_0 T_2] / [1+(\omega_0-\omega)^2T_2] ---------- (1.20)$$

It can be seen [12] that a plotting of χ'' versus $(\omega_0-\omega)T_2$ shows the resonant character of absorption, while a plot of χ' versus $(\omega_0-\omega)T_2$ shows the dispersion which follows absorption.

1.7 : Relaxation Processes

At resonance, the probability of the radition of frequency ν inducing absorption is exactly equal to the probability of its inducing emission. Because there are more nuclei in the lower energy state, a net absorption will occur. But the excess of population in the lower level will gradually tends to diminish with time, while the population in the upper level will increase until they become equal; there will then be no net absorption and the signal, of a spectrometer designed to detect resonance, will tend to diminish and finally disappear. This phenomenon is known as 'saturation'. However there exist means whereby the spin system exchanges energy with its surroundings, which assists to restore the Boltzmann equilibrium. This also helps to maintain the NMR signal without disappearing. These restoring processes are known as 'relaxation'.

The relaxation processes are transitions induced by the thermal noise spectrum of the medium surrounding the nuclear spin system(i.e. the liquid structure or solid lattice in which there are many degrees of freedom other than those concerned with spin; this has components at suitable radio-frequencies, and induce thransitions in the same way as does the applied frequency v but with a tendency to restore the Boltzmann distribution instead of destroying it [3].

It is convenient to consider two different relaxation mechanisms, each of which is effectively a first-order rate process characterised by its own time constant.

1.7.1 : Spin-lattice relaxation, of time constant T_1 occurs because there is exchange of energy between the spin states and the surrounding medium (the lattice, which acts as a heat sink for the energy released when the nuclei decay to their ground state). In any actual physical system the nuclear spins are never entirely bereft of interaction with the lattice, although very often the interaction is quite small. Such interaction between the two systems strives to bring both of them into thermal equilibrium having the same temperature, which is almost identical to the lattice temperature. Thus, while the radiofrequency radiation begins to reduce the excess population in the lower energy state, the interaction with the lattice are tending to restore the excess to its original value. Hence the T_1 process can be considered as affecting the life times of population of spin energy levels.

The values of T_1 which are encountered experimentally usually lie within the range 10^{-4} to 10^4 sec [12]. The value is usually larger for solids than for liquids and gases. For solids it is rarely shorter than 10^{-2} sec at normal temperature, while at low temperatures it may be much longer. For pure liquids T_1 may be as short as 10^{-2} or 10^{-3} sec, and rarely it exceeds 10 sec. The prescence of paramagnetic ions in a liquid promotes the relaxation processes, and may reduce T_1 to less than 10^{-4} sec. In general the value T_1 of also depends on the strength H_0 of the steady magnetic field.

1.7.2: Spin-spin interaction, of time constant T_2, occurs due to exchange of energy between different nuclear spins. Instead of transferring energy from the spin system to an external sink (the lattice), spin-spin relaxation involves the interchange of energy within the spin system. Quantum mechanically, it is best described as being a process which limits the lifetimes of the nuclear spin states and consequently causes line broadening.

Since each nucleus possess a small magnetic dipole moment there will be a magnetic dipole-dipole interection between each pair of nuclei. Each nuclear magnet finds itself not only in the applied steady magnetic field H_0, but also in a small local magnetic field $H_{local} \sim 5$ gauss produced by the neighbouring nuclear magnets [12]. The effective steady magnetic field will not therefore be the same for each nucleus, but will vary over a range of several gauss from one nucleus to another. It follows that the resonance condition will not be perfectly sharp. Instead, the energy levels are broadened by an amount of the order of $\gamma \hbar H_{local}$. If we keep a fixed radio frequency v_0 and sweep the steady magnetic field, the resonance will be found to be spread about H_0 over a range of values of the order of H_{local}.

The spin-spin interaction time T_2 is of the order of the maximum value of the line shape function, $g(v)_{max}$. It has been shown that $T_2 = 1/2g(v)_{max}$ [13]. The T_2 processes can be considered to be affecting the relative energies of the spin levels. The spin-spin interaction time $T_2 \sim 1/\delta\omega_0 \sim 1/\gamma H_{local} \sim 10^{-4}$ sec [12].

For liquids and gases the reorientation and diffusion of the molecules is usually so rapid that the local magnetic field is smoothed out to a very small average value, yielding quite a narrow resonance line. This effect is found in some solids also.

1.8 : The two branches of NMR

Nuclear magnetic resonance can be broadly classified into two branches(a) Wideline NMR, characterised by resonance linewidths ranging from 100Hz upto several KHz (and even higher in ferromagnetic materials), normally using solids.
(b) High resolution NMR in liquids, where the characteristic linewidth is ~ 1Hz.

The two sections have completely different requirements for instrument performance, and use generally rather different techniques for the detection and amplification of signals. While wideline NMR method is mainly adopted by the physicists for the investigation of the solid state high resolution NMR is of enormous value to chemists both as a theoretical and as a structural tool.

1.8.1 : Wideline NMR spectra are those in which the observed width of the resonance line is as large or larger than the major resonance shifts caused by differences in the chemical environment of the observed nucleus [14].

Information in wideline NMR is obtained through the intensity, width and shape of the signal (commonly the first derivative of the absorption signal is taken) but very often only one or two parameters are used [15]. This type of spectrum gives mostly information concerning the concentration and physical environment of the observed nucleus, though it does not yield much insight concerning its exact chemical environment. The Larmor precession frequency, which is a function of the magnetic moment and spin quantum number of the isotope as well as a function of the magnetic field, is used to identify the isotope being observed.

For the present thesis work the wideline NMR method has been adopted so as to carry out investigations in the solid state. A detailed theoretical survey of wideline NMR is given in chapter II of this thesis.

1.8.2 : High resolution NMR spectra are those in which the observed width of the resonance lines are smaller than the major resonance shifts caused by differences in the chemical environment of the observed nucleus. In this case the experimental conditions are such that it is possible to distinguish between the absorption lines of the same nuclear species in different chemical environments. Besides fine-structure splitting of the resonance signals due to spin-spin interaction is also usually observed.

One of the most important features of high resulation spectra is the chemical shift, which is a function of the chemical environment of the observed nucleus. The spectrum supplies unique information about the distribution of an isotope according to its chemical environment and is, therefore, of great importance in the determination of molecular structure. The information on the chemical and structural environment near nuclei in molecules is obtained from the positions, widths and relative intensities of the resonance lines in the high resolution spectrum.

Another very fruitful application of high resolution NMR is in studies of

hydrogen bonding, as well as other molecular interactions. Even rather weak hydrogen bonds can be detected by this method. The method can also be used to study certain proton-exchange phenomena as well as dissociation equilibria of acids and bases in aqueous solutions [16].

1.9 : Applications of NMR

NMR spectroscopy has found a wide variety of applications. Some of the basic applications include the accurate measurement of nuclear magnetic moments, determination of relaxation times in liquids and crystalline media, the measurement of frequency accurate to 1 part in 10^8 etc. Magnetic resonance magnetometers have proved to be a useful instrument not only in the accurate determination of the magnetic field, but also in the measurement of field variations for geological applications [17].

An important and growing application of standard NMR techniques is the study of water content in a variety of materials, including food stuffs and fuels. Other applications of NMR include quantitative evaluation of liquid components in solid-liquid mixtures, study of fuels, prospecting and discovery of oils, estimation of water content in old manuscript and books etc. (Some investigatons of water content as well as oil content in a variety of materials, carried out using the indigenous wideline NMR spectrometer fabricated during the present thesis work, are described in section 8.5 of this thesis).

The width and shape of the resonance spectra have yielded information concerning crystal structure, phase transitions [18] and hindered internal motions in solids [19]. Self-diffusion may be studied both in non-metals and in metals. The resonance spectrum sometimes provides information concerning short-range order in alloys and defects in both metals and non-metallic solids [12].

The subject therefore is of interest to not only physicists and chemists, but also to biologists, metallurgists, and elc :tronics engineers. There has even been some geophysical application to NMR. However, recently, the most important application of NMR has turned out to be the technique of NMR imaging.

1.9.1 : NMR Imaging

Conventional NMR applications do not permit the location of the resonating nuclei to be determined, but it is now possible to obtain this information by spatially encoding the emitted signals. This is achieved by applying some kind of a linear field gradient which causes different regions of the sample to transmit different frequencies. Hence the different regions of the sample will become spatially determined so that it can be used to create an image of the distribution of nuclei in the sample [20]. This is the basic principle involved in the NMR imaging technique.

If a sample of water is placed in a homogeneous magnetic field, the NMR frequency spectrum of the hydrogen nuclei in the water molecules is a single narrow line. If the magnetic field is perfectly uniform, the shape of the line will be independent of the geometry of the sample. Now, if a linear magnetic field gradient is superimposed the resonant nuclei at one side of the sample will feel a weaker total magnetic field than those at the other side. There will thus be a linear distribution of Larmor frequencies across the sample. Then the free induction decay signal is subjected to Fourier transformation, a mathematical procedure that transforms the data from a curve representing signal

strength versus time into one representing signal strength versus frequency. The result is a spectrum that is broadened to a shape corresponding to the one-dimensional projection of the strength of NMR signal onto the frequency axis. By rotating the magnetic field gradient electronically one can get a projection from a slightly different angle. Computer analysis of many such projections reconstructs the sample's geometry. In the two-dimensional application of the technique the direction of the gradient is rotated within a single plane. In the three-dimensional extension of the method the gradient is rotated in three-dimension space through at least half a sphere [21].

The foremost application of NMR imaging is in the field of medicine [22]. Magnetic Resonance Imaging (MRI) exposes the internal landscape of the body as never before. Without painful injection of contrast material, it can reveal damage from a stroke buried deep beneath the skull, find tiny spinal cord injuries, detect multiple sclerosis, metabolic loss of brain function etc, and make it possible to differentiate the white and gray matter of the brain. For the soft tissues of the body, MRI comes close to being the perfect imaging technique - by enabling sensitive discrimination of healthy and diseased tissues. MRI finds its true application not in the study of anatomy, but rather in the study of physiological functions of the body. Since there are no known hazards associated with MRI, this makes the technique attractive from the point of view of prolonged time course studies, which would be either difficult, impossible or hazardous by X-ray techniques, but which would fit in well with the emerging physiological role of NMR.

Other useful biological application of NMR imaging includes measurement of fluid velocity (as in blood flowmeter), in the study of small biological systems like small animals, excised organs etc..

Proton imaging also finds much application in the area of building science and technology. Non-destructive testing of building materials when subjected to various conditions of dampness could well lead to new methods of dampness proofing [22].

REFERENCES

[1]   C.P. Slichter : Principles of Magnetic Resonance (USA; Springer:1978)

[2]   S.P. Parker Mc Graw-Hill concise Encyclopedia of Sciene& Technology (USA; McGraw-Hill : 1984)

[3]   B.P. Straughan and S.Walker; Spectroscopy-Volume I (New York; John Wiley: 1976)

[4]   J.S. Rigden; Rev. Modern Phys.; 58 (1986) 433

[5]   E.M. Purcell, H.C. Torrey and R.V. Pound; Phys. Rev.; 69 (1946) 37

[6]   H.C. Torrey, E.M. Purcell and R.V. Pound; Phys. Rev.; 69 (1946) 680

[7]   F.Bloch, W.W.Hansen and M.Packard; Phys. Rev.; 69 (1946) 680

[8]   F.Bloch, W.W. Hansen and M.Pacard; Phys. Rev.; 70 (1946) 474

[9]   E.L. Hahn; Phys. Rev.; 80 (1950) 580

[10] N.F. Ramsey; Nuclear Moments (London; Chapman & Hall: 1953)

[11] W.V.House; IEEE Trans. Nucl. Sci.; NS-27 (1980) 1220

[12] E.R. Andrew; Nuclear Magnetic Resonance (Great Britain; Cambridge University Press:1969)

[13] N.Bloembergen, E.M. Purcell and R.V. Pound; Phys. Rev.; 73 (1948) 679

[14] G.L.Clark; The Encyclopedia of Spectroscopy (USA; Reinhold:1960)

[15] F.Kasler; Quantitative analysis by NMR spectroscopy (Great Britain; Academic Press: 1973)

[16] J.A. Pople, W.G. Schneider and H.J.Bernstein; High-resolution Nuclear Magnetic Resonance (USA; Mc Graw-Hill:1959)

[17] F.A. Rushworth and D.P. Tunstall; Nuclear Magnetic Resonance (New York; Gordon and Breach: 1973)

[18] F.J. Owens, C.P. Poole and H.A. Farach; Magnetic Resonance of PhaseTransitions (USA; Academic Press:1979)

[19] G.E.Pake; Am. J. Phys.; 18 (1950) 438

[20] A.R.Meragi, B.Naraghi, K.H.Mikhchi & N. Banaji; Indian J. Pure & Applied Phys.; 24 (1982) 54

[21] I.L. Pykett; Sci.American; (May 1982) 54

[22] P.Mansfield and P.G. Morris; NMR Imaging in Biomedicine (USA; Academic Press: 1982)

Chapter II

WIDELINE N.M.R. - A THEORETICAL SURVEY

Abstract

A theoretical survey of the topic of wideline NMR is made in this chapter. The chapter begins with a brief introduction to NMR in solids. This is followed by a discussion of NMR sbsorption spectrum for rigid structures. The method of moments, leading to the expression for second moment in solids, is then mentioned. The techniques of structural determination from NMR absorption spectrum and the phenomenon of molecular motion in solids are also discussed. At the end of the chapter the important applications of wideline NMR has been given.

2.1 : Introduction to NMR in solids

From the viewpoint of spectroscopy the essential difference between liquids and gases on the one hand and solids on the other is that in the former case the molecules possess a good deal of translational and rotational freedom, whereas in the solid state these aspects are constrained to a great extent. This lack of free molecular motion in solids has two important consequences. In the first place the local magnetic field due to neighbouring magnetic dipoles is static, which causes the resonance absorption lineshape to be broad. On the other hand, in liquids and gases the rapid motions of the molecules smooths out the local field to a very small average value so that the line is quite narrow. This time-varying local field in liquids is also the all-important source of spin lattice relaxation. Since this is usually absent in solids a second important consequence is that solids generally have much longer spin-lattice relaxation times than liquids. It follows therefore that for solids the spin-lattice relaxation time T_1 is usually much longer than the spin-spin interaction time T_2, whereas for liquids the two times are frequently of the same order. Thus, for example, it is quite possible for a crystal to have $T_1 \sim 10^4$ sec and $T_2 \sim 10^{-5}$ sec [1].

The magnetic dipole-dipole interaction between nuclei of non-zero spin normally determines the NMR line-shape in non-metallic molecular solids, since this interaction is usually much greater than those due to quadrupolar effects, lifetime broadening, electron-nuclear effects and magnetic field inhomogeniety. The actual field that any one nucleus experiences is a combination of H_0 - the applied external field, and H_{local} - the resultant local magnetic field due to the neighbouring spins. This local field can be~0.5mT(5gauss). The actual value will depend also on the angle θ which each internuclear vector makes with H_0, and this will lead to a broadening of the resonance line since for varying value of H (=H_0+H_{local}) there will be correspondingly different resonant frequencies. The precise nature of this broadening will also depend on the type of sample assembly(e.g. single crystal or powder) [2].

2.2 : NMR absorption spectrum for rigid structures.

Analysis of lineshapes for solid specimens in which nuclear magnets occur in pairs have been done by Pake [3]. Example of such solids are many hydrated salts, such as gypsum ($CaSO_4 \bullet 2H_2O$). The resultant magnetic field H experienced by each proton dipole in the crystal lattice, including the local field produced by the nearest neighbours, is given by the relation

$$H = H_0 \pm \mu r^{-3}(3\cos^2\theta - 1) - - - - - - - (2.1)$$

Where H_0→the applied steady field
  μ→proton moment
  r→the pair seperation
  θ→angle between $\vec{H}_0$ and $\vec{r}$

It has been shown [1] that a single crystal of a specimen like gypsum should give two pairs of symmetrically disposed resonance lines. By examining the displacement of the peaks from the centre with respect to the variation with orientation, and using equation (2.1) the angular disposition of the proton pairs in the unit cell can be found. The spectrum for polycrystalline material is obtained by summing the spectra for isotropically oriented crystal grains. The experimental curve for a polycrystalline sample (like polycrystalline gypsum) shows a double-humped curve. From the shape of the line and the seperation of the humps, the inter proton distance in the water molecules of the polycrystalline sample can be found, though the accuracy is less than that afforded by use of a single crystal. The use of polycrystalline material however precludes the information on the anugular disposition of proton pairs.

Some materials contain nuclei clustered in relatively seperate groups of three. As examples, a number of solid organic compounds contain methyl groups (CH_3), and a number of acid hydrates contain oxonium ions (H_3O^+), each containing three protons at the vertices of an equilateral triangle. Consider a single crystal containing identical triangular groups similarly oriented. Neglecting at first the broadening caused by nuclei in other triangular groups, the analysis shows that the spectrum consists of a central line, and three pairs of lines symmetrically disposed about the centre. The seperation of these lines and their relative intensity are functions of the size and shape of the triangles and their orientation relative to the applied field H_0. A polycrystalline material containing groups of three identical nuclei should, from a theoretical consideration, exhibit a complicated shape. However in the experimental spectrum the rich detail is largely removed by the broadening caused by nucler dipoles in neighbouring groups [4]. By fitting experimental spectra to theoretical line shapes the arrangement of nuclei in the oxonium ion has been deduced by Richards et al [4] and by Kakiuchi et al [5,6].

Ammonium halides and methane are typical examples of the four-spin configurations [7,8]. The calculated spectra for these groups show considerable fine structure simply taking into accountant intractions within the group itself, but the broadening effect of inter-group interactons often destroys this fine structure. Besides many of these groups (e.g. methyl groups) are not rigid in the solid state. Thus in the general case, the calculation of detailed line-shape becomes unrealistic because of the complexity of the problem.

Fortunately, a theory developed by Van Vleck [9] enables structural information to be abstracted by a simple procedure from experimental line-shapes using the method of moments, and this gives more information than can be obtained from simple line-widths.

2.3 : Method of moments

If the absorption spectrum is described by a normalised lineshape function $g(\omega)$ then the nth moment of this line-shape about a point is given by

$$M_n = \int_0^\infty (\omega - \omega_0)^n g(\omega)d\omega - - - - - - (2.2)$$

If this line is symmetrical about ω_0, the odd moments vanish and only the even moments have significance. The second moment M_2 is the one used mostly.

The method of moments is usually applied to solids, where the phase sensitive technique used to detect the broad lines has an output proportional to the first derivative of the absorption curve. It is therefore convenient to calculate the second moment directly from this derivative curve rather than from the integrated absorption curve. In magnetic field units, where $h = H - H_0$, the second moment can be written as

$$M_2 = \int_{-\infty}^{+\infty} h^2 f(h)dh \Big/ \int_{-\infty}^{+\infty} f(h)dh - - - - - - - - - (2.3) \quad ,$$

where $f(h)$ is the unnormalised shape of the absorption curve. Integration by part gives

$$M_2 = (1/3) \int_{-\infty}^{+\infty} h^3 f'(h)dh \Big/ \int_{-\infty}^{+\infty} hf'(h)dh - - - - - - - (2.4),$$

where $f'(h)$ is the first derivative of $f(h)$ and is therefore proportional to the output from a phase-sensitive detector [2]. The calculation is performed by numerical integration from the curve, and this can conveniently be done using computer methods, for instance by using conducting ink and feeding the output from a curve-follower to an analogue computer, or arranging the output from the curve follower to be digitised, or by recording the output from the phase sensitive detector on paper tape to feed directly as input data for a computer programme.

In order to avoid spurious broadening (and smearing of any fine structure) the peak-to peak modulation must be kept as small as is compatible with good signal strength. A correction for the broadening effect which results from a modulation of amplitude h_m is given by

$$M_2(true) = M_2(measured) - (1/4) h_m^2 - - - - - - - - (2.5)$$

$$\therefore \quad M_2(true) = \Big\{ (1/3) [\Sigma h^3 f'(h)] / [\Sigma hf'(h)] \Big\} - (1/4) h_m^2 - - - - - - - (2.6)$$

Van Vleck's second moment formula has proved to be an important tool in structure determination, and the consistent results which have been obtained with its use in a large number of investigations testify to its correctness.

2.4 : Structural determination from NMR absorption spectrum

It has been shown [9,1] that if a nuclear magnetic resonance spectrum owes its width to nuclear magnetic dipolar broadening, the second moment or mean-square width of the spectrum may be calculated from a knowledge of the disposition of all nuclei of non-zero spin in the crystal lattice, and of their spin numbers and magnetic moments.

Since the spin numbers and magnetic moments are usually known, and since the second moment may be derived from the experimentally determined spectrum, it follows that information concerning the disposition of the nuclei may be obtained. The method is especially valuable in locating the positions of hydrogen nuclei in crystals since hydrogen atoms are very weak scatterersof X-rays, and cannot readily be located by the X-ray method.

If one is working with polycrystalline material, there is only one measured quantity, namely, the second moment. Consequently only one parameter of the crystal structure can be determined unambiguously, and all others must be known from other sources. More information is usually to be obtained from single crystals, especially when the anisotropy of the second moment is marked. Moreover, the spectrum for a single crystal is more likely to display fine structure, and this can give valuable information about the prescence of simple groups of nuclei in the structure. As an example, Andrew and Hyndman [10] have been able to show from the anisotropy of the second moment, using a single crystal, that the urea molecule, $OC(NH_2)_2$, is wholly planar.

Certain experimental aspects of these structural investigations are worthy of note. By contrast with liquids the spectrum is broad (T_2 short) and the spin-lattice relaxation time T_1 is long. Both these features operate against the occurrence of a good S/N ratio. Indeed, the spectrum can rarely be presented on an oscillograph, and instead only the first derivative of the spectrum is usually recorded using a phase-sensitive amplifier.

2.5 : Moleclular motion in solids

In many solids constituent molecules or atomic groups undergo rotational motion about one or more axis with a frequency which increases with temperature. Such motion causes a considerable change in the resonance absorption spectrum. Looking at the situation in terms of the local field produced at any resonant nucleus by its neighbouring dipoles, we observe that this field is now time-varying and that if the variation is sufficiently rapid, the time average of the local field must be taken to express the dipole interaction. Since the time average over all permitted orientations of the dipole pairs can in general be supposed to be less than the steady local field for a rigid system, the spectrum may be expected to become more narrow when the rotation sets in. A narrowing of the absorption line with increasing temperature has been observed in many solids and has been ascribed to molecular motion within the crystal lattice [1].

Molecular motion in crystals is sometimes sufficiently marked to bring about anomalies in the specific heat and transitions in the crystal structure. However, such transitions can have other causes, and unambiguous evidence of molecular motion had hitherto been obtainable mainly from X-ray or dielectric measurements. X-ray method gives such information only if each molecule spends a large proportion of its time rotating whereas the nuclear resonance linewidth is affected even though each molecule spends only a small fraction of its time rotating. Resonance line narrows when the reorientation (or rotation) rate is of the order of the frequency linewidth itself; in practlice this frequency is usually about 10^4 or 10^5 Hz.

For a polycrystalline material containing relatively isolated systems of two nuclei, in which the internuclear vector of the isolated pair is effectively stationary at low temperatures but reorients rapidly at higher temperatures about a perpendicular axis, the absorption line undergoes a transition, becoming half as wide and correspondingly more

intense at higher temperatures. This behaviour is exhibited by dichloro ethane, $(CH_2Cl)_2$ [11].

The case of triangular groups of identical nuclei of spin number 1/2 reorienting about any given axis has been worked out by Andrew and Bersohn [12]. In general it leads, as in the rigid case discussed in Section 2.2, to a spectrum consisting of a central line and three pairs of lines symmetrically disposed about the centre. However, in the special case frequently encountered, in which the axis of reorientation is normal to the plane of the triangle, two pairs of lines disappear, and we are left with the central line and just one pair of lines. For a polycrystalline sample of acetonitrile, CH_3CN, the theoretical line shape is in agreement with that observed by Gutowsky and Pake [11] at 93° K, and indicates that in this molecule the methyl group reorients about the C-C bond.

As in the case of rigid structures, it is difficult to calculate the lineshape for reorienting systems containing more than three nuclei, and here again one has to make use of Van Vleck's second-moment formula. Using this method the transition from an effectively rigid system to a rapidly reorienting system has been observed in a number of compounds. In the spectrum of polycrystalline benzene, C_6H_6, the second moment is seen to decrease from a constant value of 9.7gauss^2 below to a constant value of 1.6gauss^2 above 120°K [13]. A more interesting behaviour exhibited by polycrystalline cyclohexane, C_6H_{12}has been studied by Andrew and Eades [14,15].

Molecular reorientation has already been established from evidences obtained by nuclear magnetic resonance measurements in a great many compounds; in inorganic compounds such as ammonium salts, in almost spherical molecules such as methane and neopentane, in flat ones such as benzene, in long ones such as the long-chain paraffins and polymers, in liquid crystals, and in many others. It is important to note that materials investigated should be of the highest purity, since foreign molecules may deform the crystal lattice and thus assist, induce or prevent a reorientation process, or in other ways produce misleading results [16].

2.6 : Applications of Wideline NMR

Wideline NMR has considerable application to organic quantitative analysis, particularly for the determination of water, oil and solid fat content in industrial and agricultural materials. The wideline method can be easily adopted to on-stream measurement and control, and needs only relatively inexpensive equipment [17].

Wideline NMR is potentially capable of determining the concentration of a sizeable number of the elements. One important application of the method is the non-destructive determination of the oil content of seeds. This allows retention of desirable specimen for subsequent breeding.

For many applications the crucial point is that the linewidths for a compound in the liquid state are much smaller than those for the sample in solid state, so that the phases can be distinguished. Hence a NMR measurement can provide a quantitative determination of the fraction of the protons (or other NMR sensitive nuclei) that are in rigid or frozen environments and fraction that are in solutions [18]. Conditions can be chosen so that the resonance of liquid water is saturated and gives only a very small signal, while that of bound water is diminished very little. In mixtures of dry material and water, the process

of hydration can thus be followed by the increase in the signal strength [17].

The width and shape of the resonance line may indicate the physical environment of the isotope under study. The multiplicity of spectral peaks resulting from dipole-dipole interaction in solids has been used to determine the arrangements of atoms in solids. The width of the resonance is indicative of the degree of motional freedom of the isotope in the physical environment in which it is located. This is useful for determining the degree of "crystallinity" of polymers, for determining water or hydrocarbons adsorbed in solids, etc and for solving similar problems where there are wide differences in the degree of motional freedom of the observed atoms. Changes in motional freedom with changes in composition, temperature, pressure and other environmental factors can also be studied by observing changes in linewidth and shape [19].

REFERENCES

[1] E.R. Andrew; Nuclear Magnetic Resonance (Great Britain; Cambridge University Press: 1969)

[2] F.A.Rushworth and D.P.Tunstall; Nuclear Magnetic Resonance (New York; Gordon and Breach: 1973)

[3] G.E.Pake; J.Chem. Phys.; 16 (1948) 327

[4] R.E. Richards and J.A.S Smith; Trans. Faraday Soc.; 47 (1951) 1261

[5] Y.Kakiuchi, H.Shono, H.Komatsu; J. Chem. Phys.; 19 (1951) 1069

[6] Y.Kakiuchi, H.Shono, H.Komatsu and K.Kigoshi; J.Phys. Soc.Japan; 7 (1952) 102

[7] R.Bersohn and H.S.Gutowsky; J.Chem. Phys.; 22 (1954) 651

[8] J.Itoh, R.Kusaka, Y.Yamagata, R.Kiriyama and H. Ibamoto; J Phys. Soc.Japan; 8 (1952) 293.

[9] J.H.Van Vleck; Phys. Rev.; 74 (1948) 1168

[10] E.R.Andrew and D.Hyndman; Proc. Phys. Soc. Lond. A; 66 (1953) 1187

[11] H.S.Gutowsky and G.E.Pake; J.Chem. Phys.; 18 (1950) 162

[12] E.R.Andrew and R.Bersohn; J.Chem. Phys.;18 (1950) 159

[13] E.R. Andrew and R.G. Eades; Proc. Phys. Soc. Lond. A; 218 (1953) 537

[14] E.R.Andrew and R.G.Eades; Proc. Phys. Soc. Lond. A; 66 (1952) 371

[15] E.R.Andrew and R.G.Eades; Proc. Phys. Soc. Lond. A; 216 (1953) 398

[16] F.A.Rushworth; J.Chem. Phys.; 20 (1952) 920

[17] F.Kasler; Quantitative analysis by NMR spectroscopy (Great Britain; Academic Press:1973)

[18] C.Biscegli, H.Panepucci, A.Farach and C.P.Poole; Am.J. Phys.; 50 (1982) 48

[19] G.L.Clark; The Encyclopedia of Spectroscopy (U.S.A; Reinhold:1960)

Chapter III

EXPERIMENTAL TECHNIQUES -
WIDELINE N.M.R. SPECTROMETER

Abstract

A general description of the requirements and functioning of the different systems of a typical wideline NMR spectrometer set up is given in this chapter. The necessity for adequate magnetic field homogeneity and stability is discussed along with the means of meeting these stringent conditions. The purpose of the field modulation as well as the field sweep arrangements is also discussed. Following this, conventional NMR detector circuits are outlined. The role of phase-sensitive detection in the processing of NMR signal is then given, followed by a discussion of the essential conditions for the observation of NMR absorption. At the end of the chapter a typical wideline NMR experimental set up and its operation are briefly described.

As the interaction energy between the nuclear magnetic moment and the static magnetic field is very small ($\sim 10^{-5}$ to 10^{-7}eV) the detection of nuclear magnetism is inherently a problem of very low signal-to-noise (S/N). On a microscopic level, these energies, at least at room temperature, are significantly smaller than the thermal noise [1]] However, by virtue of the resonance phenomenon and coherence effects we are able to observe the nuclear magnetism indirectly through NMR. In this context it is worthwhile to consider the different experimental techniques and the various spectrometer systems that enable one to extract the weak NMR signal deeply embedded in noise.

3.1 : The spectrometer - basic requirements

All resonance detection techniques (in principle) and NMR (in practise) can be implemented by two basic approaches, which are called CW (continuous wave) and pulsed (transient response) methods in the case of NMR. In the first approach, either the static magnetic field or the radiofrequency is swept slowly and the absorbed (or emitted) energy monitored as a function of either of these quantities. A resonance will thus be characterised as a peak in the corresponding parameter (the spectrum). In the second case, energy of a wide frequency range is given as input to the system for a short period of time and the subsequent output is observed. The system itself provides information by its transient "ringing" after the excitation [1].

For wideline NMR studies the CW method is usually adopted. The basic requirements of a typical CW spectrometer are as follows:
(i) A powerful magnet into which the sample is placed. A net magnetization will then be induced in the sample in the direction of the applied magnetic induction.
(ii) A radiofrequency transmitter, which supplies the (Larmor) frequency appropriate for the particular field strength and nucleus under examinaton. The linearly oscillating r.f.field is applied perpendicular to the direction of B_0 and the magnetic vector of this field has a component rotating at the Larmor frequency.
(iii) A radiofrequency reciever, which detects the resonance absorption.
(iv) A recorder, to provide a permanent record of the signals observed by the reciever.

The detection and display of the resonance signal usually involves some more additional subsystems, such as slow linear field sweep, field modulation, detection systems involving signal recovery techniques etc.

3.2 : Magnet - field homogeneity and field stability

The two main requirements to be met by the magnetic field employed in NMR experiments are high degree of homogeneity in space and excellent stability in time [2].

3.2.1 : Field homogeneity

The magnetic field employed for NMR experiments should be homogeneous within the volume of space occupied by the sample. The basic requirement for such homogeneity lies in very precise pole-piece design; these must be metallurgically uniform, precisely parallel to each other and free from machining marks [3]. Besides polepieces should have a diameter about ten times larger than the air gap in order to achieve better field uniformity [4]. The requirement of better field homogeniety will indirectly restrict the sample volume that can be adopted for the experiment.

For wideline NMR studies in the solid-state the magnetic field should be uniform to about 0.1 gauss over the sample volume. Otherwise, inhomogeneities in the magnetic field will completely mask the resonance signal [5].

3.2.2 : Field stability

For achieving the maximum field stability three steps are to be adopted : a high-precision curent stabilizer, a flux stabilizer (or 'super stabilizer') and a field-frequency lock. With the first device, the magnet current is stabilized to about 1 part in 10^6. The flux stabilizer is designed to compensate for rapid fluctuations in the magnetic field. For this purpose, pick up coils are mounted on the polepieces; the voltage induced in these coils by field fluctuations are amplified, integrated and fed as a correction signal to the current stabilizer, giving a field stability of around 1 part in 10^{10} per second. As a last step, long-term variations are compensated by a correction signal derived from the 'lock circuit' and this signal is fed to the input of the flux stabilizer [4].

For wideline NMR experiments, since a field stability of the order of 1 part in 10^6 is adequate, only a precision current stabilizer need be employed for achieving the required field stability. For this purpose highly regulated alternating currents are rectified, and the direct current that is supplied to the magnet is stabilized using a feedback system. The magnet current is passed through a standard resistor and the resultant voltage is compared with that from a reference source of high stability (e.g. a Weston cell); the difference voltage is amplified and fed as an error signal to the current control through which the magnet current has passed and this causes self-compensaton. By this method a field stability of the order of 1 part in 10^6 can be obtained [3].

In the case of wideline NMR, because of the width of the line, the requirements for field homogeneity and field stability are not as critical as in high resolution NMR. Besides larger sample volumes can also be used in this case.

3.3 : Field modulation system

In order to display the nuclear magnetic resonance absorption or dispersion line on an oscillograph it is necessary to modulate the 'steady' magnetic field at a low audio frequency, often about 30Hz. Usually, a sinusoidally varying field having an amplitude of several times the width of the absorption line is applied by means of auxiliary coils. Now, if the mean value of the steady field is close to the resonant value, the field is swept twice through the resonance condition in each cycle, providing an audio-amplitude modulation of the r.f. carrier. After rectification, the audio signal is further amplified and it is then displayed on a CRO, the time-base of which is synchronised with the modulation.

On the other hand, when a phase-sensitive amplifier is employed during the recording of the signal, the modulation current is so adjusted that the maximum variation in the field at the sample is much less than the width of its resonance line. The output signal of the lock-in amplifier is then sinusoidal with an amplitude proportional to the first derivative of the line shape; strictly this is only true for a very small amplitude of modulation such that the portion of the line shape which is traversed during the field sweep can be treated as linear. On the contrary, if the modulating field is set too high considerable distortion, known as 'modulation broadening' of the output, occurs; its elimination becomes essential for the observation of true lineshapes. Provided the modulation amplitude is not more than about one-sixth of the linewidth, the curve obtained is a reasonably faithful reproduction of the derivative [6].

The process of field modulation will lead to the generation of some additional noise in the spectrometer. It has been shown that the sensitivity of NMR spectrometers with signal modulation and subsequent detection is limited to a considerable extent by the noise at the modulation frequency [7]. Since the modulation noise in the gap of the electromagnet are determined mostly by the modulating field and is proportional to it, the problem of attenuation of modulation noise reduces to stabilization of the amplitude and phase of the modulating magnetic field. Using feedback which is sensitive to variations of the amplitude and phase of the modulating field, the modulation current is stabilized, and this lowers the noise level.

3.4 : Field Sweep arrangement

Field sweep at a very slow rate is necessary for the convenient recording of NMR signal (there being a limit to the fast response capability of the recording system). The field sweep is effected either by scanning the reference voltage of the magnet current stabilizer between appropriate limit and at the desired rate [5,8,9] or by using a seperate field sweep unit, having independent field sweep coils, that generate linearly varying fields of desired strength and duration [3,10,11]. For the faithful recording of the resonance spectra this field sweep should be highly linear.

The correct choice of sweep rate is important as well as complicated because there are a number of requirements which contradict one another [4]. The best procedure for recording single scan spectrum consists of using the lowest possible sweep rate-mainly determined by the maximum allowed recording time - and the corresponding optimum saturation parameter. For systems with a high T_1/T_2 ratio, however, it may be preferable that the sweep rate be raised as this has the advantage of saving time without loss of sensitivity or resolution.

3.5 : The NMR probe

The NMR probe is the system which performs the dual function of transmitting the r.f.field as well as detecting the resonance signal. The conventional methods for detecting the existence of the NMR effect can be broadly split into two catagories:
(i) Single coil method in which the change in susceptibility of the sample when resonance occurs changes the effective inductance of a coil which is part of a tuned circuit and which surrounds the sample.
(ii) Double coil method in which one coil is fed from an r.f.signal generator and the second coil, mutually orthogonal to the transmitting coil axis and to the steady magnetic induction B_0, has a voltage induced in it due to the forced precession of the nuclear spins at their Larmor frequency.

Method (i) is often referred to as 'nuclear magnetic resonance absorption', since one picture of the process is of a heating of the spin system due to the absorption of energy at resonance, resulting in a decrease in the effective Q of the resonant circuit. Method (ii) is aptly described as 'nuclear induction'.

One important piece of information which the nuclear induction method yields, but which the resonance absorption method does not yield, is the sign of the nuclear magnetic moment. However, apart from this advantage, which is not of importance in all types of work, there is little to choose between the single- and double- coil methods of observing nuclear magnetic resonance. In practise the choice is frequently determined by local experience and tradition. For work at low temperatures one frequently desires simplicity within the cryostat even at the expense of complication outside it. The single-coil methods are preferable in such cases, since only one coil and two leads are required inside the cryostat, while the nuclear induction methods require two coils, flux leakage controls and at least three electrical leads within the cryostat [12]. Based on these considerations the single coil method of NMR detection has been adopted for the investigations presented in this work.

3.6 : Phase sensitive detection

In conventional broadline NMR the principle objective is to obtain the lineshape of the broad signal as accurately as possible, often over a wide range of temperature. The main difficulty encountered here is the very weak signal strength of the broad lines. This difficulty arises from the spread of the absorption over a range of field values due to the large nuclear spin-spin interactions which are dominant in many solids. The signal strength at any one point in the spectrum is comparable with the inherent noise of the system and invariably signal recovery techniques have to be used [13].

For extracting the weak NMR signal embedded in large interference noise, a lock-in amplifier is the most ideal signal processing instrument that can be used [14]. This is a sophisticated low-level signal measurement system using phase sensitive detection principle. The system has two inputs: a signal that is to be measured (which in a NMR spectrometer corresponds to the output of the NMR probe that varies at the modulation frequency), and a reference that has the same frequency as the input (here, the modulation frequency) and having an arbitrary but constant phase shift with respect to the input. The signal is prefiltered after amplification and is fed to a phase-sensitive detector (PSD). The reference signal is also filtered and, after passing through a 0 to 360° continuously-

controllable phase shifter, is fed to the PSD through a driver.

The operation of a phase-sensitive detector is similar to that of a half-wave detector. The reference voltage at the modulation frequency (often transformed into a square wave) switches on and off a gate into which the signal and noise are fed. The gate will be opened for one half of each cycle. Over several hundred periods any random signals present tend to cancel out provided the integrating time is long enough. This time determines the effective bandwidth of the system and, provided the speed of traverse through the line is slow enough, the important factor is the time constant of the smoothing circuit. A relatively large value for the time constant helps to narrow down the effective bandwidth considerably. This will then be equivalent to passing the input through a tuned circuit having a very high Q-factor, so that the noise components outside the bandwidth will get eliminated. Only the Fourier components of the input at the reference frequency (and odd harmonics) will contribute to the net d.c.component [13]. When the magnetic field is swept, the output of the PSD will vary in amplitude and in phase as the field modulation effected at different region of the normal signal line shape. As a result the original signal will get converted into its derivative at the detector's output. This output of the PSD is low-pass filtered and after further amplification, becomes the final output of the lock-in amplifier. The setting of the 0 to 360° phase shifter is in general adjusted to optimize the output signal.

The main advantage of phase sensitive detection is that only those components of the noise in the input which occur at the reference frequency are detected, whereas in normal detectors all frequencies contribute to the electrical noise of the output: thus a considerable gain in S/N ratio ensues. As its name implies, the output from the phase-sensitive detector depends on the phase of the input signal and since it also depends on the slope of the normal line the final output will constitute the derivative of the original signal [15].

3.7 : Condition for the observation of NMR absorption

If a nuclear magnetic resonance signal is to be detected at all, it must be discriminated from the background of random electrical fluctuations or 'noise'; in fact the signal power available at the detection apparatus must be at least of the same order as the noise power. If, further, accurate measurments are to be made of the shape of the resonance absorption line, the ratio of signal power to noise power must be much greater than unity [12].

Bloembergen, Purcell and Pound have derived an expression for the signal-to noise voltage ratio [16], which for a given nuclear species can be shown as

$$V_s/V_n \propto \zeta N \left[(v_0^3 V_c Q T_2) / (T^3 B_2 F T_1) \right]^{1/2}, \quad \text{where}$$

$\zeta \longrightarrow$ is the filling factor denoting the proportion of the effective coil area which is occupied by the spin system

$N \longrightarrow$ is the total number of nuclei per cc

$v_0 \longrightarrow$ is the applied radio frequency

$V_c \longrightarrow$ is the effective volume in which the r.f.magnetic field energy is stored and is very nearly equal to the volume of the coil

$Q \longrightarrow$ is the quality factor of the coil

T_2 ⟶ is the spin-spin interaction time

T ⟶ is the temperature of the experimental sample

B_2 ⟶ is the effective bandwidth of the phase sensitive amplifier

F ⟶ is the noise factor of the detection apparatus   and

T_1 ⟶ is the spin-lattice relaxation time.

The above expression leads to the following conclusions:

(a) Frequency v_0 : The radio frequency occurs explicitly as $v_0^{3/2}$, but also enters implicitly into Q (which usually increases more slowly with frequency), F and V_c (which may slowly decrease with an increase of frequency). Hence it can be concluded that it generally pays to work at as high a frequency as possible. This frequency is often limited by the magnetic fields available, which should therefore be as high as possible.

(b) Number of nuclei present : The proportionality of S/N ratio to $\zeta N V_c^{1/2}$ indicates that the specimen should contain as many resonating nuclei as possible.

(c) Temperature : The factor $T^{-3/2}$ in the expression indicates that a very low sample temperature will considerably enhance the S/N, though at the expense of experimental simplicity.

(d) Relaxation times : The term $(T_2/T_1)^{1/2}$ implies that the linewidth should be small, as for example in a liquid, and that the spin lattice relaxation time should be short. T_1 may often be shortened by the addition of a paramagnetic impurity to the specimen.

(e) Detection system : The factor $(Q/B_2F)^{1/2}$ leads to the obvious statement that the S/N ratio is improved by use of a high-Q coil, an amplifier of low noise-factor, and a narrow bandwidth. B_2 is of the order of $1/t_c$, where t_c is the time constant of the output circuit of the phase-sensitive amplifier; therefore B_2 is only reduced at the expense of a slower speed of recording information.

Thus the main choices that permits optimisation of the signal strength will be (i) a high, steady magnetic field, (ii) a large sample volume and (iii) as low a specimen temperature as possible.

The basic requirements for observing nuclear magnetic resonance absorption can now be considered. A sample of material, containing large number of nuclei in which one is interested, is subjected to a strong and steady magnetic field H_0. It is then necessary to wait for a period several times longer than the spin-lattice relaxation time for the spin system to come into thermal equilibrium with the lattice. Facilities must now be provided for subjecting the sample to a radiofrequency magnetic field of appropriate strength in a direction at right angles to H_0. This is achieved by winding a coil around the sample, its axis in the direction of the desired oscillatory field, and by passing an r.f. current through the coil. Provision must now be made for adjustment either of the magnitude of the steady field H_0, or of the radio frequency v, until the resonance condition is reached. Under this condition the maximum power is absorbed from the radiofrequency field. This resonance condition is detected by observing the additional power flow, equivalent to extra losses in the coil supplying the radiofrequency [12].

3.8 : A Typical wideline NMR spectrometer

A typical arrangement for wideline continuous wave NMR spectrometer is as shown in Fig.3.1. The magnetic field is ~1 Tesla (10,000 gauss) with reasonable (but not necessarily outstanding) stability and homogeneity, capable of being swept linearly over
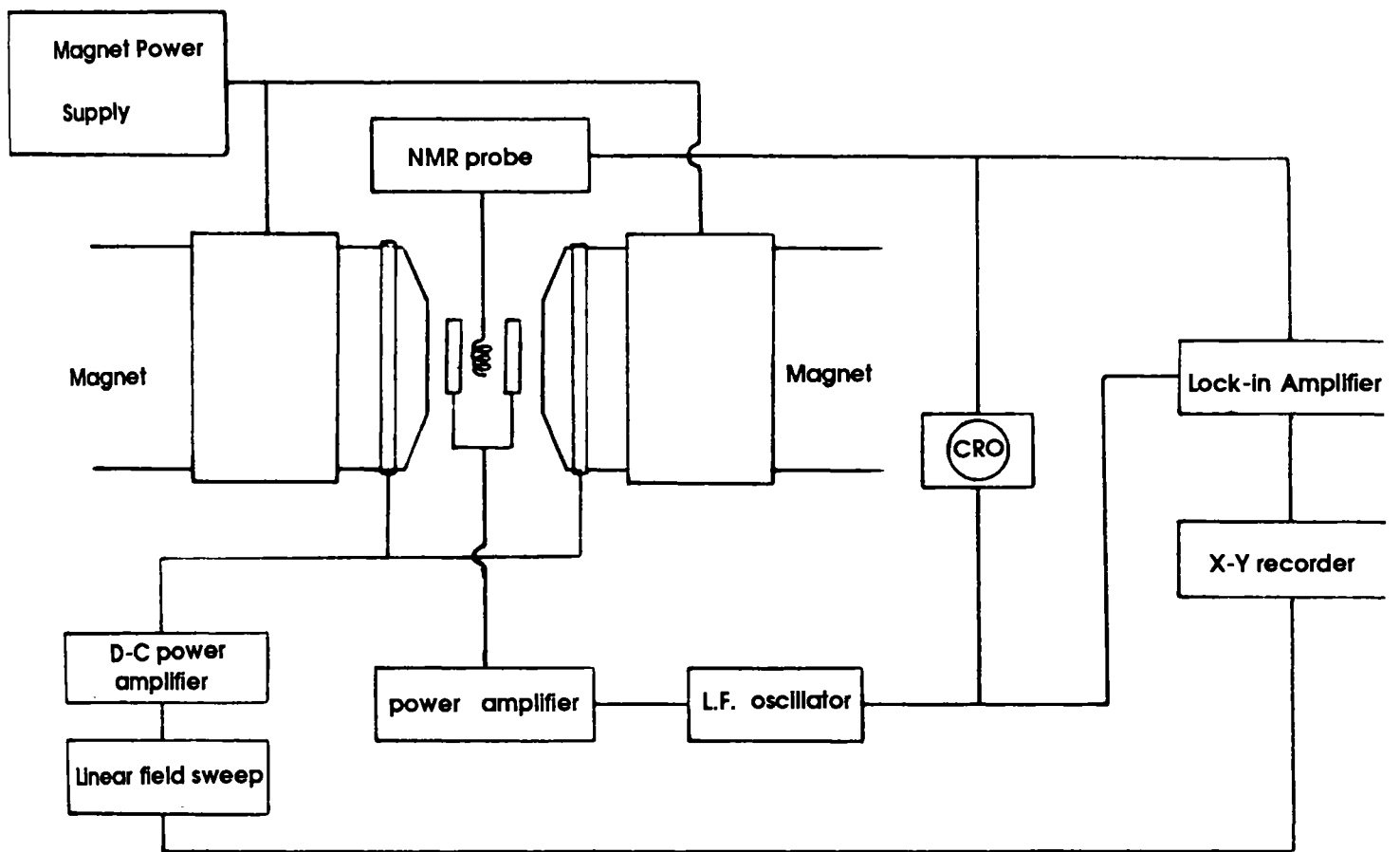
Fig. 3.1 : Block diagram of typical CW wideline NMR spectrometer

field ranges upto ~5mT at rates varying down to ~0.1mT per minute. Additional audio frequency field modulation is used by superimposing a small sinusoidal field variation by modulation coils fixed round the polecaps. The absorption signal detected by the NMR probe can be displayed on an oscilloscope, in which case the modulation strength should be around five to ten times the width of the resonance line under investigation.

For recording of the NMR signal, the output of the NMR probe is fed into the lock-in amplifier, the reference for which is derived from the modulation oscillator. Besides, to avoid any distortion of the lineshape, the amplitude of field modulation is reduced to less than one fourth the linewidth [13]. The derivative output of the lock-in amplifier is then recorded either on a strip chart recorder or on an X-Y recorder, whose X-sweep is linked with the slow linear field sweep.

REFERENCES

[1]   W.V. House; IEEE Trans. Nucl. Sci.; NS-27 (1980) 1220

[2]   A.Abragam; The Principles of Nuclear Magnetism (Great Britian; Oxford University Press:1962)

[3]   B.P.Straughan and S.Walker; Spectroscopy-Volume I (New York; John Wiley: 1976)

[4]   M.L. Martin, J.-J. Delpuech and G.J. Martin; Practical NMR Spectroscopy (Great Britain;Heyden: 1980)

[5]   S.Ganapathy and K.Ramani; J.Instn. Electronics & Telecom.Engrs.(India); 23 (1977)152

[6]   E.R.Andrew; Phys.Rev.; 91 (1953) 425

[7]   N.I. Shpin'kov; Instrum. & Exp. Tech. (USA); 15 (1972) 149

[8]   J.B.Cook, R.E. George and E.H.Grant; J.Sci.Instrum.; 41 (1964) 390

[9]   J.Sthanapathi, A.K.Ghosal, D.K.Dey, A.K.Pal and S.N.Battacharya; J.Phys. E; 10 (1977) 221

[10]   K.J.Wilson, C.Raghavan and C.P.G.Vallabhan; J.Instrum. Society of India; 18 (1988) 265

[11]   K.J.Wilson and C.P.G.Vallabhan; J. Phys. E;22 (1989) 131

[12]   E.R Andrew; Nuclear Magnetic Resonance (Great Britain; Oxford University Press1969)

[13]   F.A. Rushworth and D.P. Tunstall; Nuclear Magnetic Resonance (NewYork; Gordon and Breach: 1973)

[14]   C.S.Rangan, G.R.Sarma and V.S.V Mani; Instrumentation-Devices and Systems (New Delhi; Tata Mc Graw-Hill:1983)

[15]   K.A.Mc Lauchlan; Magnetic Resonace (Great Britain; Oxford University Press : 1972)

[16]   N.Bloembergen, E.M. Purcell and R.V. Pound; Phys. Rev.;73 (1948) 679

Chapter IV

IMPROVED MAGNET CURRENT STABILIZER

Abstract

The chapter begins with a consideration of the requirements for magnetic field stability needed for NMR experiments. After reviewing some of the earlier transistorised magnet current stabilizing circuits the necessity of an alternate design is highlighted. Following this a modified current sensing technique developed for high current applications is given. The improved high current stabilizer circuit, which totally eliminates the need for a seperate current sensing unit, is described in detail. The chapter also gives a theoretical analysis of conventional reference voltage selector circuit that has led to an improved design which provides a better resolution for scanning the magnetic field.

4.1 : Magnetic field stability requirement

The static magnetic field employed for NMR experiments should be highly stable so that the sample under investigation experiences a very steady field throughout the duration of the experiment [1]. This is especially important when the derivative of the spectrum is obtained with a pen recorder as against oscilloscope display, since in this case one has to sweep through the resonance very slowly [2].

The minimum field stability required can be approximated to be of the order of a fraction of the width of the narrowest resonance line intended to be studied. In the case of wideline NMR, assuming a linewidth~0.2 gauss for the typically narrow resonance line that will be studied, the degree of field stability required in a steady field of, say, 2000 gauss will be ~(0.02/2000)~ $1/10^5$ over the sample volume. This amount of field stability can be achieved by using appropriate design for the electromagnet.

If very rigorously thermostated and shielded from stray magnetic influences, permanent magnets are capable of providing extremely stable fields [3]. However the permanent magnets suffer from a major drawback in that their relatively narrow polegap cannot accomodate wide probeheads, thus ruling out the use of large diameter sample tubes and multinuclear versatility [4]. Besides there are difficulties in using permanent magnets at very high fields [3]. These limitations of permanent magnets can be overcome by the use of electromagnets, providing a major advantage of adjustable magnetic field. Further, the electromagnets can generate much higher fields and field stability equivalent to that of the very best permanent magnets can be routinely achieved [3].

The stability of the field produced by an electromagnet depends largely upon the stability of the current that passes through its coils. Since a field stability of the order of one part in 10^5 can be obtained by stabilizing the magnet current alone [3], the task of achieving the necessary field stability for a wideline NMR spectrometer reduces to the proper stabilizaton of the magnet current.

4,2 : Earlier magnet current stabilizers

The major causes of field instability in an electromagnet are random voltage fluctuations in the mains and changes in coil resistance due to temperature variations. The latter can largely be overcome by allowing the magnet to reach thermal equilibrium (which may take about two hours). The mains fluctuations produce field changes that may reach as much as several hundred gauss and to counteract such changes proper current stabilizer has to be incorporated in the power supply to the magnet [5].

A typical current stabilizer is represented by the block diagram of Fig.4.1. The total current that flows through the current sensor (a standard resistor) will develop a proportional voltage that is compared with a reference voltage (say, from a battery) by the comparator. The error voltage so developed is amplified and fed to the control unit (an appropriate network of power transistors). The control unit will regulate the current flowing through it such that any tendency for fluctuation in the load current from the value set by the reference voltage will be countered and thus a steady current will flow through the load. Any change in the set current will cause either an increase or decrease in the potential drop (or power dissipation) across the control unit.

The earlier current stabilizers were fabricated using vacuum tubes [6,7,8]. With the arrival of power transistors the vacuum tube circuits have become outdated. A number of transistorised magnet current stabilizer circuits [9, 10, 11, 15, 12, 2] have been described in literature. The operation of these circuits is identical to that of the typical current stabilizer described above; with a single low value standard resistor functioning as the current sensor and a series pass bank of parallel connected power transistors acting as the control unit.

In these circuits the standard resistor plays an important role in the stability of the whole system and hence proper care has to be taken in its design and construction. The resistor should be made of a wire having a low temperature coefficient of resistivity so that its value does not change significantly with temperature. Either manganin or eureka wire of appropriate gauge has to be selected for this purpose. Then there lies the task of removing the heat generated in the standard resistor so as to maintain its resistance at a constant value. Some circuits (e.g.[5,2]) achieved this by immersing the standard resistance coil in transformer oil and by circulating cold water through a copper spiral tube surrounding the resistor coil. Some other circuits, (e.g.[12]), had used thermostated chambers to keep the temperature of the standard resistor regulated to a good extent, thus getting better results. These types of cooling arrangements can work satisfactorily in circuits meant to stabilize relatively low currents (say,upto~10A).

4.3 : Need for an alternate design

A serious drawback encountered with the earlier magnet current stabilizer circuits is that considerable effors are needed to remove the heat generated across the current sensing standard resistor. The current sensing methods employed in these circuits are not only cumbersome and costly but also unsuitable when high magnet currents are involved, since the power dissipation across the sensing resistor will then increase substantially.

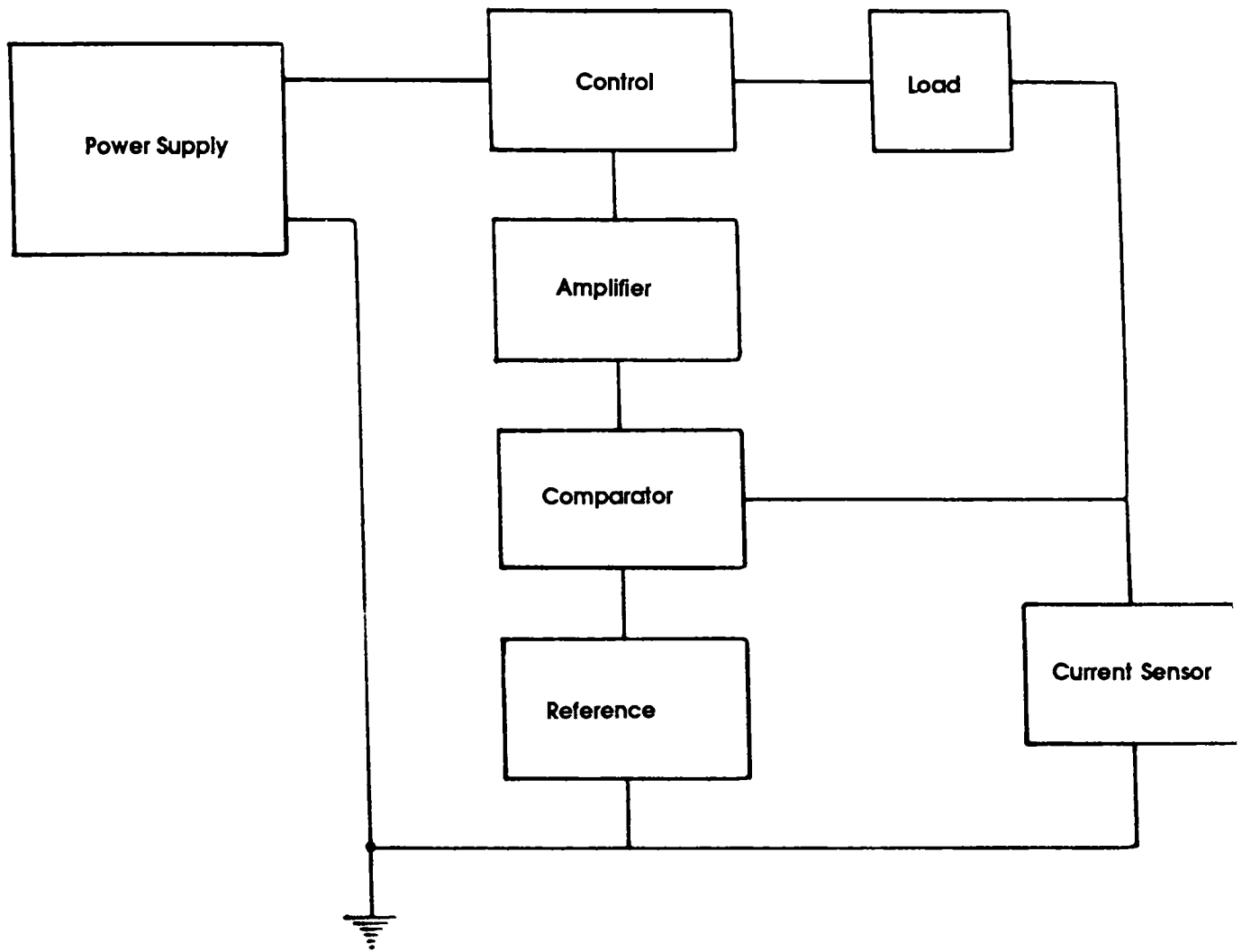The electromagnet around which the wideling NMR Spectrometer has been

Fig. 4.1 : Block diagram of a current stabilizing system

fabricated here does not permit any of the above mentioned conventional current stabilizer circuits to be utilised for effecting field regulation. This situation arises because the electromagnet (Magnion Inc.,USA) is a high current type, which will yield its maximum field strength of 1.1T (11,000 gauss) only at 50A. For stabilizing a current of such a high magnitude none of the conventional current sensing methods is viable. This has prompted us to adopt an altogether different approach for stabilizing the high current, with special emphasis on high current sensing.

4.4 : A modified current sensing technique

For eliminating the complex and costly cooling arrangements that usually become necessary for sensing high currents a simple and effective technique has been developed [13]. In this innovative method the total current is made to devide itself among a network consisting of an appropriate number of low value standard resistors connected in parallel. This helps to keep the power dissipation in the individual resistors to a low value but at the same time allows an adequate sensing voltage to be developed across the network as a whole to be utilised for current stabilization.

4.4.1 : Selection of the sensing network

The number of individual resistors in the network is chosen by considering the maximum sensing voltage required and the maximum power dissipation that may be allowed across each individual resistor. The individual resistors are made by giving due consideration to the apropriate dimension (length and thickness) of the standard resistor wire to be used. A suitable thickness gauge has to be selected that not only permits efficient radiation of heat developed but at the same time will necessitate only a reasonably convenient length of the wire to be used for making the resistors.

In our case, for sensing the alterations in a maximum current of $I_{max} = 50A$, the maximum feedback voltage was chosen as $E_{f \cdot max} = 0.2V$. Then the effective resistance of the network to be fabricated is obtained as

$$R_{eff} = E_{f \cdot max}/I_{max} = 0.2V/50A = 0.004 \ \Omega$$

The maximum power dissipation across the current sensing network at the maximum current value then become

$$P_N = I_{max}^2 \cdot R_{eff} = (50)^2 \times 0.004 = 10W$$

Choosing the maximum power dissipation that may be allowed across the individual resistors of the network to be less than 0.5W, say, as $p_i = 0.4W$, the total number of resistors to be formed into the network becomes

$$N = P_N/p_i = 10/0.4 = 25$$

Then the resistance value, R, for the individual resistors of the network is obtained from the relation

$$p_i = E_{f \cdot max}^2/R$$

$$\therefore \quad R = (0.02)^2/0.4 = 0.1\Omega$$

For making the resistors eureka wire was chosen because of its low temperature coefficient of resistivity ($\sim 10^{-5}$/°C). An adequate thickness gauge for the wire, that may enable faster dissipation of heat developed, was chosen as 18s.w.g. Then the length of the wire required to make 0.1Ω resistors will be approximately 25cms.

Thus for the sensing of current fluctuations in a maximum current of 50A the sensing resistor network is effected by connecting in parallel 25 numbers of 0.1Ω resistors, made by winding approximately 25cms of 18 s.w.g. eureka wire. Since the power dissipated in each individual resistor is very small (a maximum of 0.4W only) its resistance value remains virtually a constant. The voltage developed across this network as a whole can be used as the feedback voltage for the current stabilizer system.

4.4.2 : Advantages of the technique

Besides eliminating the need for cumbersome and costly cooling arrangements the novel technique employed here has a major advantage in that any tendency for change in the individual resistor values (mainly due to Joule heating) will not affect appreciably the effective resistance of the network. Hence the probability for current drifting is less. Further, though the method has been formulated here for high current systems, it can be utilised in low current applications as well with even greater effectiveness.

4.4.3 : Current stabilizer using the new current sensing method

Utilising the sensing technique described above a high current stabilizer has been designed and fabricated for regulating upto 50A current through the electromagnet. The schematic circuit of the stabilizing unit is shown in Fig. 4.2.

Unregulated DC at 100V (50A) from a variable 3-phase rectifier unit was chosen as the input to the stabilizing system. A very high value capacitor ($12000\mu F$; 200V DC) is connected at the rectifier output to filter off the ripple content from it. The additional low value capacitor ($10\mu F$) will take care of voltage transients during mains failure.

The series element consists of 31 power transistors (Q_2 to Q_{32}) having V_{CEO} of 140V. The $1/2\Omega$ resistors made of eureka wire in each emitter lead serves to equalise currents in the different power transistors. The very low temperature coefficient of resistivity of eureka helps in preventing fluctuation in emitter resistance. Power transistors (2N 3442) having approximately identical current gain values are selected for making up the pass bank. The transistors are intially mounted in pairs on standard heat sinks meant for two power transistors. These are in turn mounted on a thick, blackened, aluminium sheet having a number of additional radiating fins fitted onto it.

The control unit essentially consists of an op-amp A(LM 741), working in the inverting mode with a closed loop gain of around 10^4. The non-inverting input of A is supplied with a stable reference voltage, derived from a dry cell. The transistors T_1(SL100), T_2(BD139) and Q_1(2N3442) follow A and provide the necessary current gain to the transistors of the series element. The +12V,-12V regulated supply voltages for the op-amp are derived from a pair of voltage doubler circuits followed by L 7812 regulator chips, as shown in Fig.4.3. The voltage doubler circuit was chosen as it permits the most compact transformer to be used for a given DC output voltage requirement [14,15].
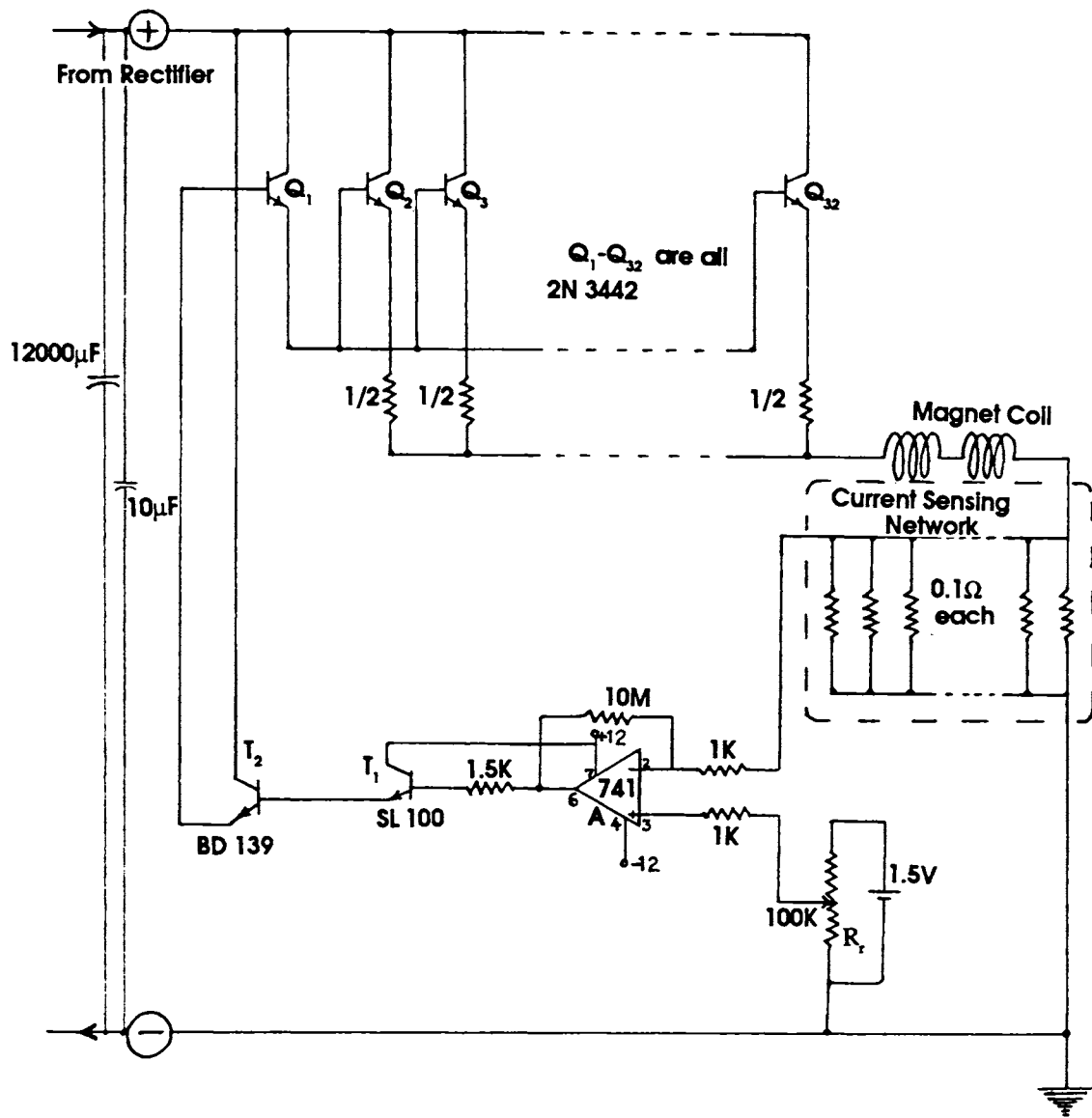
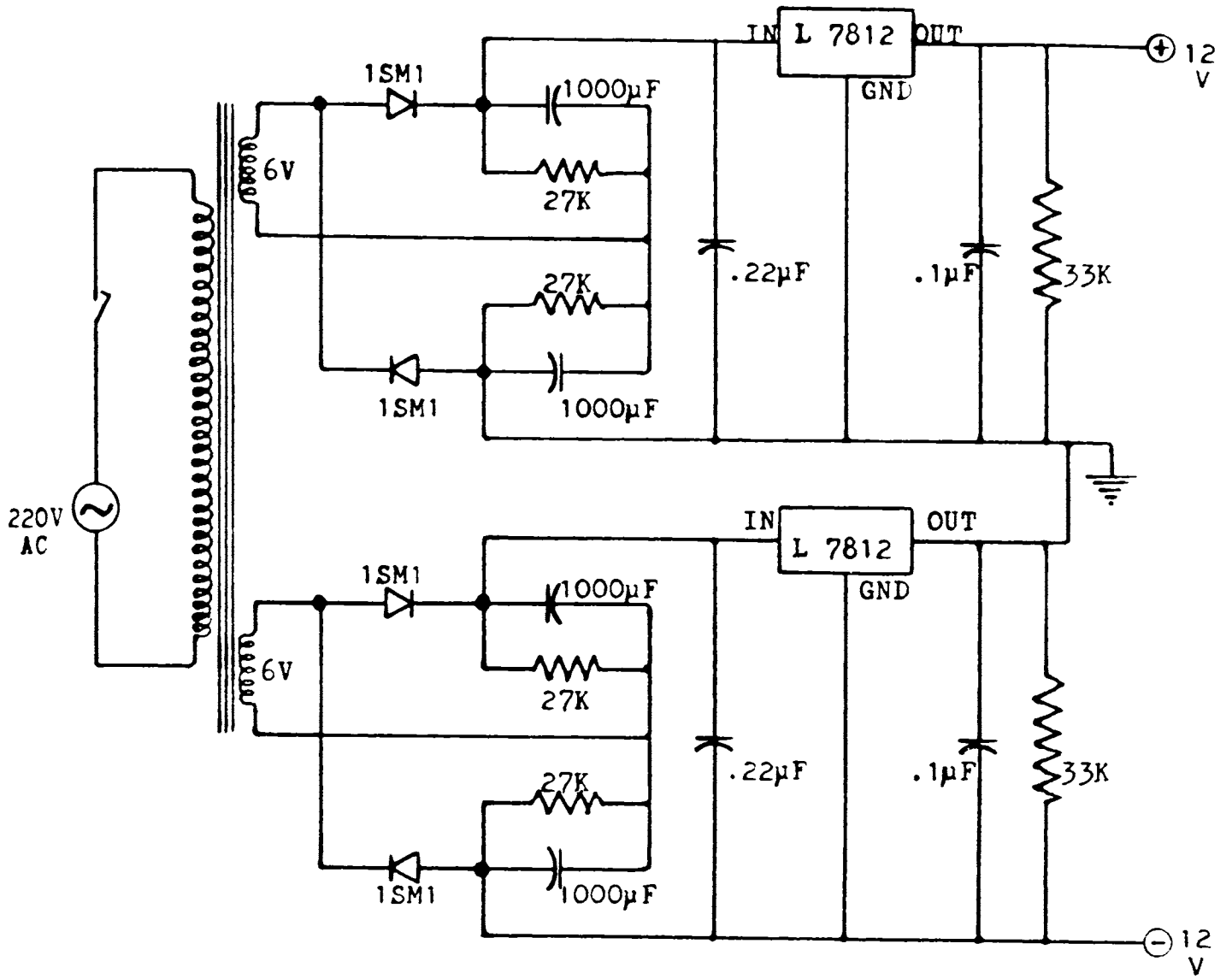**Fig. 4.2 : Schematic circuit of the stabilizing unit**

Fig. 4.3 : Schematic circuit of the + 12V and - 12V regulated power supplies for the op-amp.

4.4.4 : Operation and performance of the current stabilizer

Any drift in the magnet current will alter the sensing voltage in the same direction. This fluctuation in the sensing voltage gets compared with the reference voltage set by the potentiometer R_r. The amplified error signal produced by A then undergoes initial current boosting by T_1. The transistors T_2 and Q_1 functioning as a Darlington pair, which effect further current boosting, will alter the base currents of Q_2 - Q_{32} such that the initial tendency for current fluctuation is countered, thereby achieving current stabilization.

The current through the magnet coil can be varied from zero to maximum value by varying the reference voltage. Fine control of the current is achieved by using an additional ten turn helical potentiometer in R_r.

The stability of the magnetic field was tested visually by displaying the proton signal in water on an oscilloscope. A reasonably stable absorption pattern was obtained indicating good stability for the magnetic field. Subsequent recording of the signal on a chart recorder was found to give satisfactory results.

4.5 : An improved high current stabilizer

Though the current stabilizer described above has several advantages compared with earlier circuits and has been found to be operating satisfactorily, it is not free from certain drawbacks. The main limitation arises from the fact that for getting better performance from this stabilizer greater number of resistors will have to be employed in the network. This is so because for getting better current stability the reference voltage should have as high a value as possible, which in turn means that the sensed voltage should also be correspondingly higher. An increased sensing voltage will lead to greater power dissipation across the network and hence to remove this much power larger number of resistors will have to be used to form the network. Thus for achieving better results not only greater number of resistors will have to be used but also additional power will have to be wasted.

4.5.1 : A better current sensing method

To overcome the practical inconveniences involved in the previous method as well as to keep the power dissipation involved in the current sensing to a minimum it becomes necessary to search for a better current sensing method. Serious efforts in this direction have led to a far superior method which entirely eliminates the need of a seperate current sensing unit [16]. In this method the feedback signal is derived by detecting and adding together the fluctuations across the emitter resistance of each power transistor of the series element. Since this method keeps the power dissipation involved in the current sensing process to a minimum, It can be adapted with greater convenience for stabilizing much higher currents.

4.5.2. : Description of the improved current stabilizer circuit

The current stabilizing arrangement employing this innovative current sensing method is represented symbolically by the block diagram of Fig.4.4. The actual schematic circuit of the current stabilizer designed to regulate the 50A current, to be
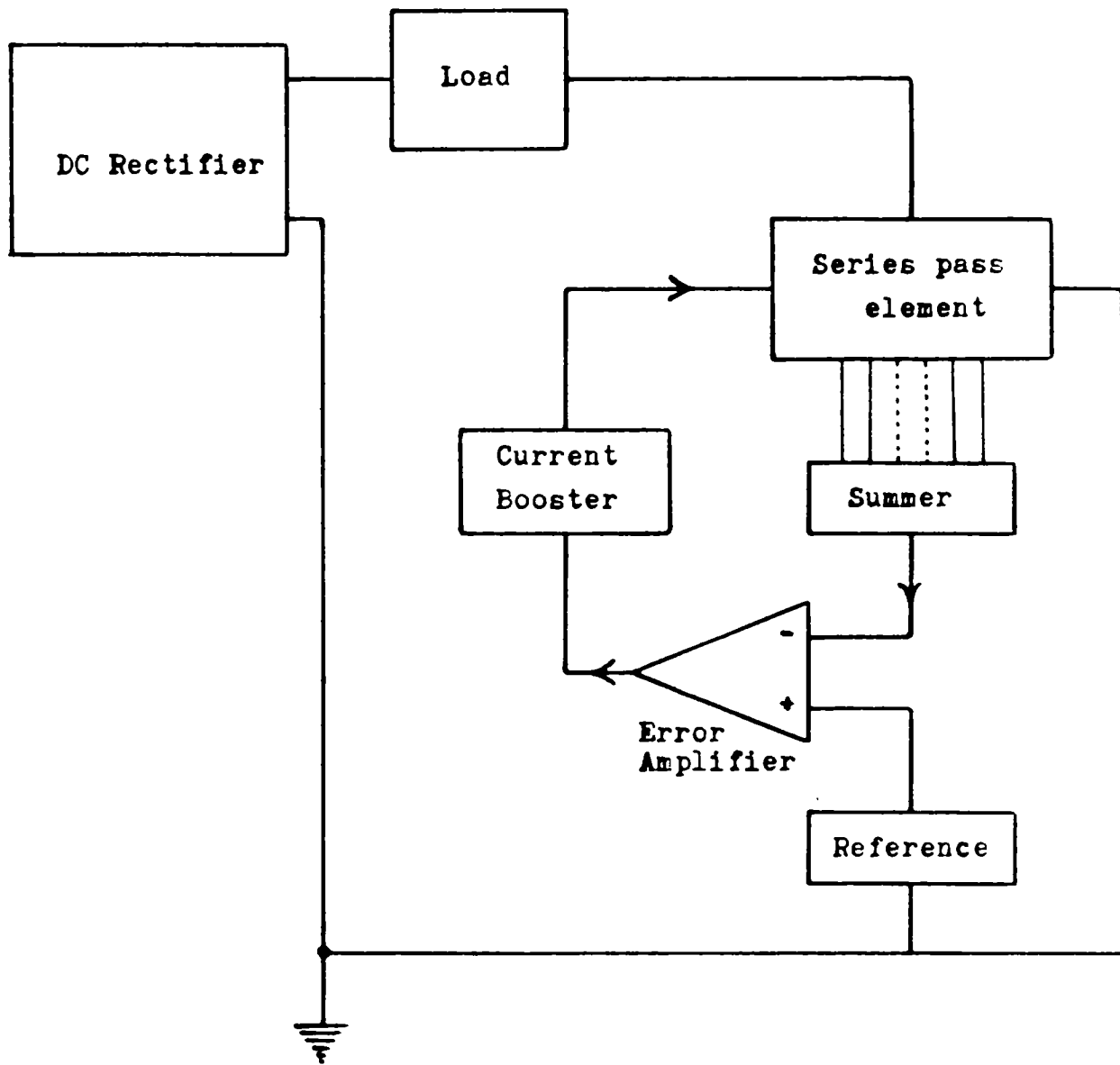
Fig. 4.4 : Block digram of the improved current stabilizer

supplied to the electromagnet, is as shown in Fig.4.5. Except for the current sensing part, the circuit is more or less identical to the previous stabilizing circuit shown in Fig. 4.2. The magnet coil has been shifted to collector side of the series element for achieving faster stabilising action. The LM 741 op-amp of the comparator of the earlier circuit has been replaced by the instrumentational op-amp LM 725, for getting better performance.

The 220Ω high precision resistor at each emitter lead of the power transistors of the series element serves to sense the current fluctuations. Since all the emitter points of Q_2 - Q_{32} are connected to the inverting input of op-amp A through 220Ω resistors, this set up will comprise the adding circuit. Thus the fractional current fluctuations sensed by each 220Ω resistor will get summed up to constitute the feedback signal.

4.5.3 : Operation and performance of the improved stabilizer

Any variation in the magnet current will cause a proportional change in the emitter current of the power transistors. As a result the cumulative feedback voltage will also get altered in the same direction. These fluctuations in the feedback signal gets compared with the reference voltage at the comparator, as in the previous case. The voltage amplified error signal, after undergoing adequate current boosting, will finally alter the base currents of Q_2 - Q_{32} such that the initial tendency for current deviation is countered, thereby achieving current regulation.

The degree of the magnetic field stability produced by the current stabilizer was checked visually, as before, by displaying the proton signal in water on an oscillo-scope. A stationary and well shaped absorption pattern was obtained indicating excellent stability for the magnetic field. Subsequent recording of the signal on a chart recorder has given very satisfactory results.

The high c irrent stabilizer circuit thus fabricated has proved to be a very useful part of the whole NMR set up. The circuit not only eliminates the need for a seperate current sensing unit but also keeps the power dissipation involved in the current sensing process to a minimum. Besides, the improved current sensing technique is far more convenient to implement than the earlier methods. The circuit offers greater advantage for stabilizing fields produced by high current electromagnets used for magnetic resonance studies. It is costwise competitive and does not employ critical components.

4.6 : A better reference voltage selector design

In conventional magnet current stabilizers [5,2,12] used for NMR experi-ments, the scanning of the magnetic field and the linear field sweep required for recording the signal are effected by means of the circuit providing reference voltage to the comparator circuit of the stabilizer. A typical reference voltage circuit, as shown in Fig.4.6 will be consisting of a reference cell E_b, a single turn potentiomenter P_1 for coarse control and a ten-turn helical potentiometer P_2 for fine control of current. The voltage E_r provided by P_2 forms the effective reference voltage, to be fed to the comparator-cum-error amplifier of the current stabilizer. It was thought to be a worthwhile effort to analyse this circuit to find the relative values and the typical setting up of the two controls P_1 and P_2 that will provide maximum resolution in the scanning of magnetic field.
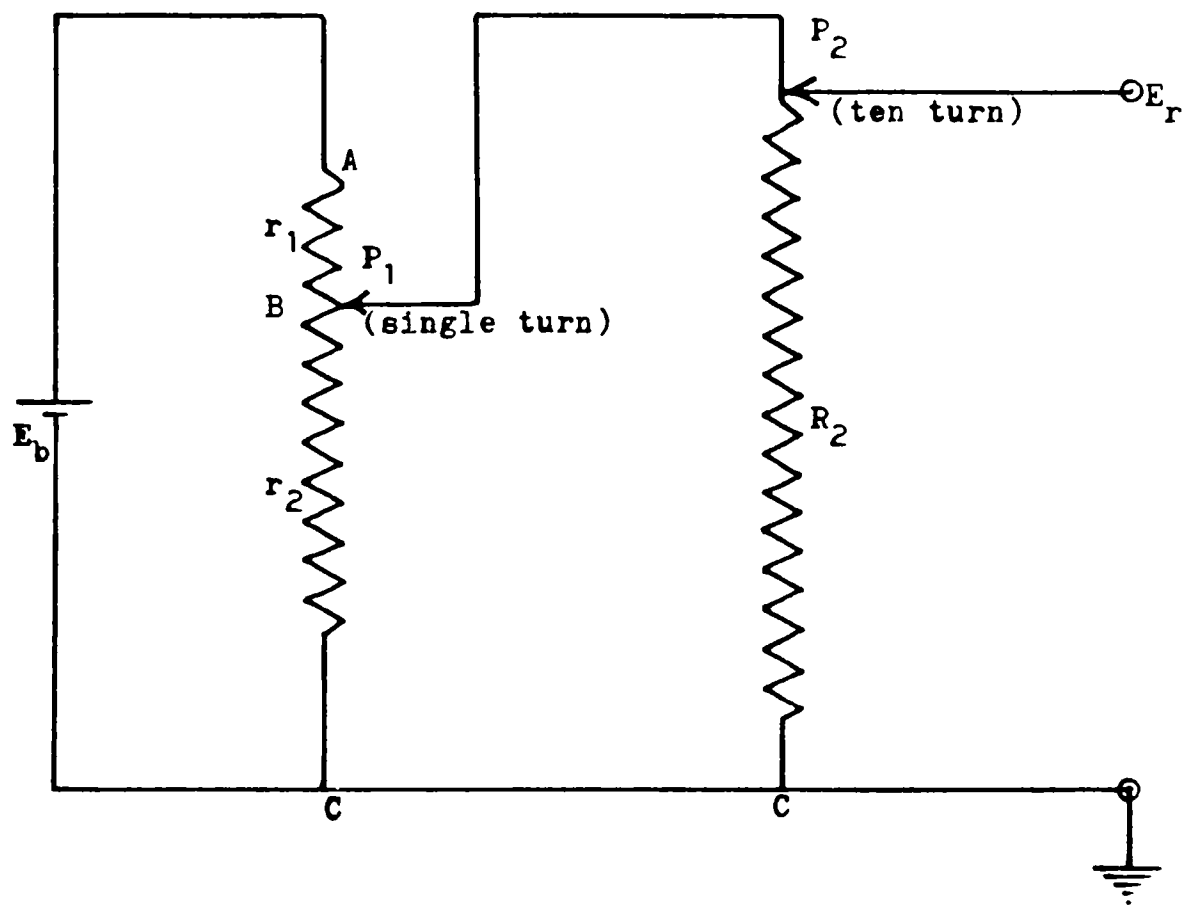
Fig. 4.5 : Schematic circuit of the improved high current stabilizer

Fig. 4.6 : Schematic circuit of a typical reference voltage selector circuit

4.6.1 : Analysis of the reference voltage selector circuit

Referring to Fig.4.6, let $R_1(=r_1+r_2)$ and R_2 be the resistance values of P_1 and P_2 respectively. For convenience, let us consider that P_2 has been so adjusted that the reference voltage E_r is developed over the entire R_2 value, a setting which provides the maximum fine scanning resolution. For a given value of E_b, R_1 and R_2 one can derive the expression for the value of r_2 required for a particular value of E_r, as follows.

Let the equivalent resistance of r_2 and R_2 in parallel, between points B & C be

$$R = r_2 R_2 / r_2 + R_2 - - - - - - - - (4.1)$$

We have $\quad E_r = [E_b / (r_1 + R)] \bullet R$

$$E_r \bullet r_1 = (E_b - E_r) R$$

$\therefore \quad r_1 = [(E_b - E_r)/E_r] \bullet R$

or $\quad (R_1 - r_2) = [(E_b - E_r)/E_r] \bullet [(r_2 R_2)/(r_2 + R_2)]$

i.e., $\quad -r_2^2 + r_2(R_1 - R_2) + R_1 R_2 = [(E_b - E_r)/E_r] \bullet r_2 R_2$

or $\quad r_2^2 - r_2[R_1 - (E_b/E_r)R_2] - R_1 R_2 = 0 - - - - - - - (4.2)$

Equation (4.2) is a quadratic one in r_2 ,whose only acceptable solution can be shown as

$$r_2 = (a + X^{1/2})/2 - - - - - - - (4.3), \text{ where}$$

$$X = a^2 + 4b - - - - - - - - - - - (4.4), \text{ with}$$

$$a = R_1 - (E_b/E_r)R_2 - - - - - - (4.5) \text{ and}$$

$$b = R_1 R_2 - - - - - - - - - - - - (4.6)$$

By giving typical values of R_1, R_2, E_b and E_r, the performance of the circuit can be understood. P_2 being a ten-turn helical potentiometer set at its maximum value, the resolution obtainable for fine scanning of magnetic field is independent of R_2 value; the maximum resolution being fixed, equal to $E_r/10$ per turn. However the extent of coarse scanning resolution does depend on the value of R_1.

Consider a typical case of a current stabilizer requiring a reference voltage of $E_r = 0.8V$ for a maximum current of 50A, like the one fabricated for the electromagnet in our NMR set up. Let R_2 be a ten-turn helical potentiometer and let E_b 1.5V. Then, using equations (4.3) to (4.6) we get that for $R_1 = 1K$, $r_2 \approx 0.55K$ while for $R_1 = 100K$, $r_2 = 92K$. This indicates that while $R_1 = 1K$ enables coarse scanning of E_r in the range of 0-0.8V by only 55% of a turn, $R_1 = 100K$ improves this to 92% of a turn. This means that a greater value for R_1 provides enhanced coarse scanning resolution. The significance of this conclusion can be realised by considering the situation when one has to work at much lower current. e.g., if the magnet current is to be 5A, then $R_1 = 1K$ potentiometer will necessitate a value of $r_2 \approx 0.05K$. This means that the coarse scanning in this case will have to be done within 5%

of a turn, which will be very inconvenient. A 100K potentiometer for R_1, in this case, can enhance the resolution to $\approx 17\%$ of a turn.

4.6.2 : An improved reference voltge selector design

In the case of the conventional reference voltage selector circuit of Fig.4.6 employiong a ten-turn helipot for fine control, the fine scanning resolution is restricted to $E_r/10$ per turn. Besides, it is susceptible to electrical noise produced by the movement of the slider contact on the precision potentiometer. Also, after some continuous usage, a wirewound helipot may develop 'contact problem' whereby the center tap contact may break occassionally. This may cause abrupt change in the reference voltage and hence in the circuit current, which may lead to damages in the stabilizer circuit. To overcome these drawbacks an improved reference voltage selector circuit has been developed, utilising single turn carbon potentiometers. This arrangement will enable the scanning resolution to be enhanced considerably while at the same time keeping the electrical noise and contact problem to a minimum.

In this circuit, as shown in Fig.4.7, the single ten-turn potentiometer of conventional circuit (Fig.4.6) is replaced by a 1K single turn potentiometer P_2 in series with a resistance devider network. By varying the position of switch `S', different scanning resolution can be selected.

In the particular circuit shown in Fig.4.7 the position `5' enable a scanning resolution $\sim E_r/20$ per turn. In the current stabilizer system used in our NMR work, this much resolution means that, at 50A over one complete turn of the potentiometer P_2, a relatively narrow magnetic field range of the order of 575 gauss can be carefully scanned. On the other hand, if the circuit of Fig.4.6 were used, by one turn of P_2 the field range would have been broadened to a value ~ 1150 gauss - thus lowering the scanning resolution. If the position `1' of the resistance devider network is selected the potentiometer P_2 will act as a medium-coarse scanning control, enabling greater convenience.

4.6.3 : Operation and performance of the circuit

The improved resolution of the circuit enables the careful and accurate searching of weak NMR signals on an oscilloscope. For this an appropriate resolution range is first selected by `S'. Then the coarse control potentiometer P_1 is adjusted for the required approximate current value. P_2 is then turned slowly till the signal appears on the oscilloscope screen.

If good quality carbon potentiometers are used as P_2 and P_1, the electrical noise that occur in precision potentiometers due to the movement of the slider can be avoided almost completely. These carbon potentiometers can also be used for extended period without being affected by the `contact problem' of wirewound helipots. The scanning resolution of the above circuit can be enhanced as desired by raising the value of resistors in the devider network.

4.6.4 : Conclusion

The theoretical analysis of conventional reference voltage selector circuit has led to the design of an improved, but simple, circuit that provides enhanced resolution for
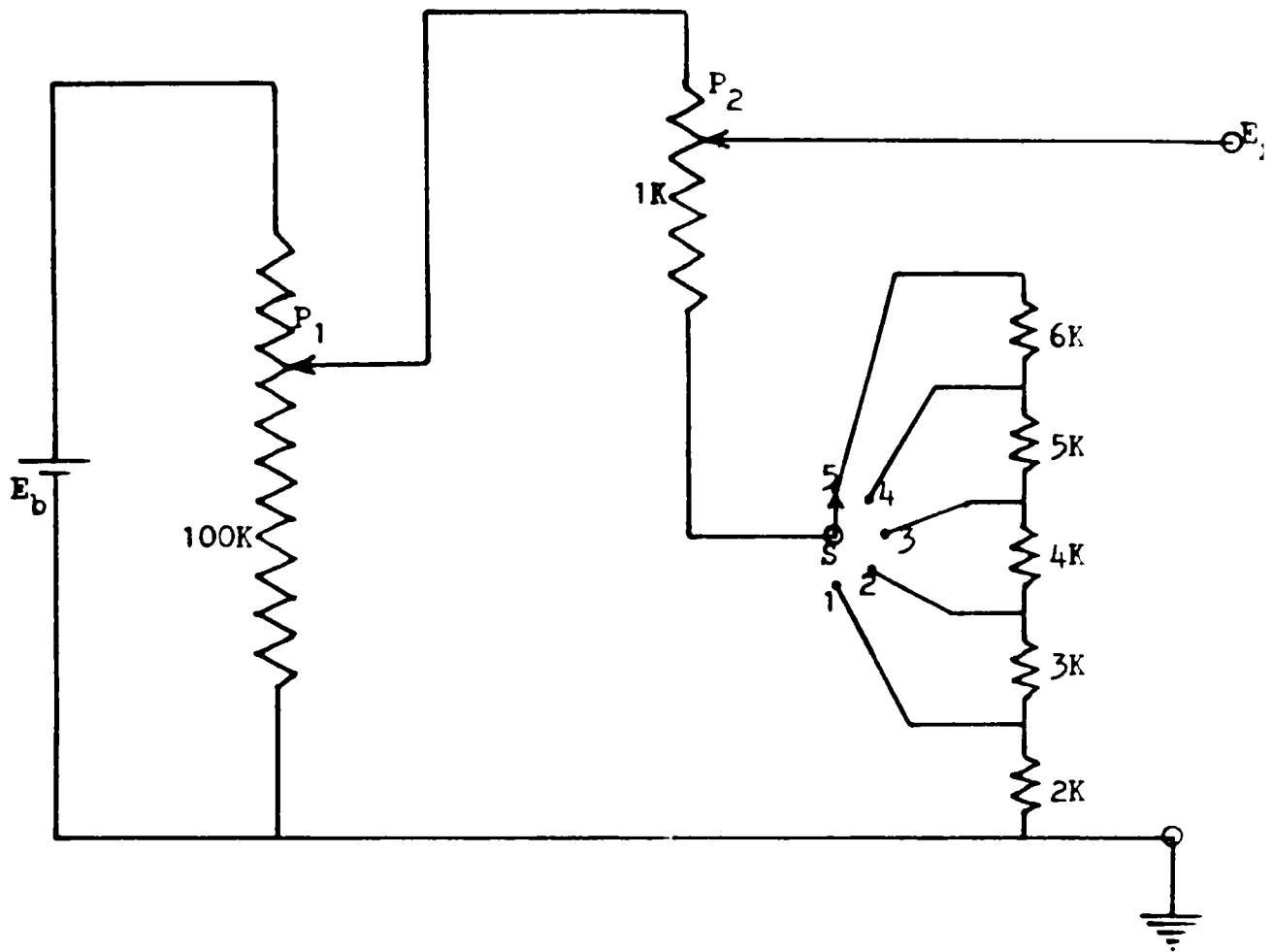
Fig. 4.7 : Schematic circuit of the improved reference voltage selector

scanning the magnetic field. This design is free from some of the inherent drawbacks of conventional multiturn helical potentiometer circuit. The circuit will enable the searching of weak NMR signals with greater accuracy and ease of operation.

REFERENCES

[1]   E.R. Andrew; Nuclear Magnetic Resonance (Great Britain; Cambridge University Press: 1969)

[2]   S.Ganapathy and K. Ramani; J.Instn. Electronics & Telecom. Engrs. (India); 23 (1977) 152

[3]   B.P. Straughan and S. Walker; Spectroscopy-volume I (New York; John Wiley: 1976)

[4]   M.L.Martin, J.-J.Delpuech and G.J. Martin; Practical NMR Spectroscopy (Great Britain; Heyden: 1980)

[5]   J.B. Cook, R.E.George and E.H. Grant; J. Sci. Instrum.; 41 (1964) 390

[6]   H.S.Somers, P.R. Weiss and W. Halpern; Rev. Sci. Instrum.; 22 (1951) 612

[7]   R. Bailey and E.C.Fellows; J. Brit. I.R.E.; 19 (1959) 309

[8]   R.J. Abraham, D.W.Ovenall and D.H. Whiffen; J.Sci. Instrum.; 34(1957) 269

[9]   R.L.Garwin; Rev. Sci. Instrum.; 29 (1958) 223

[10] S.D.Johnson and J.R. Singer; Ibid; 29 (1958) 1026

[11] K.C. Borg and F.J. Milford; Ibid; 31 (1960) 321

[12] J.Sathanapathi, A.K. Ghoshal , D.K. Dey, A.K. Pal and S.N.Battacharya; J. Phys. E; 10 (1977) 221

[13] K.J. Wilson and C.P.G Vallabhan; Proce. Solid State Phys. symp.; 28 C(1985) 327

[14] W. Waner; Troubleshooting Solid-State Circuits and Systems (USA; Reston: 1979)

[15] A.J.Diefenderfer; Principles of electronic instrumentation (Japan; Holt-Saunders: 1981)

[16] K.J.Wilson, C. Raghavan and C.P.G. Vallabhan; Int. J. Electrn.; 63 (1987) 105

Chapter V

AN INNOVATIVE MAGNETIC FIELD SWEEP UNIT

Abstract

The chapter begins with a consideration of the basic requirements for the magnetic field sweep used in NMR experiments. The earlier field sweep circuits and their drawbacks are briefly mentioned. Following this, an electronic magnetic field sweep circuit, that functions as a seperate unit, is described in detail. The design and fabrication of an improved electronic field sweep system which generates almost perfectly linear field sweeps is then discussed. At the end of the chapter the performance of the improved field sweep unit and its various advantages over the earlier systems are highlighted.

5.1 : Basic requirements of the magnetic field sweep

For the recording of the NMR signals the magnetic field has to be swept linearly at a slow but well-defined rate over a small range which is usually a few times the width of the resonance line under investigation. For getting accurate and faithful recordings the field sweep should be perfectly linear over the time interval required to record the whole signal. A non-linear field sweep will pose several problems, as a result of which the recorded signal will no longer be a true reproduction of the actual signal shape. Beside the second moments calculated under this situation will hardly be accurate enough to be useful.

An appropriate sweep rate has to be selected that permits undistorted recording of the NMR signal, within a convenient duration of time. At very rapid sweep rates the nuclear magnetic moment will not be able to follow the sweep field, which then will lead to considerable distortion in the lineshape. For recording single scan spectra the best procedure is to use the lowest possible sweep rate [1].

5.2 : Earlier field sweep methods

The magnetic field sweep is conventionally effected by varying the reference voltage of the magnet current stabilizer within a prescribed range and at a desired rate using mechanical arrangements [2, 3, 4, 5, 6]. A magnetic current stabilizer which incorporates this field sweep arrangement is symbolically represented by the block diagram of Fig.5.1. In actual practice a small d.c.voltage, that can be scanned in the desired manner, is combined with the actual reference voltage and the resultant voltage is given as the effective reference signal to the comparator circuit of the current stabilizer. A typical circuit used to effect this is shown in the schematic diagram of Fig.5.2. The voltage selected by the potentiometer P_1 forms the main reference voltage. (P_1) also permits manual scanning of the magnetic field). The battery B may be a low value standard cell. 'R' essentially stands for a resistance selector circuit. P_2 is a wirewound precision potentiometer, the centre spindle of which is driven by a synchronous motor and reduction gears. By changing the gear ratio the sweep rate can be varied, while a suitably selected R value will provide the required field sweep range [4,5]
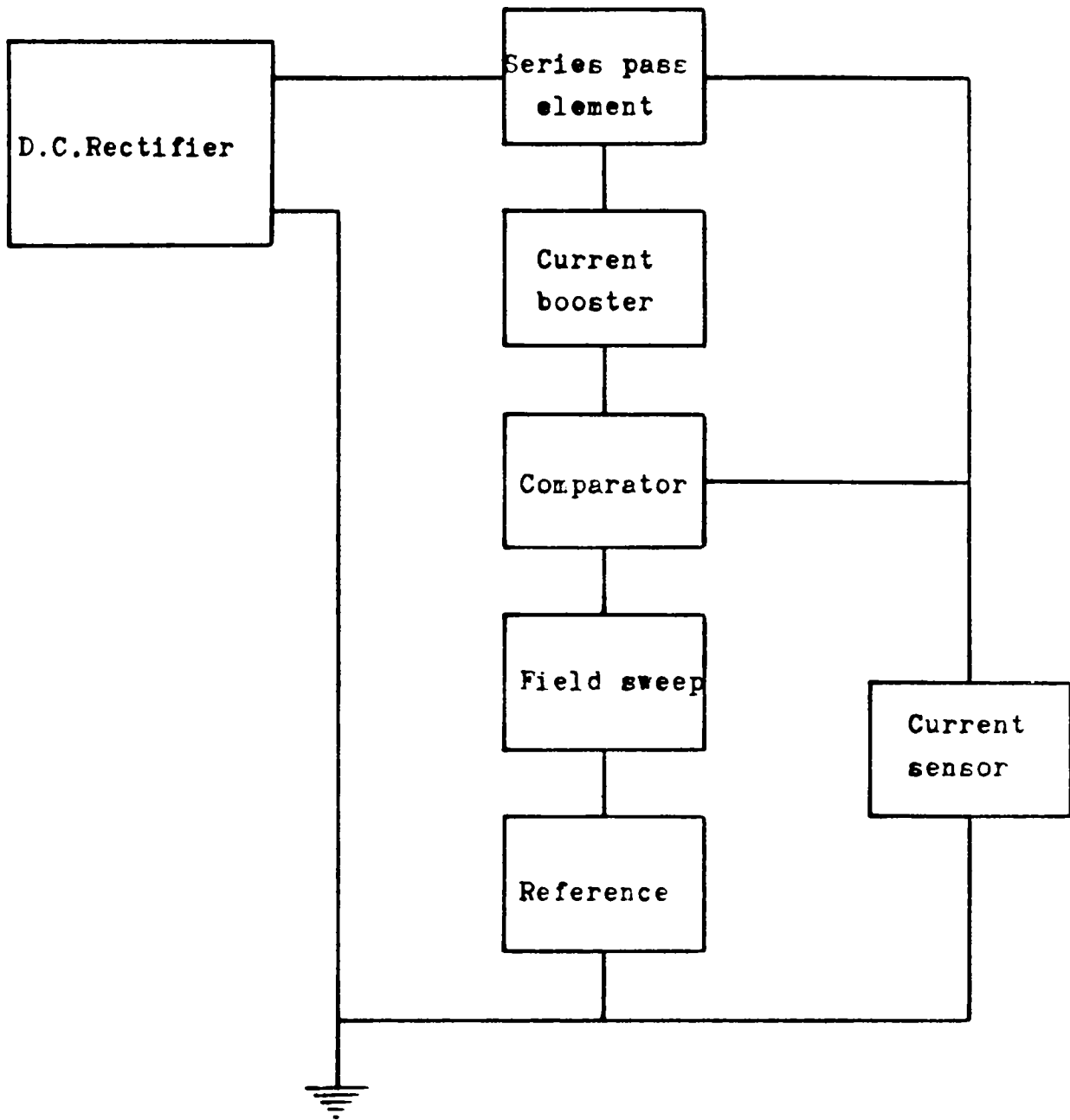
Fig. 5.1 : Block diagram of a magnetic current stabilizer incorporating field sweep
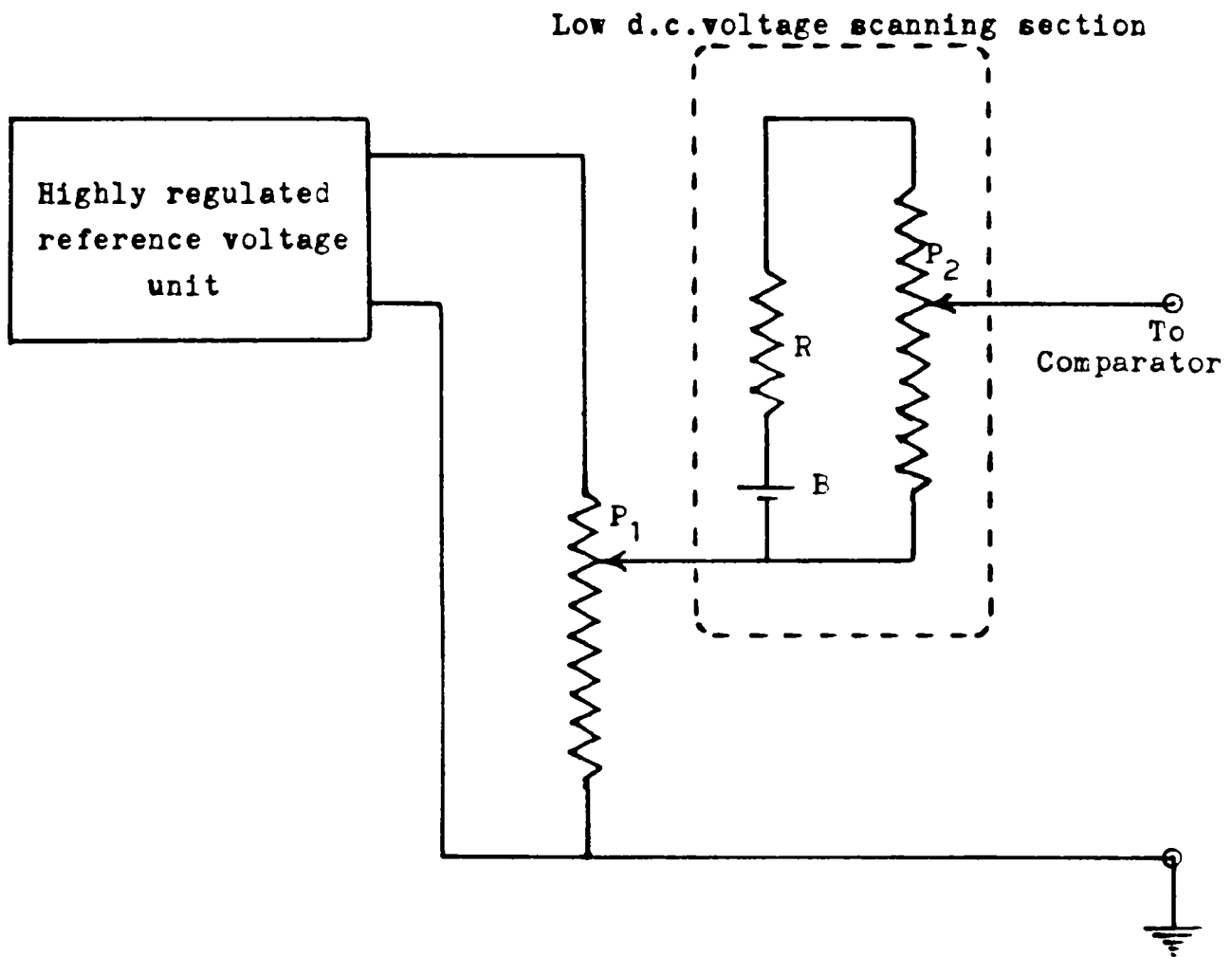
Fig. 5.2 : Schematic circuit of a reference voltage sweep set up

However the mechanical field sweep system possess several inherent draw-backs including electrical noise produced by the movement of the slider on the potentiometer, the eventual degeneration of the potentiometer through wear, etc.. With prolonged use these potentiometers will become excessively noisy and the sweep will no longer be steady. The overall flexibility of the system is very poor, as any desired change in sweep rate is very difficult to implement.

5.3 : An electronic magnetic field sweep unit

The mechanical field sweep systems can be replaced with more convenient electronically controlled field sweeps which can be made highly flexible as well as reliable. In one system [7] an op-amp integrator circuit generates a sweep voltage which is used to vary the reference voltage of the control unit of the magnet current stabilizer to effect the field sweep. But in this case there exists a possibility for interaction between the sweep circuit and the current control unit which may lead to unwanted fluctuation and noise.

With a view to eliminate the inherent limitations of mechanical field sweep systems and also to avoid any unwanted interaction between the sweep circuit and the current control unit a new electronic magnetic field sweep unit has been designed and fabricated [8]. This system functions as an entirely seperate unit without any interaction with the magnet's main current control unit. At the same time, due to the sufficient amount of d.c.amplification which is provided in this circuit, considerable output current can be derived to cover the required field sweep range.

5.3.1 : Description of the field sweep unit

The field sweep unit designed here is symbolically represented by the block diagram of Fig. 5.3. Essentially it consists of three main sections: (i) a generator of linear sweep voltage, (ii) d.c.amplifier stages for enhancing the sweep signal to the required output power level and (iii) the magnetic field sweep generator coils. Besides these is a regulated power suply section for energizing the different sub-assemblies. The actual circuit of the field sweep unit is shown in Fig.5.4.

(i) Sweep voltage generator:- The sweep voltage generator is basically an op-amp integrator circuit with provision to choose sweep speeds as required. The integrator output is given by the relation,

$$V_0 = -(1/RC) \int V_i dt.$$

If the input voltage V_i is constant the op-amp will start integrating the input voltage with a time constant (RC) till the voltage reaches a saturation value $V_{0\ max}$ determined by the supply voltage (and the limiting values of the op-amp characteristics) in a time T_S given by

$$T_S = (V_0 max/V_i) (RC)$$

Evidently the sweep speed can be varied by changing the value of V_i or (RC).

In the present circuit an LM 741 op-amp functions as the integrator A_1. The time constant is chosen to be 10 seconds. Sweep speed is selected by changing V_i by means

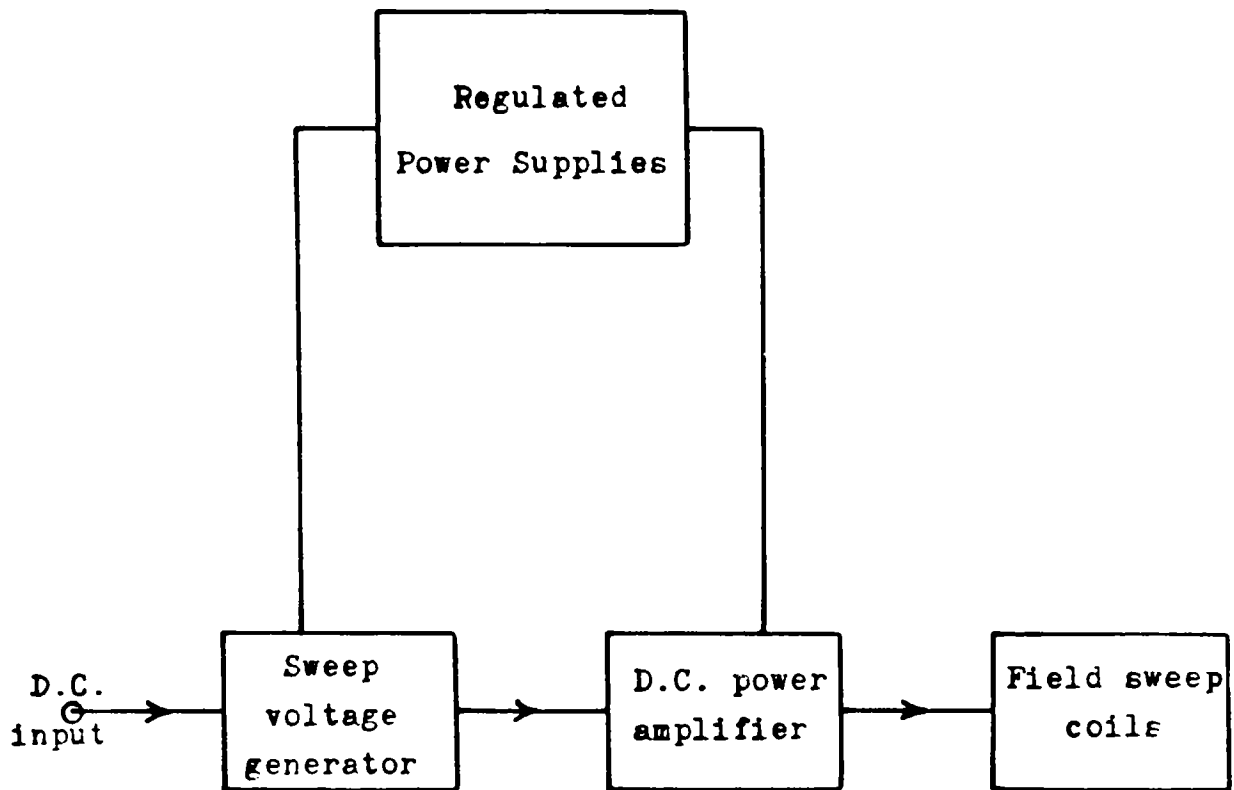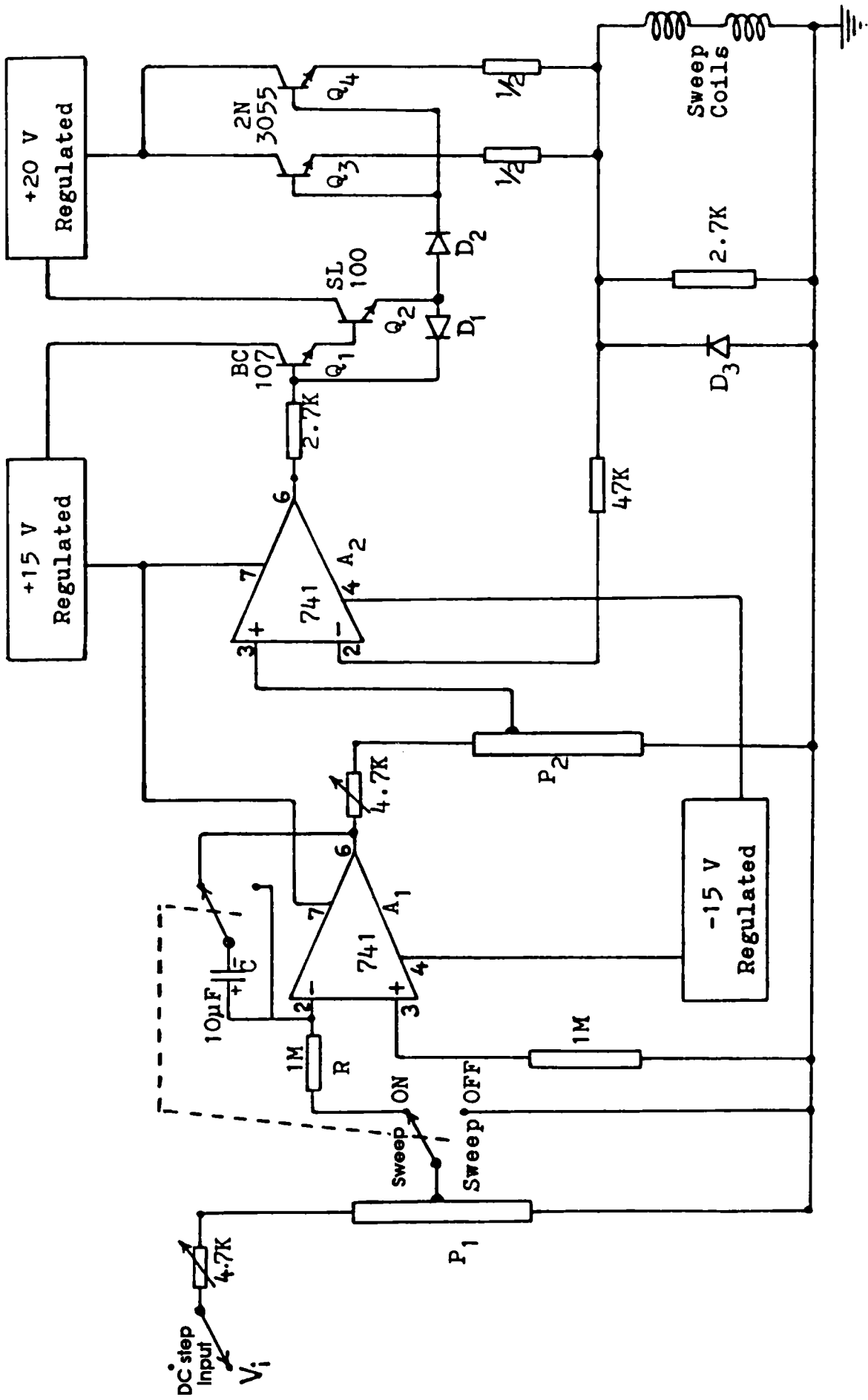Fig. 5.3 : Block diagram of the field sweep unit

Fig. 5.4 : Schematic circuit of the electronic field sweep unit

of the potential devider P_1. Sweep speeds can be varied in steps by a factor of four each from 0.5 to 128 minutes. The potential devider P_2 is so chosen that after d.c. amplification the final output when applied to the sweep coils can give magnetic field sweep variations by a factor of two each in steps from 5 to 80 gauss.

The 1MΩ resistor connected between the non-inverting input of A_1 and the circuit ground helps to reduce the effect of input bias current in the integrator. For greater advantage the op-amp A_1 should be one having high-gain, low-offset voltage and low-bias current. Chopper-stabilized amplifiers will be an ideal choice, especially because of their superior long-term d.c.stability.

The 10μF integrator capacitor should be one having very low leakage, like a polystyrene or tantalum capacitor. The 1MΩ integrating resistor as well as resistors in the output and sweep input attenuators should possess very good stability.

(ii) D C amplifying stages :- The d c amplifying section consists of an op-amp buffer followed by three stages of current boosters. The op-amp A_2 provides the necessary stability to the sweep signal before being subjected to current boosting by the Darlington pair consisting of the transistors Q_1 (BC 107) and Q_2 (SL 100). The final power amplification is effected by the power transistors Q_3 and Q_4 (2N 3055s).

A diode D_1, connected between the base of Q_1 and emitter of Q_2, serves to stabilize the current through Q_2 and thus preventing it being overdriven. At the same time D_1 keeps the base of Q_1 and emitter of Q_2 well isolated. The diode helps to prevent any positive feedback to Q_2 from the load side.

The highly regulated +15V and -15V supply voltage for the op-amps A_1 and A_2 are derived by employing μA 723 IC regulators in the high voltage regulator configuration, as shown in Fig.5.5. The μA 723 voltage regulator was chosen due to its high ripple rejection and low temperature drift [9]. The +15V regulated supply also powers the transistor Q_1. For energizing the power transistors Q_3 and Q_4 a +20V regulator capable of supplying as much as 2A current was required. The series voltage regulation principle was adopted in the design and the fabrication of this regulator unit, which is shown in Fig. 5.6. The same circuit serves to meet the power requirements of the transistor Q_2.

(iii) Sweep generator coils:-The sweep generator coils consist of two circular coils wound over aluminium frames that fit closely onto the magnet polepieces. On each coil is wound some 200 turns of 24 s.w.g. copper wire. The two coils are then connected together such that the field due to them is in conjunction. This coil system will produce a magnetic field ~ 80 gauss when a current ~ 0.6A passes through them.

The diode D_3 across the sweep coils is connected to bypass any voltage transients at the load and thus to protect the power transistors Q_3 and Q4. The 2.7KΩ resistor across the coils provide stabilizing feedback voltage to A_2, while the 47KΩ resistor limits the feedback current.

5.3.2 : Operation and performance of the field sweep unit

Initially the working of the integrator sweep circuit alone was checked. The sweep voltage was recorded on a chart recorder for the different sweep speed ranges. The
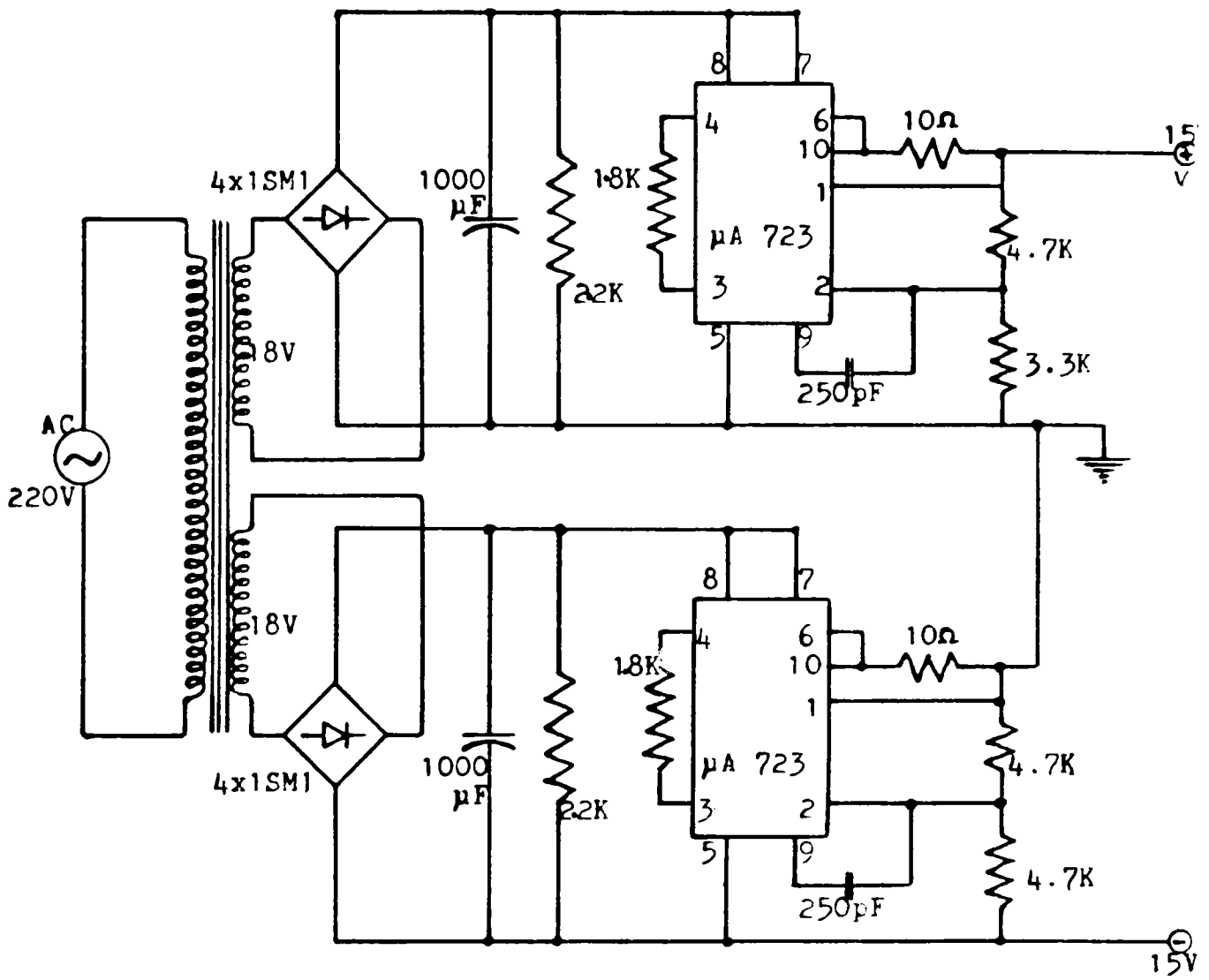
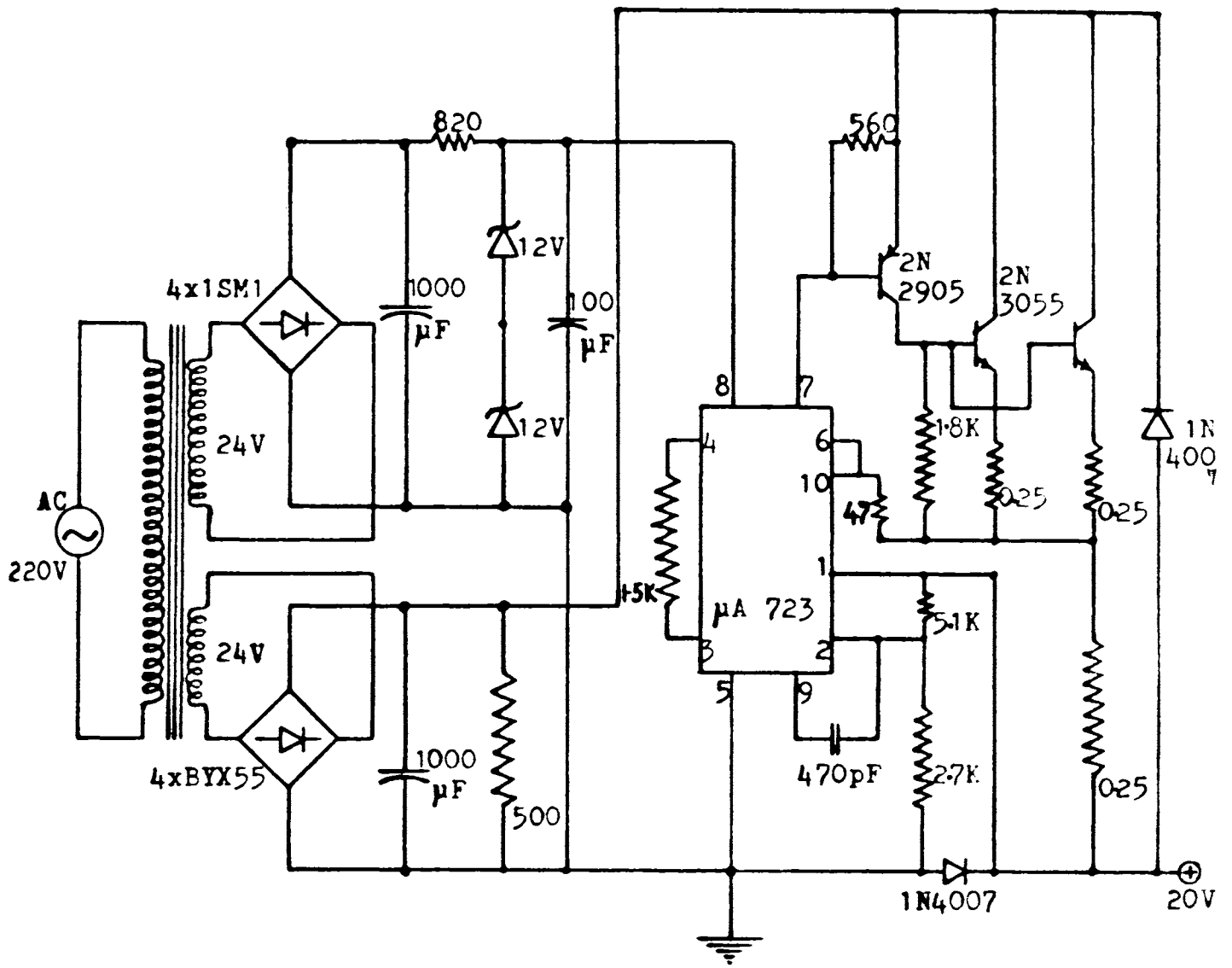Fig. 5.5 : Circuit diagram of the +15V and -15 regulated power supplies

Fig. 5.6 : Circuit diagrams of the +20V regulated high current power supply

recordings showed that the output voltage is nearly linear for the fast duration sweeps, while the long duration sweeps were observed to exhibit slight non-linearity.

The integrator was then connected to the d.c. amplifying stages and the sweep coils to constitute the complete field sweep unit. The sweeping of the magnetic field was also tested, using a Hall probe, and was seen to emulate the sweep voltage recordings approximately. The performance of the complete sweep unit was then tested by recording the proton signal in $Fe(NO_3)_3$ solution. The recording of the signal was fairly satisfactory.

5.4 : An improved electronic linear sweep circuit

As mentioned above the sweeps generated by the field sweep unit of Fig. 5.4 are not perfectly linear. Though the 1/2 min and 2 min sweeps were observed to be nearly linear the long duration sweeps were found to exhibit non-linearity that increases with increasing sweep time. Fig. 5.7 shows a tracing of the 8min field sweep, from which the non-linearity present is clearly evident.

The non - linearity of the above op-amp integrator sweep was understood to be due to a number of well-known factors [10], the most important of which being the abscence of a constant current charging of the condenser in the integrator circuit. It has been found that it is practically impossible to overcome all these factors to get perfectly linear sweeps. Though some circuits claiming better sweep linearity have been proposed recently (e.g.[11]), most of them employ rather complex circuitry with associated difficulties for implementation. This situation has prompted us to design a new circuit that will not only be very convenient to implement but at the same time give almost perfectly linear field sweeps.

The newly designed circuit [12] is an improved version of conventional IC bootstrap ramp generator, in which an appropriately selected op-amp gain is utilised to suppress the various sources of non-linearity.

5.4.1 : Bootstrap sweep generator circuits

The bootstrapping technique is based on the principle that the charging current of the capacitor in a ramp generator can be maintained constant by inserting a source of compensating e.m.f. in series with the charging capacitor. The compensating e.m.f. is supplied by an amplifier whose output voltage is an exact copy of the voltage across the charging capacitor. The circuit utilising this principle is referred to as "bootstrap sweep" circuit since its output voltage is lifted, as it were, by its own bootstraps.

Fig.5.8 is a symbolic representation of bootstrapping circuit. Here a fictitious variable source v_0 is added in series with the charging voltage V. In the schematic diagram of the circuit shown in Fig.5.9 the amplifier of voltage gain A generates the variable voltage v_0. Initially v_0 is zero and when the switch `S' (Fig. 5.9) is open the voltage across the capacitor starts rising towards V. As soon as the capacitor's voltage starts to rise, then v_0 is no longer zero; now the total voltage across the RC combination is $V+v_0$ and the capacitor aims towards this modified target value. Since the target voltage is constantly increasing, we are always operating in the initial portion of the exponential rise, which is linear. As a result a linear sweep voltage, which emulates the constant current charging of the capacitor, is obtained at the output of the amplifier.
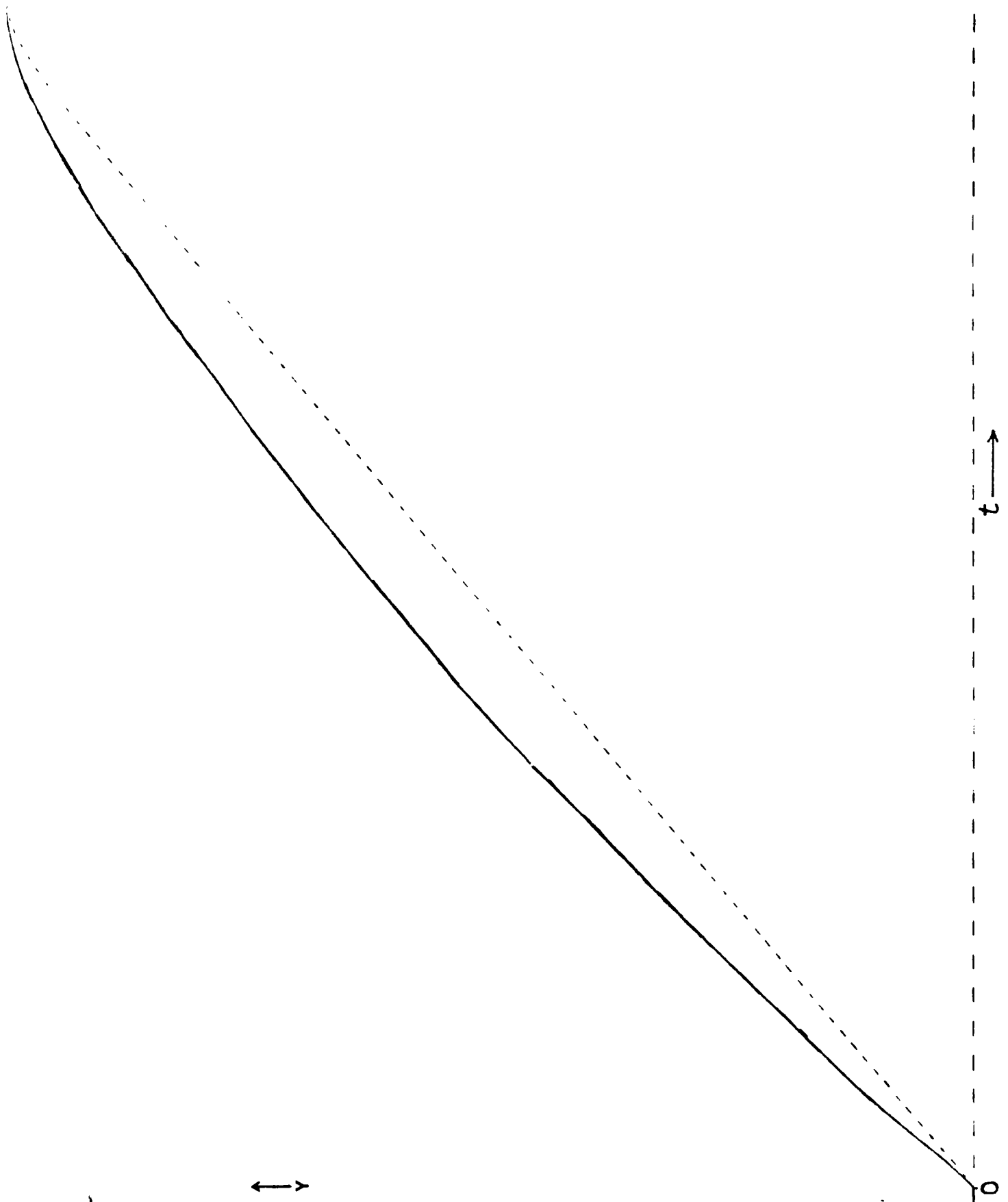
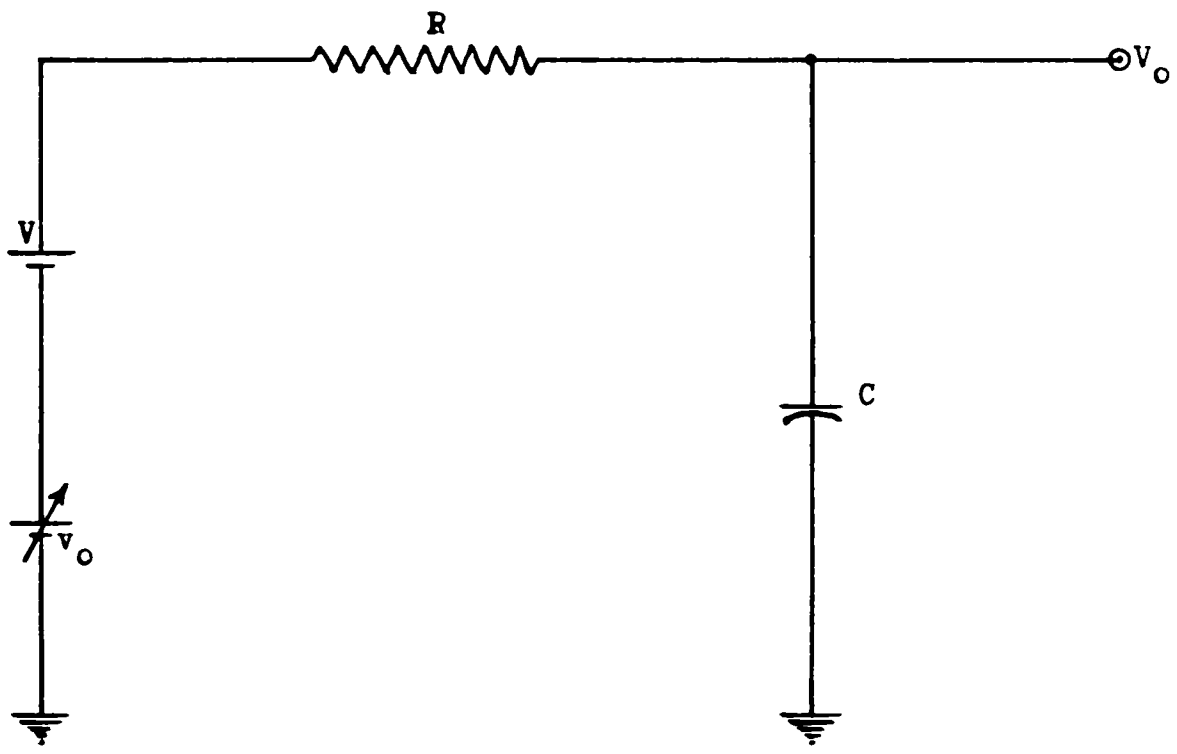Fig. 5.7 : Tracing of the integrator sweep voltage recording corresponding to 8 min (chart speed~3cm/min)

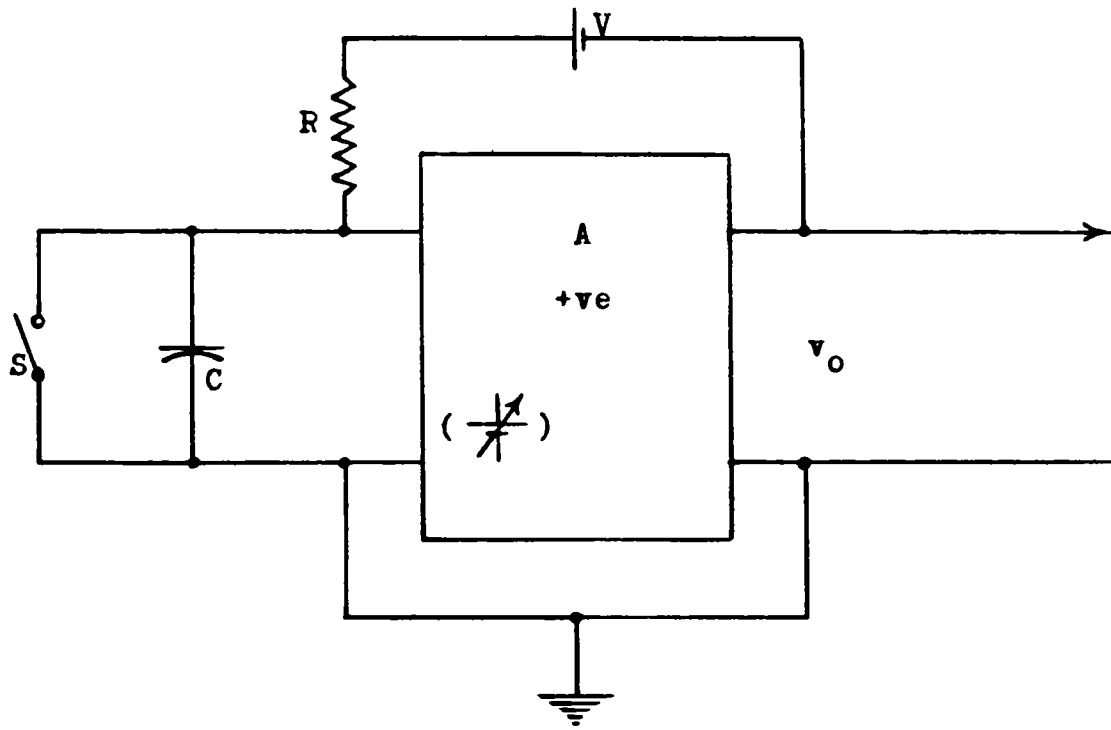Fig. 5.8 : Symbolic representation of a bootstrapping circuit

Fig. 5.9 : Schematic diagram of a bootstrapping circuit

It has been shown [13] that

(i) the sweep speed at the output of the amplifier $\approx AV/RC$ and

(ii) the slope error of the circuit = V_s/V $(1-A+R/R_i)$ where V_s is the sweep amplitude and R_i is the input impedance of the amplifier.

Fig. 5.10 shows a typical bootstrap ramp generator circuit employing an op-amp A as a voltage follower [9]. Here the high value capacitor C_1 acts as the bootstrapping capacitor, which together with the diode D, serves to establish a linearly increasing charging voltage for the RC combination. At the output of the op-amp a linear sweep voltage is generated.

5.4.2 : A modified IC bootstrap ramp generator

It has been observed that the conventional bootstrap sweep circuit incorporating unity gain voltage follower (Fig.5.10) cannot maintain good sweep linearity for different sweep durations. An analysis of the typical bootstrap ramp circuit, as given below, shows that a modified IC bootstrap ramp generator can provide a very much improved sweep linearity.

The slope error of a bootstrap sweep is known to be proportional to $(1-A+R/R_i)$, A being the amplifier gain, R_i the input impedance of the amplifier and R the charging resistance [13]. This indicates that if a unity gain voltage follower employing a commonly available op-amp is adopted as a bootstrap long-duration ramp generator, then R/R_i cannot be kept small enough to minimise the slope error. However, if FET input op-amps are used, then in principle one should get perfectly linear sweeps, since then $R/Ri=0$. Though this is true to some extent, in practice it has been observed that such perfectly linear sweeps are never generated in the case of circuits employing FET input op-amps like CA 3140 or OPA 121 wtith unity gain. The reason evidently is due to the non-ideal performance c : the remaining components such as charging capacitor, bootstrapping capacitor etc.which contribute to the slope error. The slope error of the bootstrap ramp circuit can then be taken as proportional to $(1-A+(R/R_i)+k)$, where k stands for the contribution to the slope error by components other than the op-amp. Thus one finds that even an FET input op-amp under unity gain condition cannot generate perfectly linear sweeps. If, instead, the op-amp gain is chosen to be greater than unity, as $A' = 1+(R/R_i)+k$, we see that the slope error will reduce to zero thus eliminating any non-linearity. This was indeed observed by us and we have seen that by carefully setting the op-amp gain the utmost in sweep linearity can be obtained for the desired sweep durations. It appears that an op-amp gain greater that unity serves the dual purpose of keeping the sweep time much less than the RC time constant as well as providing the excess gain required to stretch out the non-linearity of a unity gain bootstrap sweep. Both these factors help to obtain excellent sweep linearity.

5.4.3 : Description of the field sweep unit

The field sweep unit incorporating this modified bootstrap circuit is symbolically represented by the block diagram of Fig. 5.11. As in the earlier field sweep unit, the set up essentially consists of three main sections : (i) a generator of linear sweep voltage, (ii) d.c. amplifier stages for enhancing the sweep signal to the required output power level and (iii) the magnetic field sweep generator coils. The sections (ii) and (iii) are the same ones that were used in the earlier field sweep system of Fig.5.4, while for the sweep generator section the modified IC bootstrap configuration is used. The actual circuit of the field sweep unit thus fabricated is shown in Fig. 5.12.
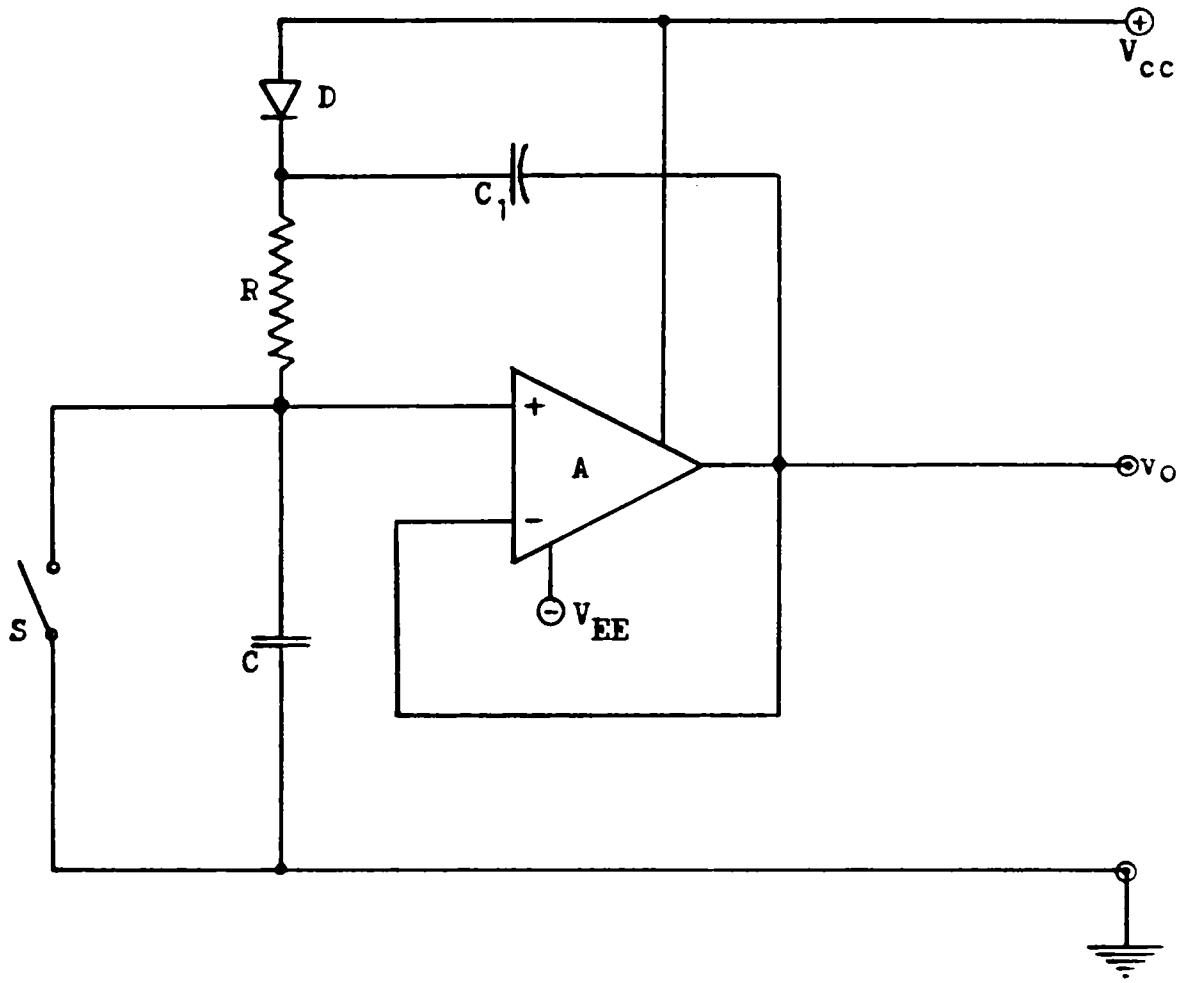
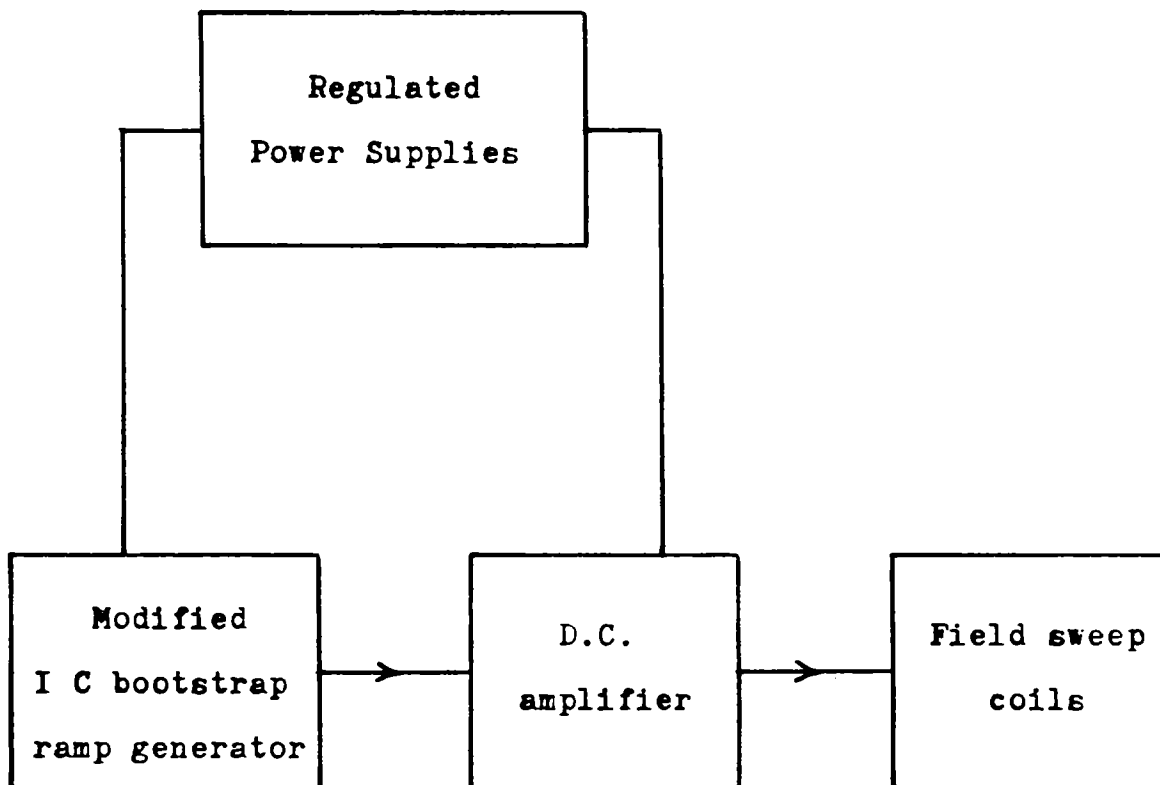Fig. 5.10 : Schematic circuit of a typical bootstrap ramp generator

```
┌─────────────────────┐
│     Regulated       │
│   Power Supplies    │
└─────────────────────┘


┌──────────────┐      ┌──────────────┐      ┌──────────────┐
│  Modified    │      │    D.C.      │      │  Field sweep │
│ I C bootstrap│ ──▶  │  amplifier   │ ──▶  │    coils     │
│ramp generator│      │              │      │              │
└──────────────┘      └──────────────┘      └──────────────┘
```

Fig. 5.11 : Block diagram of the improved field sweep unit
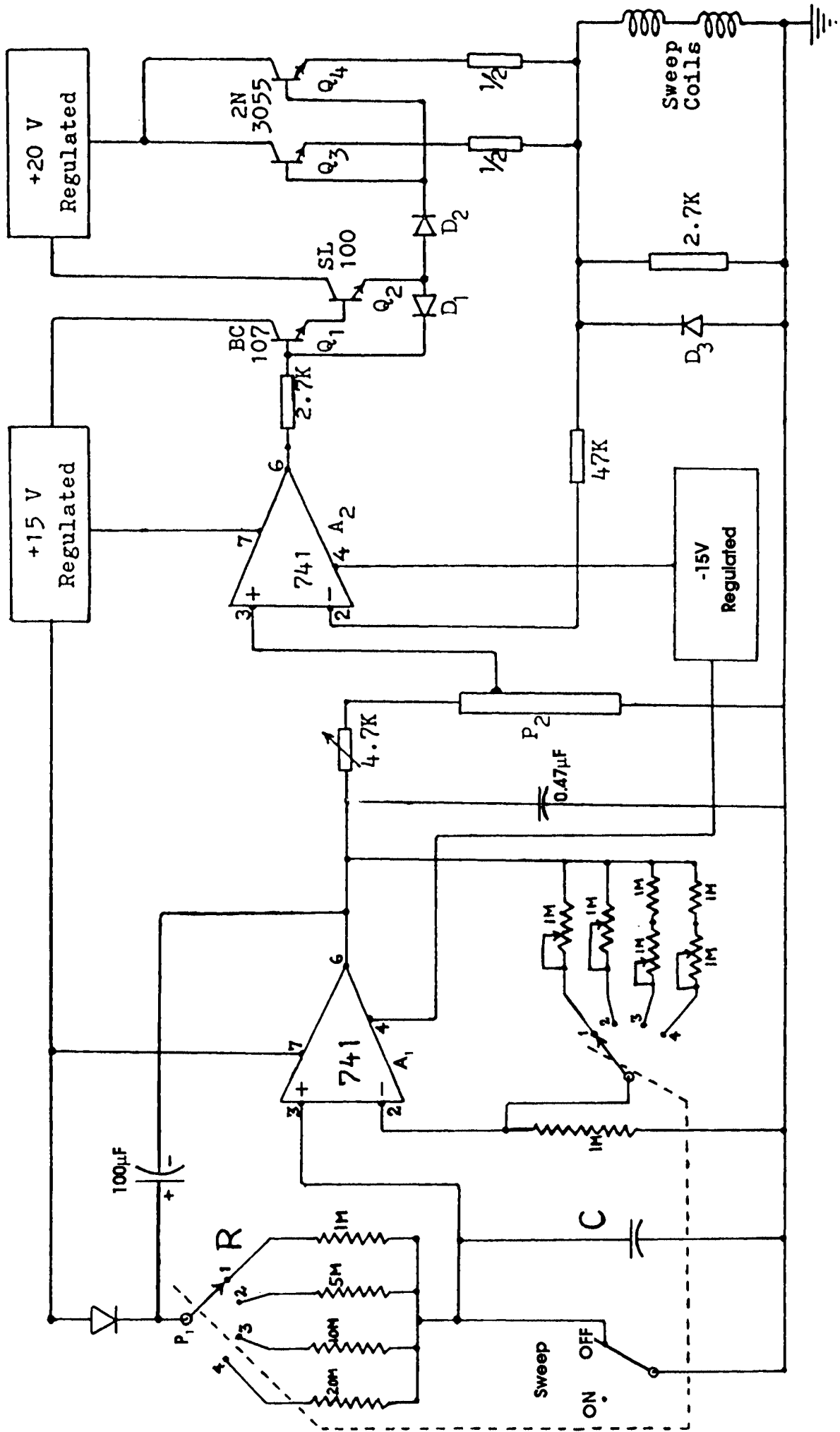
Fig. 5.12 : Schematic circuit of the improved linear field sweep generator

The modified bootstrap ramp generator forms the first part of the figure. The op-amp A_1 acts as the bootstrapping amplifier while R and C constitute the charging circuit. In this set up the sweep speed at the output will be $A'V/RC$, V being the potential difference across the bootstrapping capacitor C_1. The maximum sweep output voltage will then be $V_0 = A'VT_S/RC$ so that the sweep time $T_S = VRC/A'V$. Provided that C has a low leakage but high charge capacity, then V_0 will approach a saturated value V in a time $T_S = RC/A'$. The sweep duration can thus be varied by changing R or C.

For the present work the circuit has been designed to give sweep durations of 1/2, 5/2, 4 and 8min by choosing a constant value for C and varying R. A low value tantalum capacitor was chosen for C while an ordinary electrolytic capacitor was chosen for C_1, which should have a value much greater than C. R_2 together with R_1 sets the op-amp gain required to obtain the utmost in sweep linearity. By trial R_2 is adjusted to obtain the best linearity for each sweep duration setting.

The linear sweep voltage is then subjected to proper current boosting by the d.c. amplifying section. On passing this sweep current through a pair of field sweep generator coils the required linear variation in magnetic field is obtained. Variation of the strength of the sweep field can be conveniently done by varying the amplitude of the ramp voltage input to the d.c.amplifiers. In the present case the potential devider P_2 provides a magnetic field sweep range from 0.5 to 8mT (5 to 80 gauss) by a factor of two in successive steps.

5.5 : Performance of the improved field sweep unit

The recordings of the sweep voltages for different sweep durations have shown that the output linearity over the entire range is much better than 0.1%. This is evident from Fig. 5.13, which shows the tracing of the sweep recording corresponding to 8min duration. The lineari.y of the corresponding magnetic field sweep was also found to be excellent. The performance of the complete sweep unit was then tested by recording the broad proton resonance signals fron standard samples like polycrystalline NH_4Cl, etc. The recording of the signals were entirely satisfactory.

5.5.1 : Advantages of the innovative field sweep unit

The linear magnetic field sweep unit, which uses only commonly available components, gives a much improved performance in comparison with conventional sweep circuits. The modified bootstrap sweep generator circuit adopted here has a notable advantage in that the amplifier gain can be conveniently manipulated to obtain the utmost in sweep linearity for any desired sweep duration. Besides, unlike the earlier circuits (e.g. [7,11] and the one described in section 5.3), a seperate DC input is not required here to initiate and maintain the sweep. These advantages make the improved field sweep unit a simple but effective one as required for the recording of wideline NMR spectra. In this context it is worth mentioning that the improved sweep circuit design can as well be utilised in any other application where a highly linear long duration sweep voltage becomes necessary.
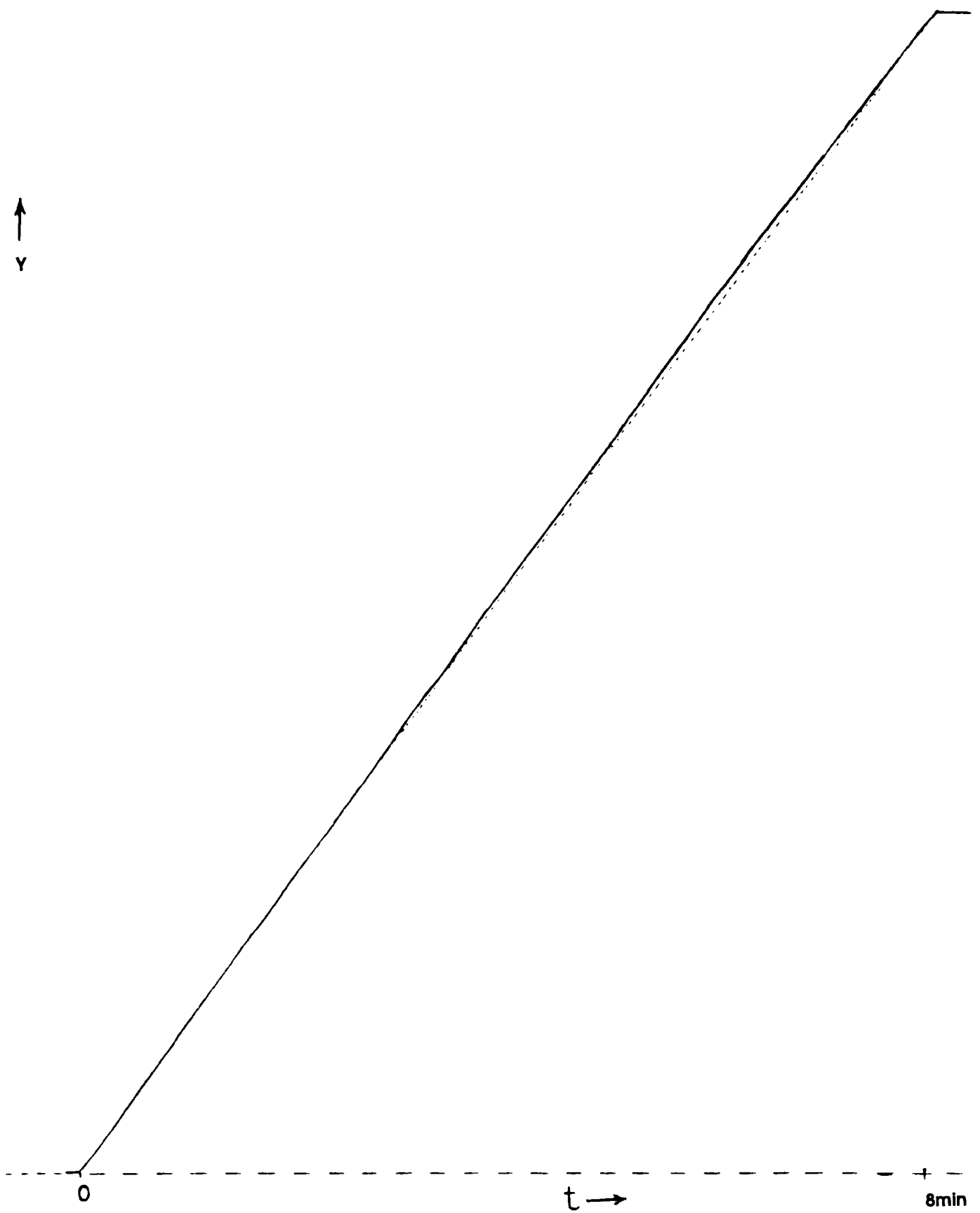
Fig. 5.13 : Tracing of the improved sweep voltage recording corresponding to 8min duration (chart speed ~ 2cm/min)

REFERENCES

[1]   M.L.Martin, J.-J.Delpuech and G.J.Martin; Practical NMR spectroscopy (Great Britain; Heyden : 1980)

[2]   R.L.Garwin, D.Hutchinson, S.Penman and G. Shapiro; Rev. Sci.Instrum.; 30 (1959) 105

[3]   P.H.Cole and R. Vaughan; J.Sci Instrum., 40(1963)411

[4]   J.B.Cook, R.E.George and E.H. Grant; J.Sci. Instrum.; 411(1964)390

[5]   S.Ganapathy and K. Ramani; J. Instn. Electronics & Telecom. Engrs. (India); 23 (1977) 221

[6]   J.Sthanapathi, A.K.Ghoshal, D.K.Dey, A.K.Pal and S.N. Battacharya; J.Phys.E.; 10 (1977) 221

[7]   N,S.Vander Ven; Rev. Sci. Instrum.; 39 (1968) 408

[8]   K.J. Wilson, C. Raghavan and C.P.G. Vallabhan; J. Instrum. Society of India; 18 (1988) 265

[9]   W.D.Cooper and H.B. Weisbecker; Solid State Devices and Integrated circuits (USA; Reston:1982)

[10]   G.E. Tobey, J.Graeme and L.P. Huelsman; Operational Amplifiers- Desigh and Applications (Tokyo; Burr-Brown: 1971)

[11]   A.G.Khandozhko, V.N.Ermakov and E.I. Slyn'ko; Instrum.Exp.Tech (USA); 23 (1980) 128

[12]   K.J.Wilson and C.P.G. Vallabhan; J.Phys. E; 22(1989)131

[13]   J.Millman and H. Taub; Pusle, Digital and Switching waveforms (Japan; McGraw-Hill : 1965)

Chapter VI

IMPROVED N.M.R. DETECTOR CIRCUIT

Abstract

A comprehensive description of the different types of NMR detector circuits fabricated for the present thesis work, with special emphasis on an improved detector circuit designed using MOSFETs is given in this chapter. Brief mention of the earlier NMR detector circuits is made at the beginning. The marginal oscillator-detector is then described in some detail. This is followed by a discussion of Robinson oscillator-detector circuits and their advantages over the marginal oscillator. The design and fabrication of a modified version of Robinson oscillator employing MOSFETs, which offers excellent sensitivity as well as capability to operate at very low r.f.levels, are then described in detail. The chapter concludes by describing the performance of the improved NMR detector circuit.

6.1 : Earlier NMR detector circuits

The earlier forms of NMR spectrometers employed either Q-meter circuits [1] or radio frequency bridges [2] for detecting resonance absorption. Although the Q-meter circuit was being used extensively for the detection of nuclear resonance absorption, especially where one is restricted to low r.f.levels and when accurate susceptibility measurements are required, it does have certain disadvantages. A highly stabilized r.f.oscillator having low AM and FM noise characteristics is required here and if it is necessary to sweep the frequency, it is difficult to track the natural frequency of the tank circuit with the variation of the oscillator frequency. This can lead to an undesirable admixture of the nuclear dispersion signal. Besides, since the Q-meter monitors the quality factor Q of the sample coil as loaded by the amplifier circuitry (including coaxial cables and connectors), it is susceptible to microphonics.

In the bridge circuits the mixing of the dispersion and absorption signals can be avoided by estabilishing an appropriate balance condition. However, slight variations of circuit conditions (say, due to temperature changes) may affect the state of balance markedly [3]. Further, since the bridge system is balanced for a particular frequency, a search for an unknown resonance involves sweeping the magnetic field over quite a range to find the resonance point and this, however, is not convenient to carry out. Instead it would be much easier experimentally if the frequency could be swept at constant field. But a frequency sweep will necessitate continuous adjustment of the bridge circuit, thus making it totally unsuitable for the slow searching of unknown resonance lines [4].

For simplicity and ease of operation it is often convenient to use a self-oscillating detector, especially where a wide frequency scan is desired. Two types of such oscillators are commonly used: the marginal oscillator and the Robinson oscillator. In these oscillators susceptibility to microphonics can be reduced by typically an order of magnitude in comparison with a similar Q-meter circuit [5].

6.2 : Marginal oscillator-detector

A marginal oscillator makes use of barely enough positive feedback so that an extremely small absorption of energy causes the amplitude of oscillations to vary by a large amount making the direct observation of the NMR signal quite easy. Marginal oscillator circuits have been extensively used as NMR detectors, a well known version being the Pound-Knight-Watkins (PKW) spectrometer [6,7,8].

The principle of this device, called usually as the 'Pound Box' is the following: the level of oscillations of an r.f. oscillator decreases when its load is increased. The lower the initial level of oscillation, sharper is the decrease. A sample containg nuclear spins placed in the coil of the tuned circuit of the oscillator will absorb r.f. energy at resonance and may be considered as an additional load. The drop in the level of oscillations is then used to detect the resonance [1].

A marginal oscillator circuit has the following major advantages as compared with the earlier bridge circuit:
(a) They are very simple to implement
(b) The circuit responds only to a variation of the absorption component χ'', since the effect of the dispersion component is to cause a frequency modulation which is not detected. The pure absorption is therefore recorded and there are no problems of maintaining good balance to ensure only this type of the signal.
(c) Wide frequency sweeps are possible when searching for unknown resonances, provided adequate feedback networks are included to keep the oscillation level constant.

6.2.1 : Transistorised marginal oscillator NMR detector systems have become much more compact and simple to fabricate. For the present thesis work the initial NMR signal, that of proton in doped water, was observed using a transistorised marginal oscillator circuit. This circuit closely follows the one put forward by Ijaz-ur-Rahman [9], which claims to give improved performance compared with earlier marginal oscillator circuits. The circuit offers the advantage that the amount of feedback and the amplitude of oscillations across the LC circuit can be independently controlled and so its setting as a marginal oscillator becomes extremely easy.

The actual circuit fabricated is shown in Fig.6.1. The circuit has its coil tapped at its centre from where sufficient current can be drawn by transformer (step down) action, to be fed back to the emitter of the oscillator transistor. The feedback capacitor of 400pF and a variable resistance (R_2) of 3KΩ enable one to control the phase and magnitude of this feedback. The circuit was fabricated using BC 178 transistors for both the oscillator transistor and the detector transistor.

The amount of d.c. bias of the detector and the amount of r.f. signal applied to it are important, as the gain of this stage depends on its quiescent point. The optimum combination of the d c bias and the r.f. signal amplitude are best found in practise as follows: After having placed the sample tube containing tap water (doped with ferric nitrate solution) in the coil, kept between the pole pieces of the magnet, power to the circuit is switched on. A d.c. voltmeter (20000Ω/V) is connected between the collector and emitter of T_2. If this transistor is not conducting, nearly full supply voltage (about 8V) will be indicated. Otherwise the preset potentiometers R_1 , R_2 and R_3 are adjusted to obtain this condition. R_3 alone is then adjusted so that the meter reads about a volt less than maximum,
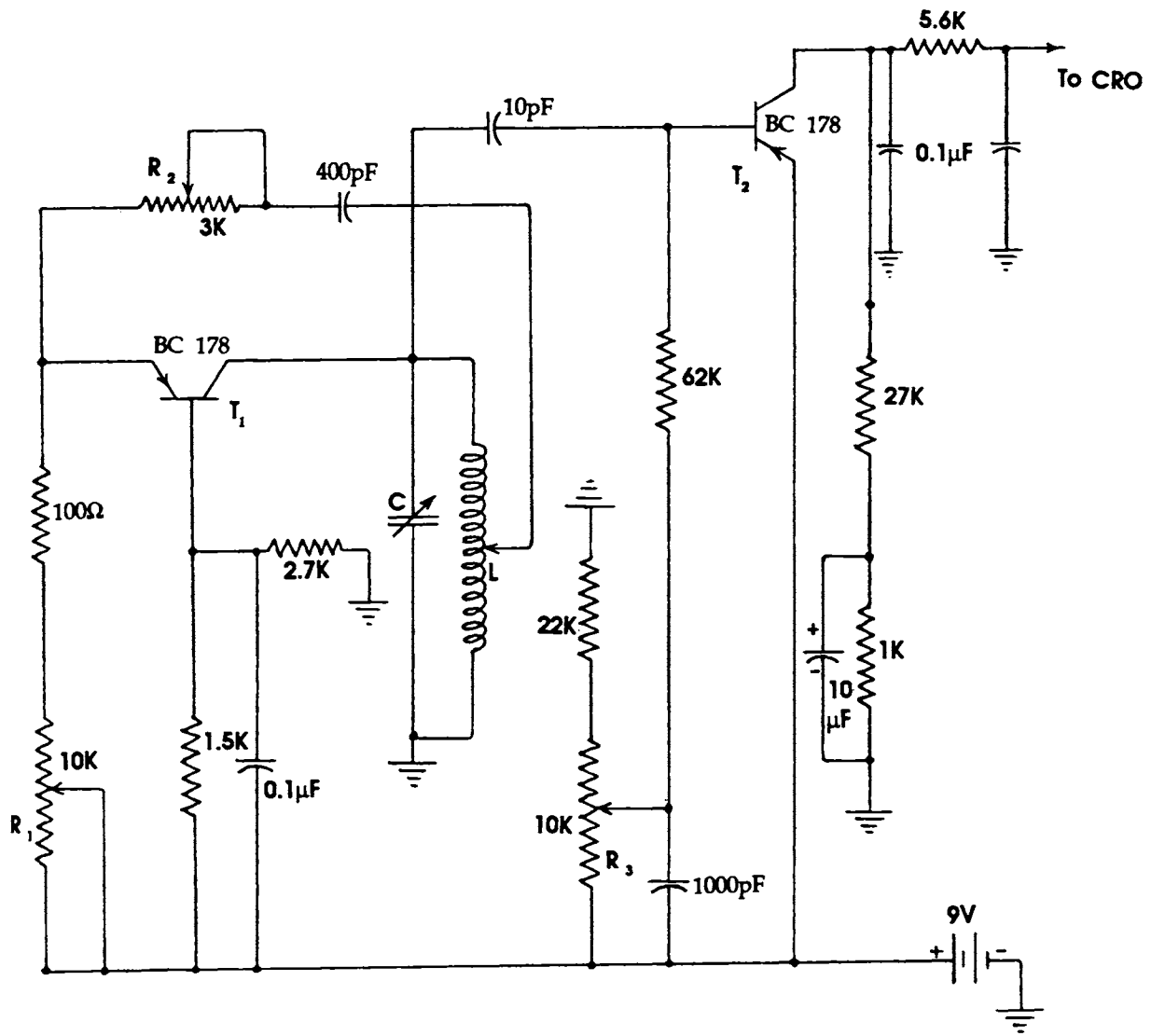
Fig. 6.1 : Circuit diagram of the marginal oscillator

indicating that T_2 is slightly conducting. R_1 and R_2 are then adjusted so that the meter reads about 2V.

After establishing the above bias condition the magnet power supply is switched on. The magnet current is now increased from zero, rather slowly, until the resonance peak appears on the oscilloscope screen. The peak will move sideways on changing the magnet current. In case the amplitude of the resonance peaks is too small, the sensitivity of the marginal oscillator is increased. This is easily done by adjusting R_2 so that the meter reading goes up, say by 1V, and then R_1 is adjusted so that the reading gets restored to its initial value.

Using the above set up proton resonance signal was observed in doped water. However the S/N ratio of the signal was not satisfactory. This was understood to be so because when the circuit is set at a high sensitivity level for obtaining better signal strength it will generate a good deal of noise, mainly due to microphonics, which will mar the appearence of the signal on the oscilloscope screen. Besides, a high sensitivity sate will lead to instability in the circuit, whereby the oscillator may flip in and out of oscillation sporadically and the same may have to be reset again and again.

6.2.2 : Disadvantages of the marginal oscillator-detector

As mentioned above, the S/N ratio of the marginal oscillator circuit shown in Fig.6.1 was not adequate enough for the satisfactory recording of the resonance signal. Also it is known that the marginal oscillator-detector suffers from a number of drawbacks, as mentioned below, which deter its usage as an efficient NMR detector.

(i) The main weakness of the marginal oscillator circuit is its non viability for producing very small r.f.fields, which sometimes become necessary for avoiding saturation in specimens like solids possessing long spin-lattice relaxation time. With a marginal oscillator maintaining stable ope.ation it is not possible to reduce the r.f.amplitude across the specimen coil much below 0.1V, whereas for the investigation of several solids it usually becomes necessary to work at a low r.f.level of the order of a few millivolts if saturation is to be avoided [4].

(ii) Since the operation of the marginal oscillator depends on the non-linear characteristics of the device used [10], their sensitivity tends to be less than that of Q-meter circuits.

(iii) For a given sample coil the marginal oscillator operates best at only one r.f.level. This precludes conveninet choice of r.f.level on the basis of sample saturation properties [11].

These disadvantages of marginal oscillator circuits in general and the poor performance of the circuit shown in Fig.6.1 in particular forced us to go for Robinson oscillator, which was learnt to be capable of providing far better performance in comparison with other NMR detectors.

6.3 : Robinson oscillator-detector

Robinson has devised a clever combination of Q-meter and marginal oscillator circuits having all the advantages of both of these, plus the ability to operate at very low r.f.levels on the sample coil [12].

Most of the drawbacks of the marginal oscillator-detector can be overcome by using a Robinson oscillator, where the r.f.feedback needed to sustain oscillations is

derived from a limiter stage. The limited oscillator [13] does not require continuous adjustment nor does it depend critically on the exact characteristics of particular devices. Besides, Robinson oscillators are considerably less sensitive to the unwanted dispersion component [5]. Because of these desirable features Robinson oscillators [13,14] have recently gained much popularity as an efficient NMR detector.

6.3.1 : An FET type Robinson oscillator

A typical Robinson oscillator circuit consists of a limited self- oscillator where seperate stages are used for regeneration and amplitude control. The essence of the Robinson system is that the only non-linearity in this occurs in the form of a simple limiter, so that both the oscillation conditions and the sensitivity to magnetic resonance absorption are predictable in a straight forward way. This is not the case in other forms of self-oscillating detectors, which are maintained in a more or less unpredictable or 'marginal' mode by the arbitrary operation of a manual or automatic control system.

For the present thesis work a Robinson oscillator employing FETs as active elements was tried out first. The actual circuit fabricated is shown in Fig. 6.2. This circuit is essentially a simplified version of the one put forward by Robinson [15]. Here bipolar transistors in the limiter stage of the Robinson's orginal circuit [15] have been replaced with the FETs Q_1 and Q_2 (BEW 10s), which posses less $1/f$ noise than a bipolar pair. This long-tailed pair of FETs acts both as the limiter and as a moderately efficient detector.

If the r.f.input to the gate of Q_1 has an amplitude exceeding about 100mV the current through Q_2 is switched on and off. A fraction (determined by C_1 and C_2) of this clipped current is fedback to the tank circuit and this sustains oscillations, the amplitude of which is linearly proportional to the Q of the circuit. Thus the resonant circuit responds directly to changes in Q due to NMR absorption. On the negative half-cycle Q_1 is switched off but on the positive half-cycle the current through it continues to rise at a rate governed by R, even after Q_2 is turned off. Thus the drain current of Q_1 contains a component which is the detected signal.

The transistors T_1 and T_2 (BC 109) and the FET - Q_3 (BFW 10) form the audio amplifier arrangement for enhancing the detected signal. The preset potentiometer R_1 enables one to set the required r.f.level across the specimen coil. The trimmer capacitor C_2 helps to select an appropriate C_1/C_2 ratio for achieving an optimum feedback and hence sensitivity. The +18V dc power for the circuit was provided from two 9V cells.

Using the above mentioned NMR detector circuit a highly satisfactory proton resonance signal from liquid samples could be observed on an oscilloscope. The S/N ratio of the signal was far better than that of the signal obtained using the marginal oscillator circuit of Fig.6.1. The Robinson oscillator circuit was found to have a high degree of frequency stability and very low sensitivity to microphonics as compared with the earlier marginal oscillator. Besides a better control over the r.f.level could be achieved using this circuit. The tracing of a typical derivative signal corresponding to proton resonance in doped water obtained using this circuit is shown in Fig.6.3.

6.4 : An improved Robinson Oscillator using MOSFETs

Though the circuit shown in Fig. 6.2 was found to give very good results for the recording of NMR signals in liquids, it could not be used effectively for recording
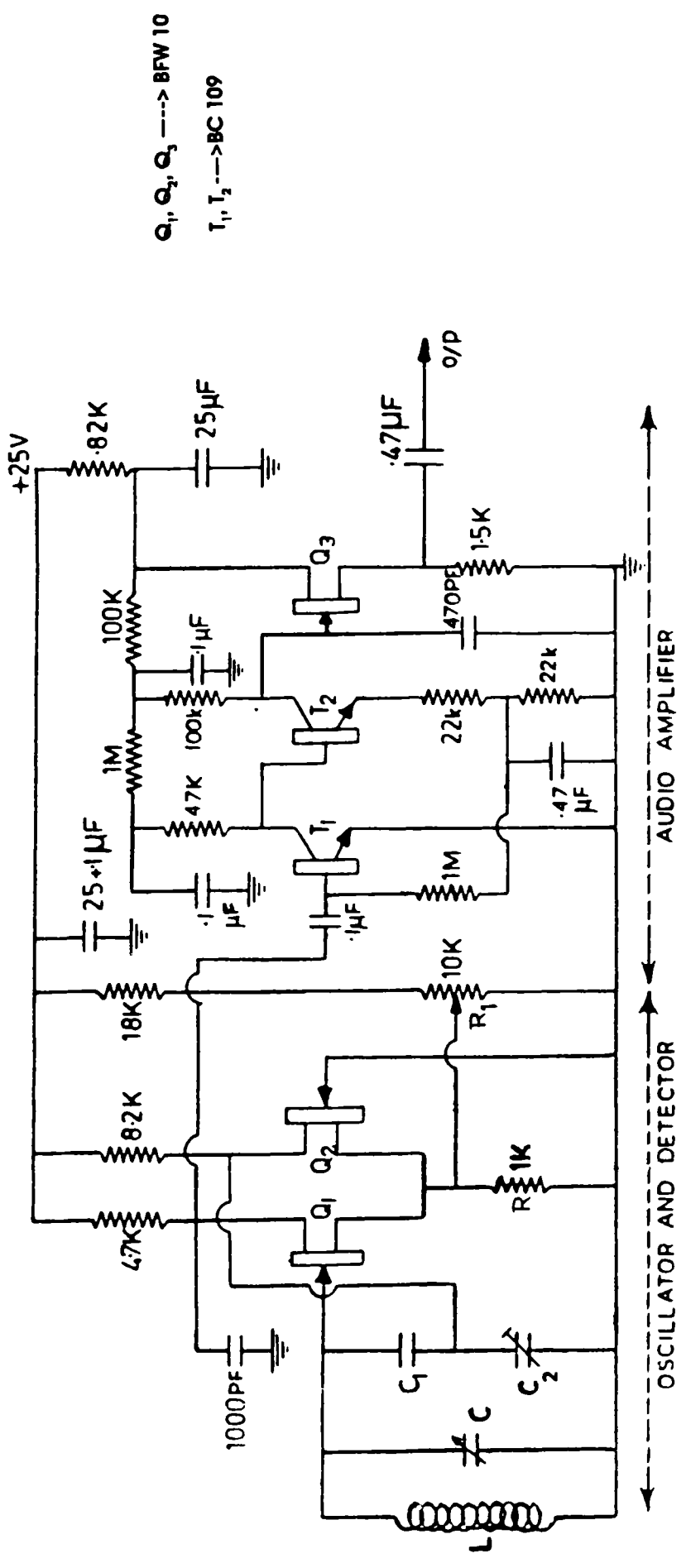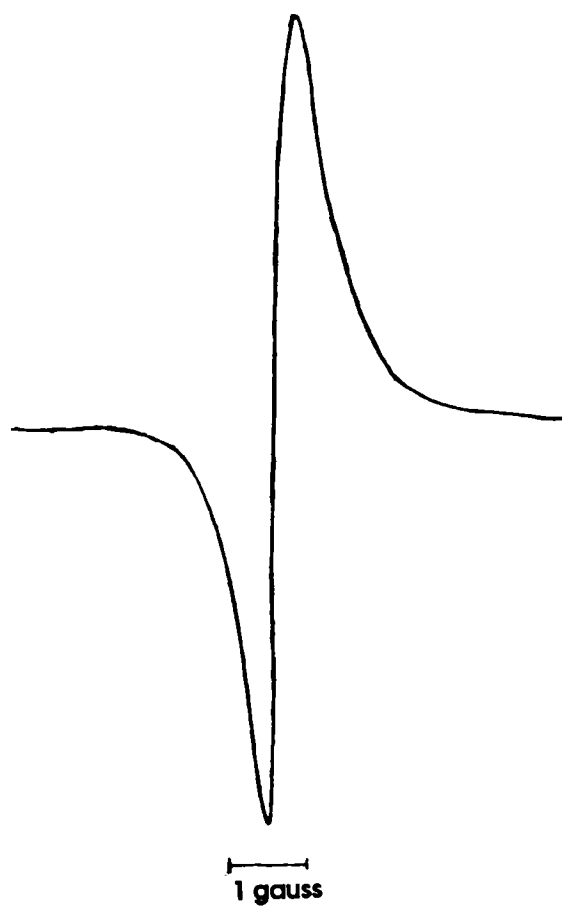
Fig. 6.2 : Circuit diagram of the FET based Robinson's oscillator

Fig. 6.3 : Tracing of the derivative curve of proton resonance from water doped with $Fe(NO_3)_3$ solution (resonance frequency ~8MHz; r.f.level ~80mV) obtained using the FET based Robinson oscillator

resonance signals from solids. This was due to the fact that the r.f. level of this circuit could not be brought down to the order of a few millivolts, as required in solids for avoiding saturation. It was found that the r.f.level of the circuit could only be brought down to a value of about 60mV. This circumstances has prompted us to search for a different circuit capable of operating at very low r.f.levels.

Though several modified versions of Robinson oscillators [16, 15, 17] including those employing integrated circuits have been published, most of them suffer from drawbacks like circuit complexity or requirement of highly critical components. The later versions using integrated circuits suffer from reduced sensitivity resulting from relatively low input impedance and the poor noise characteristics of the integrated circuits used.

With the intention of achieving enhanced sensitivity for the detector circuit as well as to obtain the ability to operate the oscillator at very low r.f. levels it was decided to design an improved, but simple, version of Robinson oscillator employing MOSFETs as the active devices for the present work. In this circuit [18] the very high input impedance and better noise characteristics combined with high transconductance of the MOSFETs have been fully exploited for achieving the required sensitivity needed for recording weak NMR signals.

6.4.1 : Description of the circuit

The circuit, which is shown in Fig. 6.4, comprises of three stages: (i) an r.f.level limited oscillator, (ii) a detector and (iii) a low noise amplifier.

Since the oscillator stage determines the minimum r.f.level at which the circuit can be operated and the maximum sensitivity that can be achieved, much importance had been given to proper design of the same. The input impedance of the active devices used for the oscillator has to be very much higher than the shunt impedance of the nuclear resonance circuit, which is typically a few thousands ohms in practical circuits. Later versions of Robinson oscillators have been using FETs as the active devices. However their input impedance ($\sim 10^6$ ohms) is not high enough to prevent Q value of the tank circuit getting affected adversly. As a result the Q factors for such circuits are only moderate. Besides operation at very low r.f.levels using such circuits is nearly impossible mainly due to poor transconductance of conventional JFETs.

To overcome these disadvantages MOSFETs (3N 200) were utilised as the active devices for the level limited oscillator in the present circuit. The MOSFETs have an input impedance ($\sim 10^{13}$ ohms) that is much higher than that of JFETs. This serves to enhance the Q of the new detector circuit considerably. MOSFET also provide excellent high frequency characteristics as well as very low 1/f moise, factors that make them desirable choice for the long-tailed pair in a Robinson oscillator. Besides the high transconductance value, better noise characteristics of MOSFETs and their high tolerance to microphonics are added benefits.

As in many versions of Robinson oscillator [16, 5], in the present design the operating conditions are chosen to give nearly perfect limiting independent of the oscillation level. As a result the absorption signal does not appear as a component of the drain current and hence a seperate demodulator is used. Conventional circuits have been employing highly specialised diodes, capable of working at very low levels, as the rectifier [16,5]. To avoid the requirement of critical components and also to facilitate the designing
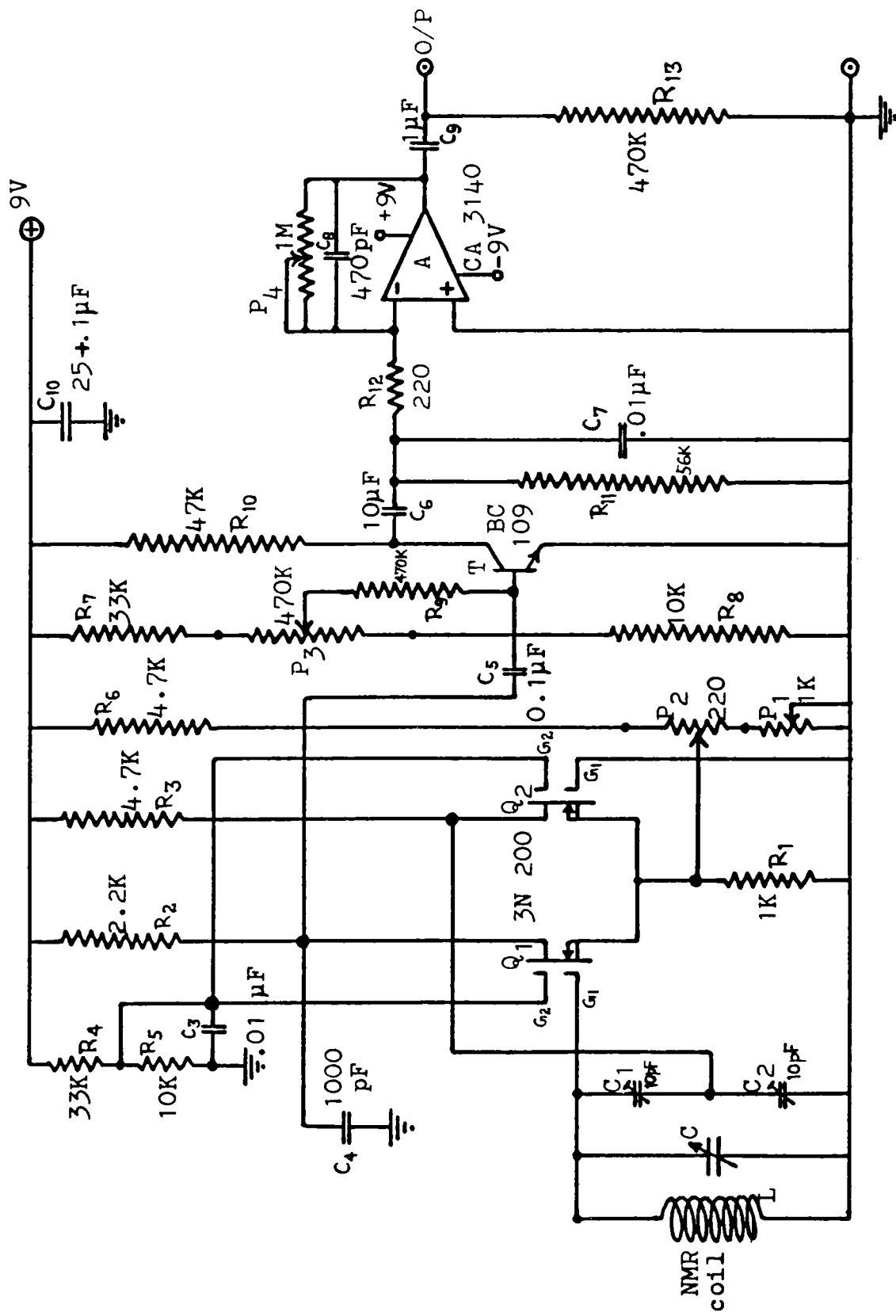
Fig. 6.4 : Schematic circuit of the Improved MOSFET based Robinson oscillator

with commonly available components the base-emitter junction of a silicon transistor (BC 109), properly biased to act as an efficient detector, was utilised for the present circuit. This arrangement can perform well at levels much lower than what the diode rectifier can respond to. Besides, at the collector of the transistor, a stage of a.f. amplification is also obtained as a bonus.

The S/N ratio of the final output signal is considerably affected by the noise contributed from the a.f.stage. In order to minimise the noise generated in the a.f.stage we have employed a single low-noise op-amp (CA 3140) for the final a.f.amplification, instead of using several transistor amplifier stages as in some earlier circuits [15, 17]. The op-amp gain can be conveniently adjusted, either for boosting weak NMR signals or for preventing saturation of the amplifier in the prescence of strong signals - by reducing the op-amp gain suitably.

Since the d.c. power requirement for the present design is rather low, it enables standard 9V cells to be used for energizing the complete circuit. As a result the interference due to additional noise generated by power supply stabilizers, as was present in some earlier circuits (e.g.[15]), also gets totally eliminated in the present design.

As in the circuit of Fig 6.2 the trimmer capacitors C_1 and C_2 in the present circuit help to select a suitable sensitivity level. Both the MOSFETs are appropriately forward biased by the positive gate-2 voltage applied to them from the potential devider circuit comprising of resistors R_4 and R_5. This serves to establish an optimum transconductance for these active devices. The a.c. grounding of gate-2 using the capacitor C_3 helps to reduce the reverse transfer capacitance of the MOSFETs, thereby minimizing stray r.f.feedback [10]. The series combination of the preset potentiometers P_1 and P_2 enables convenient selection of r.f.level. The preset P_3, connected in the potential devider network constituting resistors R_7 and R_8, serves to choose an appropriate detector bias level that can yield a good S/N ratio for the detected signal. The resistor R_9 helps to restrict the bias current. The preset P_4 is needed to vary the op-amp gain, and hence the final output signal amplitude, as desired. The +9V and -9V d c power for the circuit was provided from two 9V cells.

6.4.2 : Operation of the circuit

Keeping a reference sample in the NMR coil, initially the presets P_1 and P_2 (Fig.6.4) are adjusted to select the required r.f.level. The biasing of the detecting transistor T is then adjusted, using the preset P_3 such that T is made slightly conducting. Then, viewing the absorption signal pattern on an oscilloscope, P_3 as well P_4 are properly adjusted to get a signal having the best S/N ratio. Under this condition the circuit will yield optimum S/N for any other signal at the particular r.f.level. For recording a signal at a different r.f.level one may reoptimize the S/N by adjusting the presets P_3 and P_4.

6.5 : Performance of the improved NMR detector

The circuit shown in Fig. 6.4 has been operated at r.f.levels ranging from 150mV down to 1mV. The silicon transistor rectifier arrangement has been observed to work excellently even when the r.f.level at its base is less than 20mV. This is a real advantage compared to the diode rectifier set up in some earlier circuits (e.g.[5]). The performance of the complete circuit was tested by recording weak NMR signals, especially

from solids, at room temperature. The recording of the signals were entirely satisfactory. Fig.6.5 shows a typical tracing of the derivative curve of proton resonance in polycrystalline NH$_4$Cl recorded at room temperature (30° C).

It has been found that the new MOSFET based Robinson oscillator circuit gives a much improved performance in comparison wit conventional NMR detector circuits, even for room temperature operation. The circuit can be fabricated using commonly available components and requires no critical elements. The simple nature of the circuit enables a compact printed circuit layout (~4 cm x 6 cm) without necessitating any complex interstage shielding or any critical layout of components. The enhanced sensitivity, capability to operate at very low r.f.fields and the overall simplicity of the circuit makes it an excellent NMR detector, especially useful for probing weak signals.

4.5 gauss
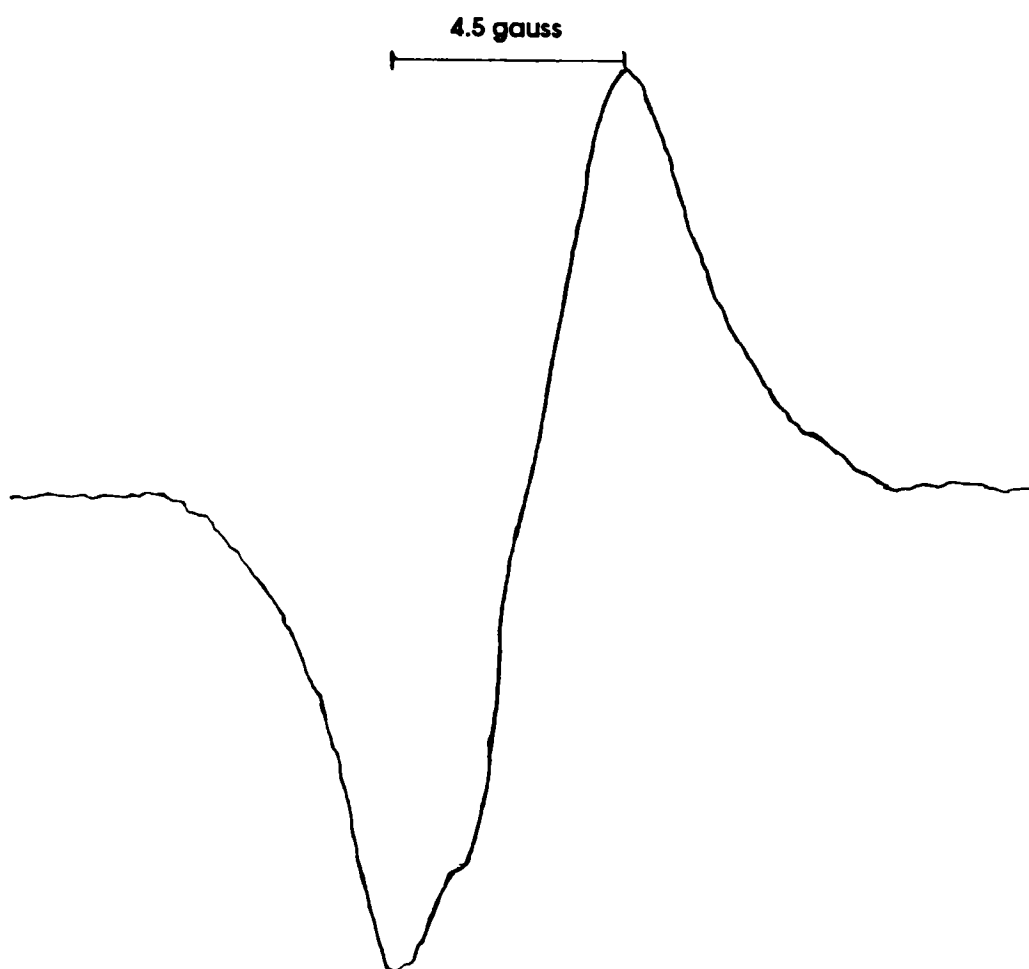
Fig. 6.5 : Tracing of the derivative curve of proton resonance from NH_4Cl (resonance frequency ~12MHz; r.f.level~20mV) obtained using the MOSFET based Robinson oscillator, at room temperature (~30° C)

REFERENCES

[1]   A.Abragam; The Principles of Nuclear Magnetism (Great Britain; Oxford University Press: 1962)

[2]   N.Bloembergen, E.M. Purcell and R.V.Pound; Phys.Rev.; 73 (1948) 679

[3]   F.A. Rushworth and D.P. Tunstall; Nuclear Magnetic Resonance (New York; Gordon and Breach Science Publishers: 1973)

[4]   E.R.Andrew; Nuclear Magnetic Resonane (Great Britain; Cambridge University Press: 1969)

[5]   P.Deschamps, J. Vaissiere and N.S. Sullivan; Rev.Sci.Instrum.; 48 (1977) 664

[6]   R.V. Pound and W.D.Knight; Rev. Sci. Instrum; 21 (1950) 219

[7]   G.D. Watkins and R.V.Pound; Phys. Rev.; 82 (1951) 343

[8]   D.G. Hughes and M.R. Smith; J. Phys. E; 4 (1971) 13

[9]   Ijaz-ur-Rahman; Am.J.Phys.; 47 (1979) 1004

[10]   N. Sullivan; Rev.Sci.Instrum.; 42 (1971) 462

[11]   D.W.Alderman; Rev.Sci.Instrum.; 42 (1970) 192

[12]   R.T. Schumacher; Introduction to Magnetic Resonance (New York; W.A.Benjamin:1970)

[13]   F.N.H. Robinson; J.Sci.Instrum.; 36 (1959) 481

[14]   F.N.H. Robinson. J. Sci.Instrum.; 42 (1965) 653

[15]   F.N.H. Robinson; J.Phys.E; 15 (1982) 814

[16]   E.A. Faulkner and A. Holman; J.Sci.Instrum.; 44 (1967) 391

[17]   F.N.H Robinson; J.Phys.E; 20 (1987) 502

[18]   K.J. Wilson and C.P.G.Vallabhan; Measurement Science and Technology (UK); (In Press)

Photograph of the Wideline NMR spectrometer fabricated, showing the electromagnet (A), high current stabilizer-cum-field sweep unit (B), NMR detector (C), modulating signal generator (D), lock-in amplifier (E), chart recorder (F), C.R.O. (G) etc.

Chapter VII

SOME STUDIES OF PROTON SIGNALS
FROM AQUEOUS SOLUTIONS

Abstract

This chapter gives a brief account of some preliminary investigations carried out in liquids using the newly fabricated NMR spectrometer. Proton resonance signal recordings from different liquid specimen as well as flourine resonance signal recording from hydro flouric acid are described in the first half of the chapter. Study of the effect of different paramagnetic impurities on NMR linewidth, carried out mainly to standardise the spectrometer set up, is discussed in the latter half. At the end of the chapter a discussion of the results of these simple investigations is given.

7.1 Introduction

The NMR spectra of liquid samples differ significantly from those of solids, and so does the information obtained from them. The liquid phase is characterised by greater freedom of molecular motion. The effect of the motion is primarily to reduce the dipolar broadening of the resonance linewidth. i.e. that width due to the direct dipole-dipole interaction between nuclear spins. Secondly, the coupling of the nuclear spins to the lattice is usually reduced, so that spin-lattice relaxation times (T_1) are increased. However addition of paramagnetic ions to a liquid will promote relaxation and help to reduce the value of T_1 so that observation of steady NMR signals become possible.

The narrowness of the NMR signals from liquids permits the oscilloscope display of such signals to be achieved very conveniently. This allows standardisation of the NMR spectrometer utilising a standard liquid sample. Further, prior to the recording of the broad NMR signal of a given nucleus from a solid sample, it is convenient and advisable to observe the resonance signal of the particular nucleus from a liquid sample. This will enable one to set the d.c. magnetic field at a value corresponding approximately to that of the centre of the broad resonance signal, whereby the recording of wideline signals will become easier.

7.2 : H¹ resonance signals from different liquids

In the present work the first NMR signals obtained were that of H^1 in water doped with $Fe(NO_3)_3$ salt. For observing the resonance a fixed radiofrequency of about 12MHz was chosen. The r.f.level was chosen to be around 60mV. For obtaining the oscilloscope display the sinusoidal modulating frequency was chosen to be 33Hz and the modulating field strength to be about 1gauss. With the complete spectrometer set up switched on the d.c.magnetic field is varied slowly till the resonance signal appears on the oscilloscope. The corresponding d.c.magnetic field strength was measured to be around 2,800gauss.

For recording the signal the modulating field strength is reduced to about 50milligauss and the modulating frequency is raised to 330Hz. The output of the NMR

detector is connected to the lock-in input. The reference input to the lock-in is derived from the modulating signal generator output. The output of the lock-in is connected to the chart recorder. The field sweep amplitude of the Field Sweep Unit was chosen to be 5 gauss while the sweep speed is selected to be one minute. The chart speed of the recorder was selected to be 10cm/min. Since sweeps generated by the electronic field sweep unit is positive the magnetic field is so adjusted to be slightly less than the value at which the resonance pattern appears on the oscilloscope. With the spectrometer set up switched on the chart drive of recorder is turned on. Then the field sweep is switched on. At the resonance condition the derivative of the absorption curve gets recorded. A tracing of the resonance signal is shown in Fig.7.1.

From the derivative tracing the linewidth in magnetic field unit, ΔH, is calculated as the interval between the points of maximum and minimum slope. For the particular tracing of Fig. 7.1, ΔH is found to be 0.2 gauss. It has been learnt that for getting a correct measure of the linewidth three conditions have to be satisfied. First of all the radiofrequency field must be small enough to prevent saturation. Secondly, the resonance line must be traversed sufficiently slowly to avoid transient effects which modify the lineshape. Thirdly, the amplifier must have an adequate bandwidth to pass the nuclear magnetic resonance signal without distortion.

Once the linewidth in frequency units, Δv, is known the spin-spin interaction time T_2 can be calculated from the relation

$$\Delta v = 1/(\sqrt{3}\pi T_2) - - - - - - - - - (7.1)$$
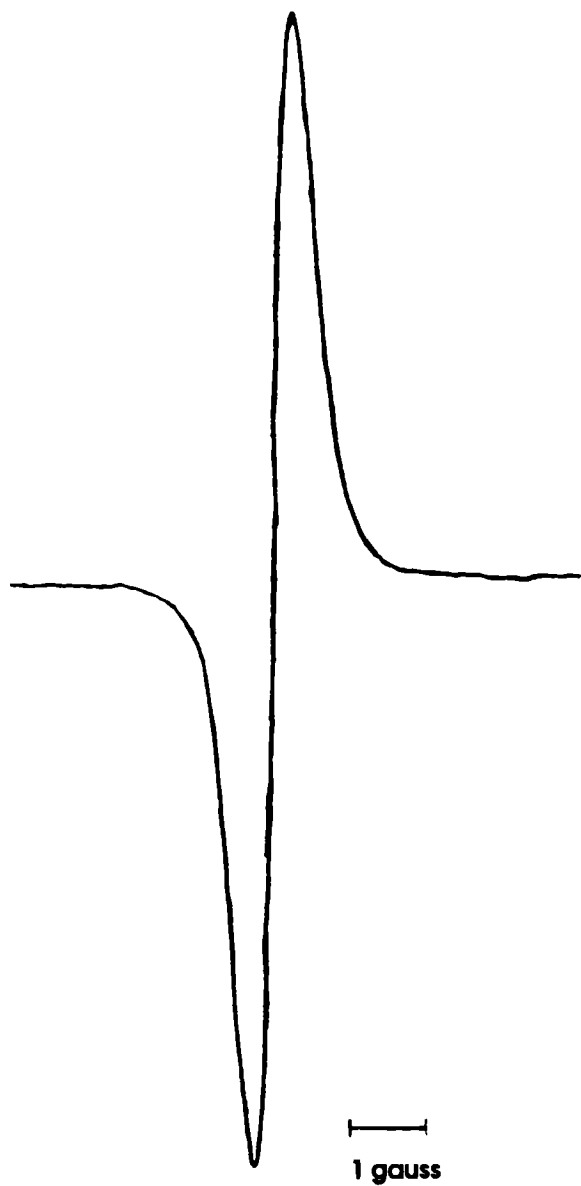
$$\therefore \quad T_2 = 1/(\sqrt{3}\pi \Delta v)$$

Since $\Delta v = \gamma \bullet \Delta H / 2\pi,$

$$T_2 = 2/(\sqrt{3} \bullet \gamma \bullet \Delta H) \text{ Secs} - - - - - - - - (7.2)$$

The effective proton spin-spin interaction time in doped water, deduced from Fig. 7.1 is found to be $\sim 2 \times 10^{-4}$ Sec.

Proton resonance signals have been recorded from various other liquid samples like tap water, distilled water, turpentine, acetone, coconut oil etc. The linewidth of these signals are tabulated in Tabe VII-1.

Table VII-1 : Linewidths of proton resonance signals from different samples	
Sample	Linewidth of H^1 signal (gauss)
Tap Water	0.15
Distilled Water	0.07
Turpentine	0.1
Acetone	0.09
Coconut oil	0.13

Fig. 7.1 : Tracing of the derivative curve of proton resonance from dilute $Fe(NO_3)_3$ solution (resonance frequency~12MHz; r.f.level~60mV)

7.3 : F^{19} resonance

For proving multi-nuclear capability of the spectrometer set up, resonance from dilute hydroflouric acid has been recorded. 40% hydroflouric acid was taken in a plastic tube and kept in the sample coil. A radio frequency of about 12MHz and an r.f.level of about 50mV were selected. When the magnetic field is varied upto a value of around 2.8Kgauss the proton resonance signal from the hydroflouric acid appears on the oscilloscope. When the field is further increased to a value approximately equal to 3Kgauss the F^{19} resonance signal appears on the oscilloscope. The tracings of the derivative recordings corresponding to these two signals are shown in Fig.7.2 for comparison purpose. The gyromagnetic ratios for H^1 and F^{19} were calculated from the values of the radiofrequencies and resonant field strengths and were found to be in close agreement with the theoretical values.

7.4 : Study of paramagnetic impurity on NMR linewidth

The resonance linewidth in most liquid samples are very small and are in practice determined by the inhomogeneity of the magnetic field over the specimen. For satisfactory observation of resonance line it becomes necessary to broaden the resonance line artificially. Bloch, Hansen and Packard [1] have observed that the addition of paramagnetic ions to water substantially reduces the proton relaxation time, which in turn serves to broaden the resonance linewidth. The effect was further examined by Bloembergen, Purcell and Pound [2], who attributed the relaxation to the diffusional Brownian motion of water molecules in the vicinity of the ion.

For the sake of calibrating our NMR spectrometer set up the study of the effect of Fe^{3+} ion concentration against spin-spin interaction time (T_2) has been repeated. Solutions of $Fe(NO_3)_3$ in water were prepared for various known concentrations and the linewidth of the proton resonance signal was calculated in each case. From the linewidth the T_2 value was deduced. It has been observed that even a weak ionic concentration markedly lower the T_2 value. This is learnt to be due to the fact that magnetic moment of a paramagnetic ion which is of the order of one Bohr magneton, is about 10^3 times larger than a nuclear magnetic moment. Hence the fluctuating local magnetic field is correspondigly larger and the relaxation time shorter. The experimental graph obtained is shown in Fig.7.3 and is in close agreement with that of earlier workers [3]. The graph indicates that the relaxation time of protons in ionic solution is inversly proportional to the ionic concentration.

Study has also been carried out using ions having totally different magnetic moment compared with that of Fe^{3+}. Ion concentration versus measurements were carried out using Cu^{2+} and Gd^{3+} ions in an identical manner as discussed above. The resultant graphs are shown in Fig. 7.4, along with the graph corresponding to Fe^{3+} ion for comparison purpose. The graphs indicates that for a given concentration the relaxation time of protons in ionic solution is greater for that solution containing paramagnetic impurities having the lowest magnetic moment (e.g. Cu^{2+}) and vice versa (e.g.Gd^{3+}). The results are found to be in agreement with the prediction of Bloembergen et al [2] that the relaxation time of protons in ionic solutions is inversly proportional to the square of the magnetic moment.

H'

$\Delta H \sim 0.23$ gauss

$(V_s \sim 20.5 mV)$

F^{19}

$\Delta H' \sim 0.3$ gauss

$(V_s \sim 3.1 mV)$

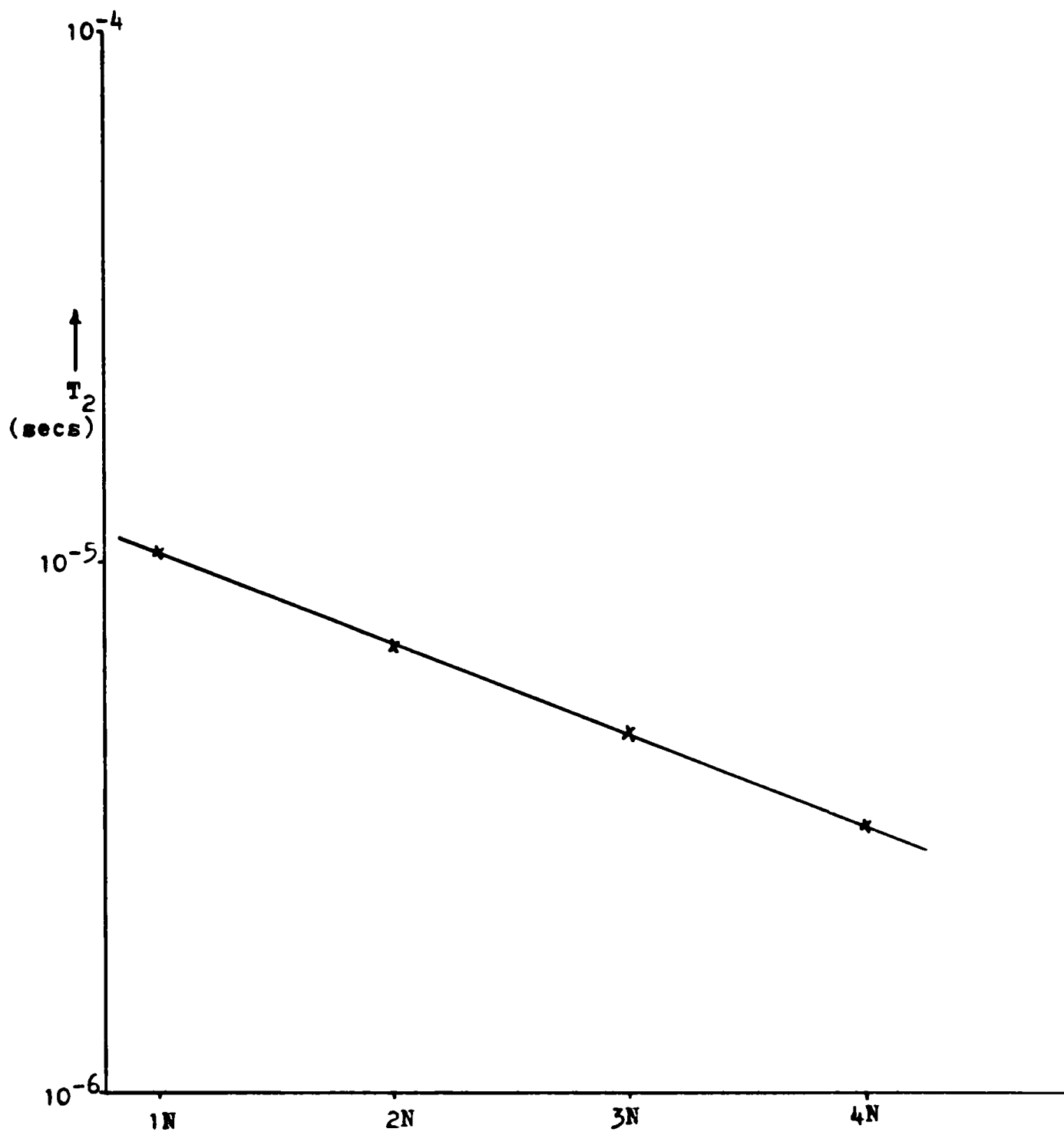Fig. 7.2 : H' and F^{19} resonances from Hydro Flouric acid

Fig. 7.3 : Graph showing the effect of Fe(NO$_3$)$_3$ concentration on T$_2$ value of proton signal
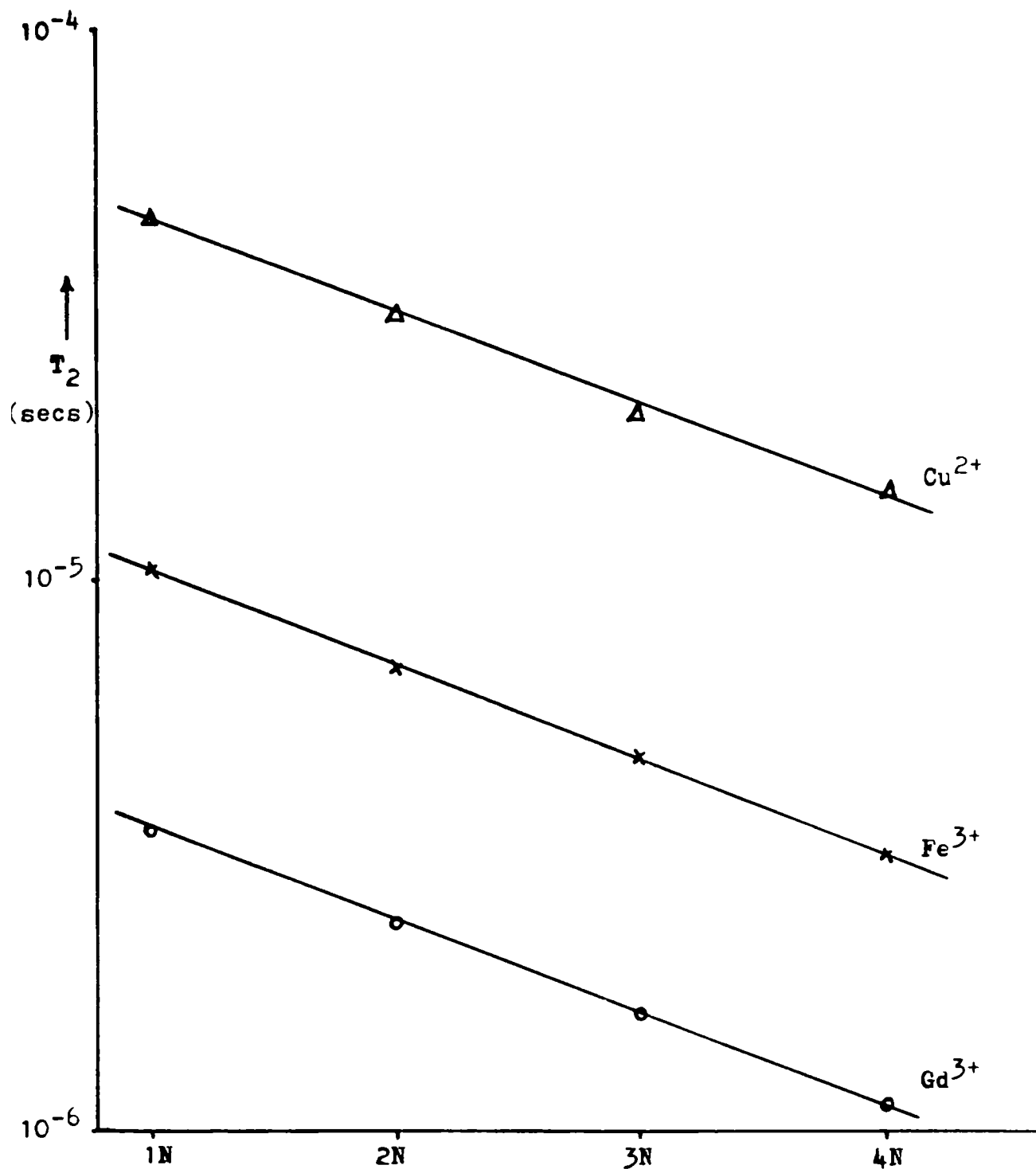
Fig. 7.4 : Graph depicting comparitive studies of effect of concentration of Fe^{3+}, Gd^{3+} and Cu^{2+} ions on T_2 value of proton signal

7.5 : Discussion

The indegenously fabricated NMR spectrometer set up has been found to be working satisfactorily. Very stable proton resonance signals could be observed on an oscilloscope using the set up. The derivative recordings of absorption signals were fully satisfactory and dependable. The versatility of the NMR spectrometer has been established by recording F^{19} resonance as well. The results of the studies carried out for standardising the set up for performing investigation in liquids were found to follow closely those obtained by earlier workers.

REFERENCES

[1]   F.Bloch, W.W.Hansen and M.Packard; Phys. Rev.; 70 (1946) 474
[2]   N.Bloembergen, E.M.Purcell and R.V.Pound; Phys.Rev.; 73 (1948) 679
[3]   E.R.Andrew; Nuclear Magnetic Resonance (Great Britain; Cambridge University Press:1969)
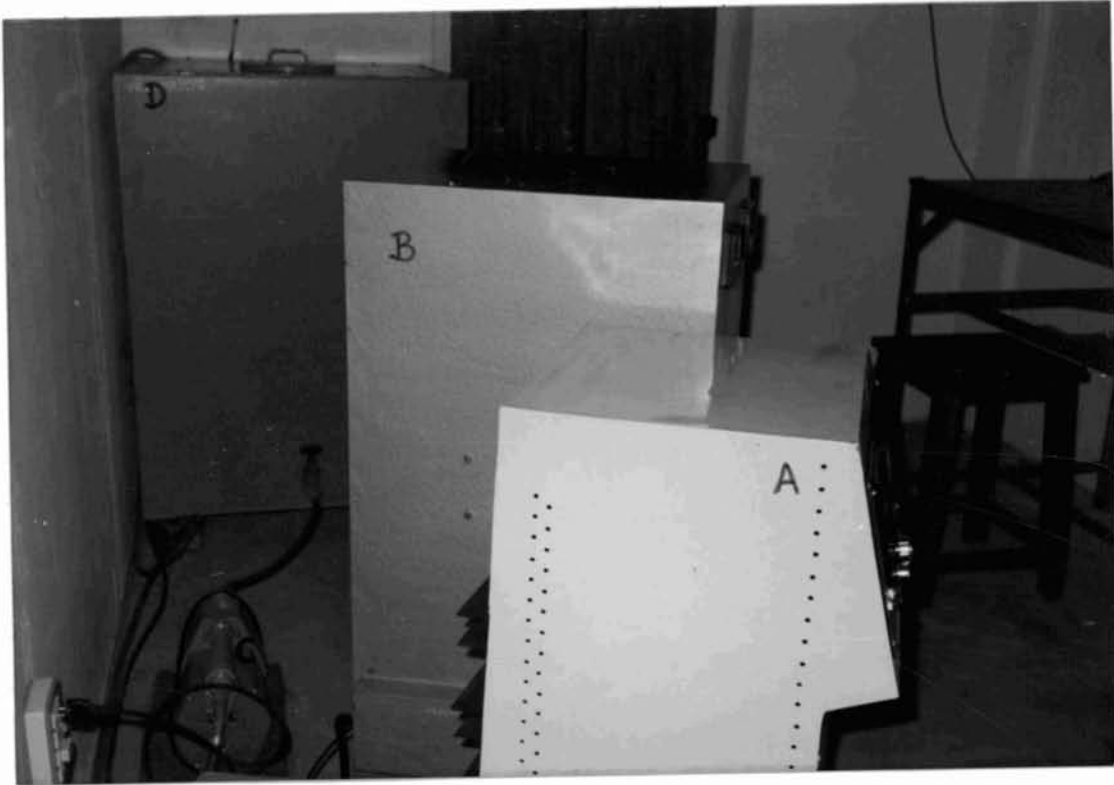
Photograph showing current stabilizer-cum-field sweep unit (A), Rectifier unit (B), monoblock pump (C) for water cooling of the electromagnet and water tank (D)

Chapter VIII

N.M.R. INVESTIGATIONS IN SOLIDS

Abstract

A descriptive survey of the investigations carried out in solid samples using the wideline NMR spectrometer fabricated in the laboratory is given in this concluding chapter. The broadline proton signal recordings from different ammonium salts in powder form are described at the beginning of the chapter. A satisfactory explanation for the anomalous features present in the proton resonance signal from ammonium chromate is then presented. Following this, the peak-to-peak strength of the proton resonance signal from zeolites is established to represent a true measure of the amount of proton containing molecules absorbed by them. A discussion of the proton signal recordings from food grains and other samples are then given. The chapter concludes by presenting a brief review of the results.

8.1 : Introduction

NMR signals from solids are generally very broad due to the large nuclear spin-spin interactions which are dominant in many solids. The linewidths may range from 100Hz upto several KHz, at an applied d.c.magnetic field of 1 Tesla. Also the strength of the wideline signals from solids are extremely weak. The signal strength at any one point in the spectrum is comparable with the inherent noise of the system and signal recovery techniques have to be used. Besides, the necessity of avoiding line distortion due to saturation effects becomes all the more important while detecting the broadline NMR signals, which can usually be achieved by reducing the radio frequency level. In the present wideline NMR spectrometer set up a lock-in amplifier is used to extract the weak wideline signals from the noisy background while the newly designed MOSFET based Robinson oscillator-detector can be conveniently adjusted to keep the r.f. field to the required low level.

8.2 : Wideline proton signals from standard solid specimen

Using the present experimental set up the first broadline proton resonance signals recorded were those from ammonium salts. Polycrystalline $(NH_4)_2SO_4$ was initially used as the sample. At first the proton signal from a liquid sample was observed on the oscilloscope, with the radio-frequency at about 12MHz. In this condition the magnitude of the d.c.magnetic field is reduced by a value approximately equal to half of the field sweep amplitude to be employed for the wideline signal recording. The liquid sample is then replaced with $(NH_4)_2SO_4$ powder. The r.f.level is reduced to about 20mV. The modulation strength is adjusted to be about 0.5gauss. The output of the NMR detector is connected to the lock-in amplifier, whose time constant is set to appropriate value to get good averaging. The field sweep amplitude is chosen to be 20gauss and the sweep time to be 9minutes. The attenuator controls of the lock-in amplifier as well as the chart recorder are adjusted so that a signal of sufficient amplitude gets recorded on the chart recorder. The tracing of a typical recording of the broadline proton signal from $(NH_4)_2SO_4$ is shown in Fig 8.1.
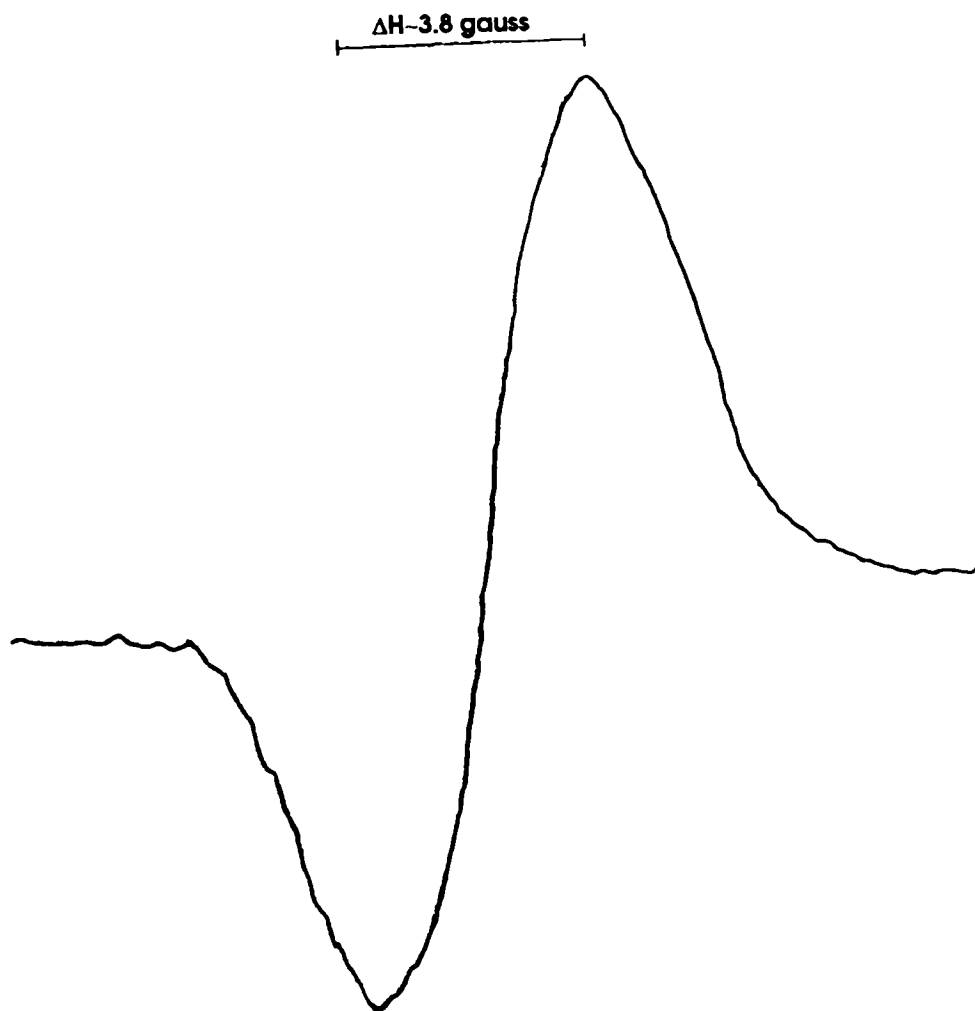
Fig. 8.1 : Tracing of proton resonance signal from polycrystalline $(NH_4)_2SO_4$ at room temperature($\sim$30° C)

Proton resonance signals were also recorded from NH_4Cl, NH_4SCN and $(NH_4)_2SeO_4$. The second moments of the proton signals from all the four ammonium salts were calculated using the method of moments discussed in chapter II, and are tabulated in Table VIII.1. The values are found to be in close agreement with the values computed by earlier workers [1].

Table VIII-1 : Second moments of proton signals from different ammonium salts at room temperature (~ 30° C)	
Sample	Second moment, M_2 (gauss²)
NH_4Cl	5.05
NH_4SCN	2.95
$(NH_4)_2SeO_4$	6.5
$(NH_4)_2SO_4$	4.1

8.3 : Proton resonance signal from ammonium chromate

Ammonium chromate,$(NH_4)_2CrO_4$, is one of the interesting compounds of ammonia which has got various applications, such as in sensitizing gelatin used in photography, in textile printing pastes, in fixing chromate dyes on wool, and as a reagent in analytical chemistry. The wideline NMR signal from polycrystalline ammonium chromate has been reported to indicate some interesting features, by earlier workers [1]. However, they were unable to explain the unusual features of the spectrum. While the anomalous features were observed by the earlier workers only at relatively low temperatures (<100°K) the improved NMR detector circuit fabricated during the present thesis work has enabled it to be observed even at room temperatures (~300°K). A tracing of the signal recording thus obtained is shown in Fig.8.2. It has further been possible to arrive at a satisfactory explanation for the anomalous features in the signal, by utilising the crystal structure of ammonium chromate, which is given below.

Ammonium chromate has a monoclinic structure, with each unit cell containing two molecules [2,3]. The crystal structure indicates two major deviations in the configuration of $(NH_4)_2CrO_4$ from what may be required for a stable and symmetrical molecule. First of all, two of the NH_4 groups in each unit cell are loosely bound, as a result of which the material has a tendency to change over to the form $(NH_4)_2Cr_2O_7$. Secondly, in this structure, each chromium atom is surrounded by a distorted tetrahedron of oxygen atoms.

The first aspect suggests that in each molecule one of the NH_4 group is rather loosely bound, as a result of which it will have a greater freedom to reorient than the other group. Calling, for convenience, the former NH_4 group as the `rotating group' and the latter one as `stationary group', we find that the average variation in the local field experienced by the protons of the `rotating group' is much less than that experienced by those of the `stationary group'. Hence the protons of the two NH_4 groups become non-equivalent in terms of the effective steady magnetic field experienced by them. Conse-
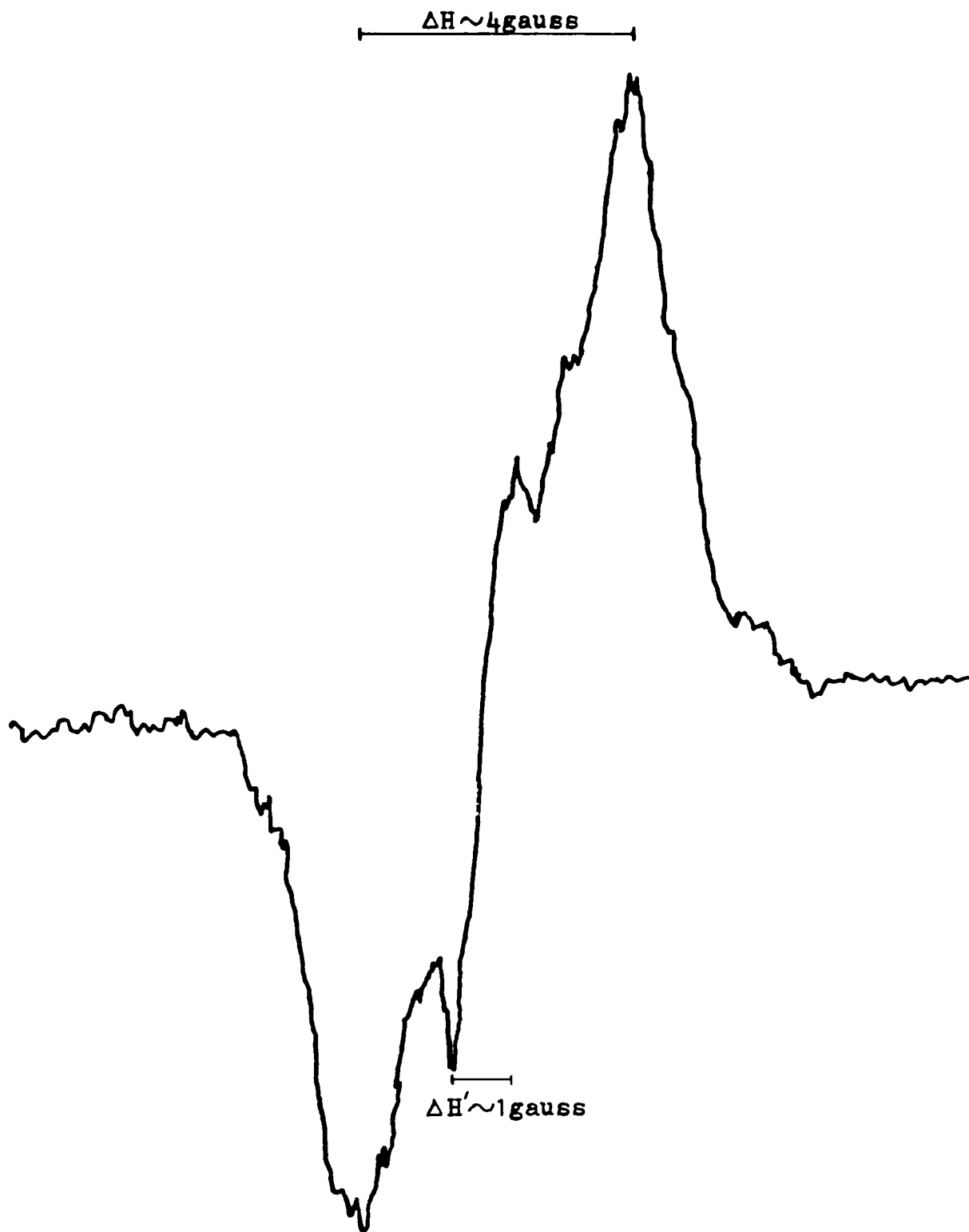
ΔH ∼ 4gauss

ΔH′ ∼ 1gauss

Fig. 8.2 : Tracing of proton NMR signal from polycrystalline $(NH_4)_2CrO_4$ at room temperature (∼30°C)

quently, in the proton resonance signal of the sample, a relatively narrow resonance line corresponding to the `rotating group' gets superposed with the broad signal originating from the protons of the `stationary group', as observed in the actual signal recorded here.

The distortions in the CrO_4 tetrahedra can also have some effect on the observed anomalous features in the NMR signal of ammonium chromate. Utilising the parameters pertaining to the crystal structure of $(NH_4)_2CrO_4$ [3] it is observed that the seperation of the two NH_4 groups with respect to Cr atom are rather unequal. This in turn makes the two NH_4 groups non-equivalent so that the proton resonance signals from them will have different linewidths, as mentioned in the above case. Hence the cumulative resonance signal from $(NH_4)_2CrO_4$ at very low temperatures will again show anomalous features. However, at room temperature, the effect of unequal paramagnetic environment of the NH_4 groups cannot lead to as marked an anomaly as that observed in the resonance signal of ammonium chromate. Hence it is concluded that the rapid reorientation of the loosely bound NH_4 group in the $(NH_4)_2CrO_4$ molecule is mainly responsible for the additional anomalous feature present in the proton resonance signal from the molecule at room temperature.

The effect of unequal paramagnetic surroundings will have a notable effect only at very low temperatures, when the reorientation of the loosely bound NH_4 group gets arrested. Indeed this effect has been observed to become predominent below about 90°K, the phase transition temperature of ammonium chromate. At the transition temperature the anomaly in the resonance signal resulting from the reorientation effect of loosely bound NH_4 groups will disappear. Only the unequal paramagnetic environment then contribute to the anomalous shape of the signal, which is apparent in the signal recording at 90°K, as reported by Richards [1]. Richards has also reported that the anomaly becomes more pronounced when the temperature is reduced below 90°K. This is clearly due to the inverse dependece of paramagnetism on temperature [4]. (Tracing of the signal recording at 78°K obtained by Richards is reproduced in Fig.8.3) However, below 78°K no further noticeable change in the lineshape was observed by Richards, even down to 20°K. This indicates that at about 78°K the paramagnetism due to Cr^{3+} reaches a saturation value. This is in true agreement with the Langevin's theory on paramagnetism, which suggests that "with very high fields applied at very low temperature the resultant magnetic moment of a paramagnetic material attains a saturation value" [4].

In the case of the signal recording at very low temperatures (<90°K), it is seen that the lineshape is modified by the unequal paramagnetic environment experienced by the NH^4 groups and the peak-to-peak seperation of the central anomalous feature is observed to be rather broad [1]. On the contrary at relatively high temperatures the linewidth of the anomalous feature is observed to be very narrow -due to the rapid reorientation/rotation of the loosely bound NH_4 group. Thus the two effects are understood to be clearly distinct. Though both of the effects are dependent on temperature, each of them becomes predominent at entirely different temperature ranges.

8.4 : Proton resonance signal from zeolite

Zeolites are the most widespread, diverse and useful framework silicates in nature [5]. They constitute a family of minerals and synthetic compounds characterised by an alumino silicate tetrahedral framework, ion exchangeable large cat-ions such as Na^+, K^+, Ca^{2+} etc and loosely held water molecules permitting reversible dehydration. The large cat-

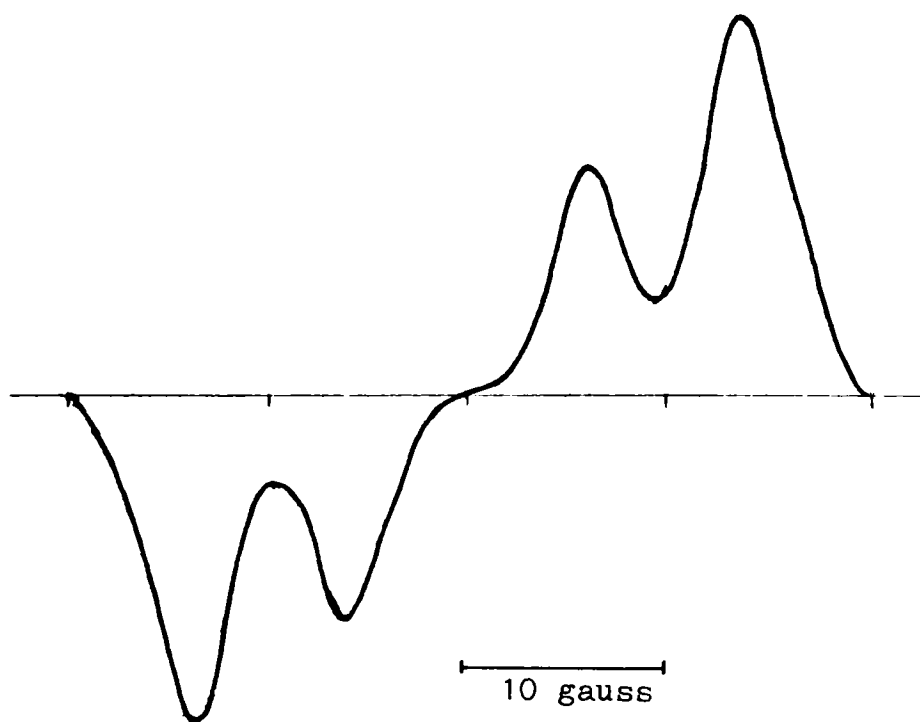Fig. 8.3 : Tracing of proton signal from $(NH_4)_2CrO_4$ at 78° K obtained by Richards(1)

ions, which are coordinated by framework oxygens and water molecules, reside in large cubo-octahedral cavities in the crystal structure. In the anhydrous state these cavities may be occupied by other molecules brought into contact with the zeolite, provided such molecules are able to squeeze through the apertures connecting cavities. Molecules within the cavities then tend to be held there by attractive forces of electrostatic and Vander Waals types. Thus, zeolites are extensively studied from scientific and technical standpoints because of their potential and actual use as "molecular sieves", catalysts, ion exchangers [6] and water softners. Dehydrated zeolites can absorb other liquids, such as ammonia, alcohol and hydrogen sulphide, instead of water.

It was felt that the wideline NMR technique can be utilised as an effective way of determining the amount of liquid molecules absorbed by zeolites. To verify this, initially, the proton resonance signal from zeolite sample at room temperature was recorded. The spectrum showed a fairly strong signal, originating from the water of hydration, with a linewidth of about three times that from pure liquid water. The tracing of the wideline NMR spectrum is shown in Fig. 8.4.

To understand a probable direct relationship between the strength of the NMR signal and the quantity of liquid molecules absorbed, the zeolite was initially heated to a high temperaure (~200°C) and then the proton signal from it were recorded at various time intervals after exposing it to moist atmosphere. A graph was plotted between the peak-to-peak strength of the NMR signal (V_s) against the time elapsed (t), which is shown in Fig 8.5. The graph indicates that as the zeolite cools to room temperature the atmospheric water vapour enters the open cavities of the zeolite till the concentration of water molecules inside it equals the water of hydration. This study has revealed that the NMR method can be adopted with greater accuracy in chemical industries for the dynamic estimation of the amount of specific molecules absorbed by zeolites.

8.5 : Proton NMR signals from food grains and other samples

As mentioned in chapters I and II the NMR technique can be effectively used to determine proton content in a wide variety of materials and products. While the conventional methods of moisture determination in seeds, food products, and pulp and paper products are time consuming as well as unsatisfactory, the NMR method enables the moisture analysis to be done very conveniently [7,8,9]. The principle underlying the NMR method is based on the fact that the water molecules contained in many substances are relatively mobile compared to those of the hydrogen containing host substance, which are usually in the form of a crystalline or amorphous solid or is a highly viscous liquid. The proton resonance of such system therefore appears as a greatly broadened signal ('solid line') superposed on which is a narrow line arising from sorbed water ('water line').

For establishing the utility of the wideline NMR spectrometer fabricated during the present thesis work for performing moisture analysis, proton resonance signals have been recorded from food grains such as rice and wheat as well as from pepper. The tracings of these signals are shown in Fig. 8.6, Fig 8.7 and Fig. 8.8 respectively. In all these cases the 'water line' is observed to have a width of about three times that of pure liquid water. The 'solid line' is prominently notable in the case of rice and wheat, whereas that in pepper is very weak and considerably broadened. The 'solid line' in rice and wheat are observed to have a linewidth of about seven times that of the 'water line'.
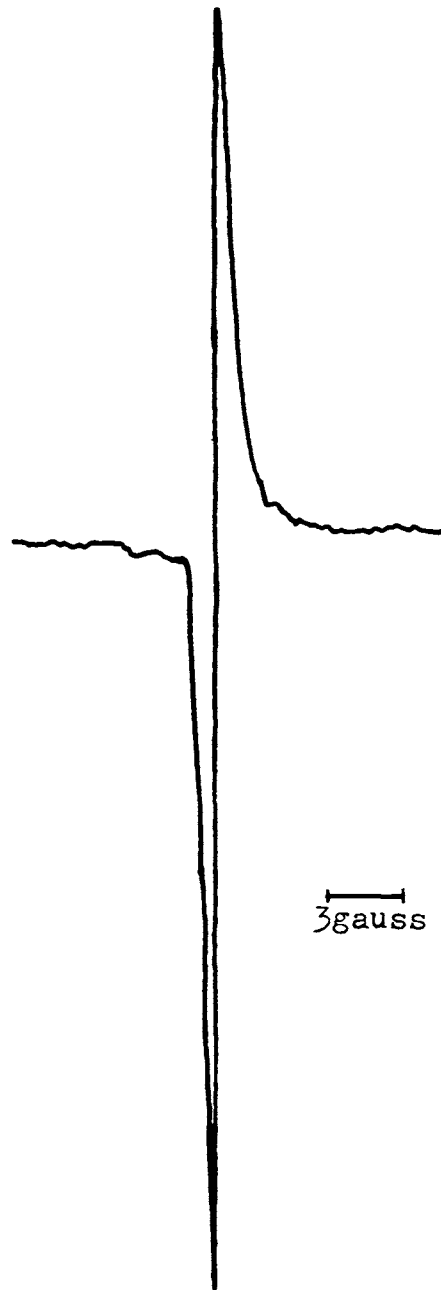
3gauss

Fig. 8.4 : Tracing of proton resonance signal from Zeolite (at room temperature)
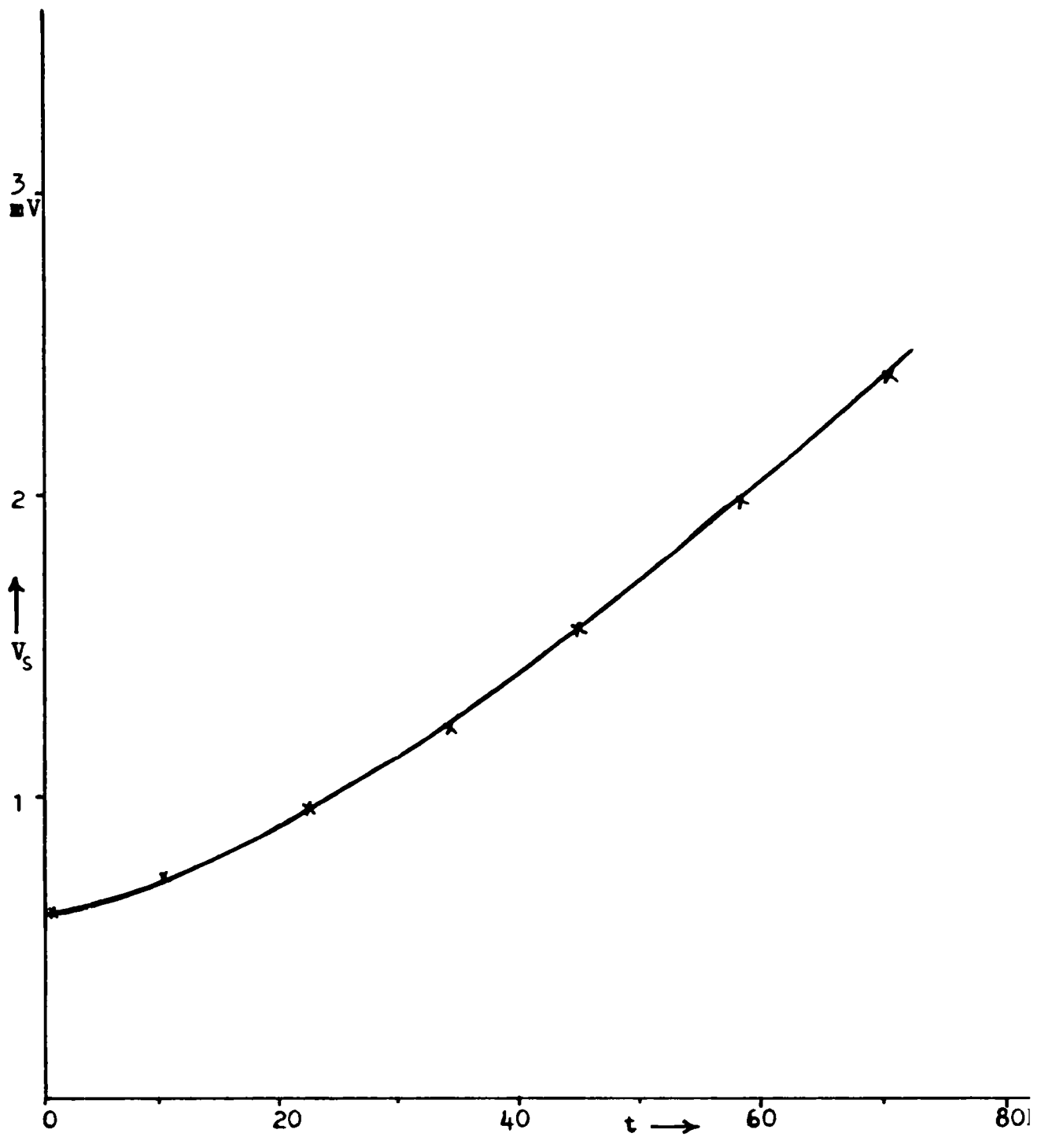
Fig. 8.5 : Graph indicating variation in the strength of proton resonance signal from zeolite with amount of proton absorbed in a given time interval
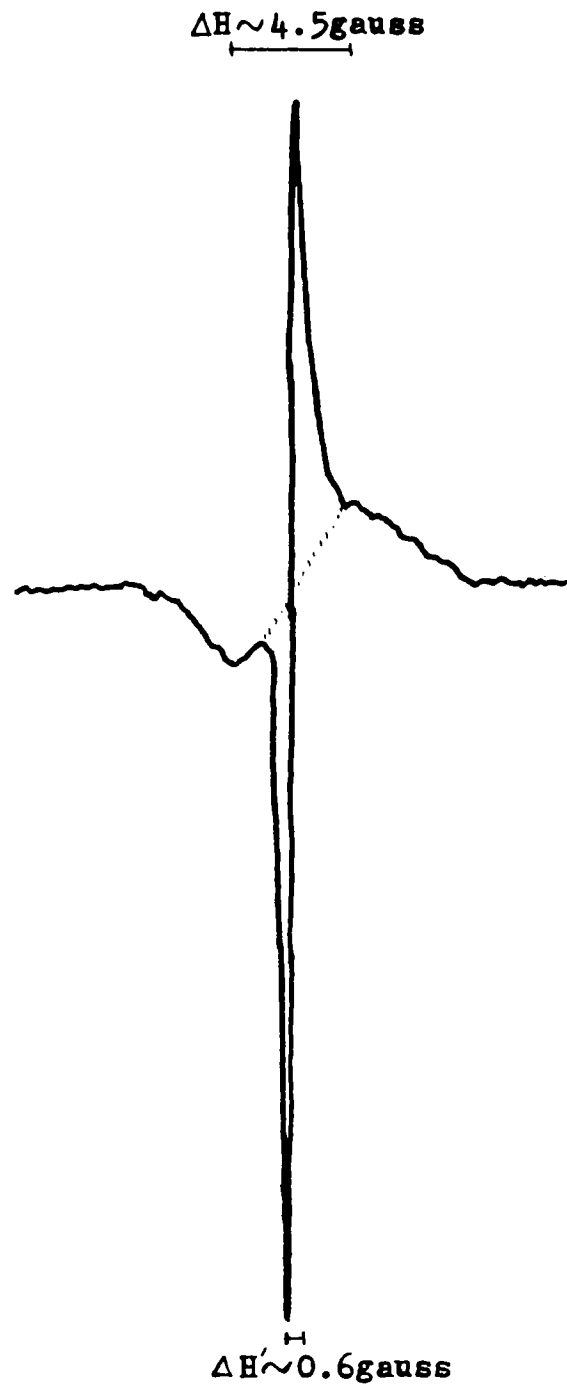
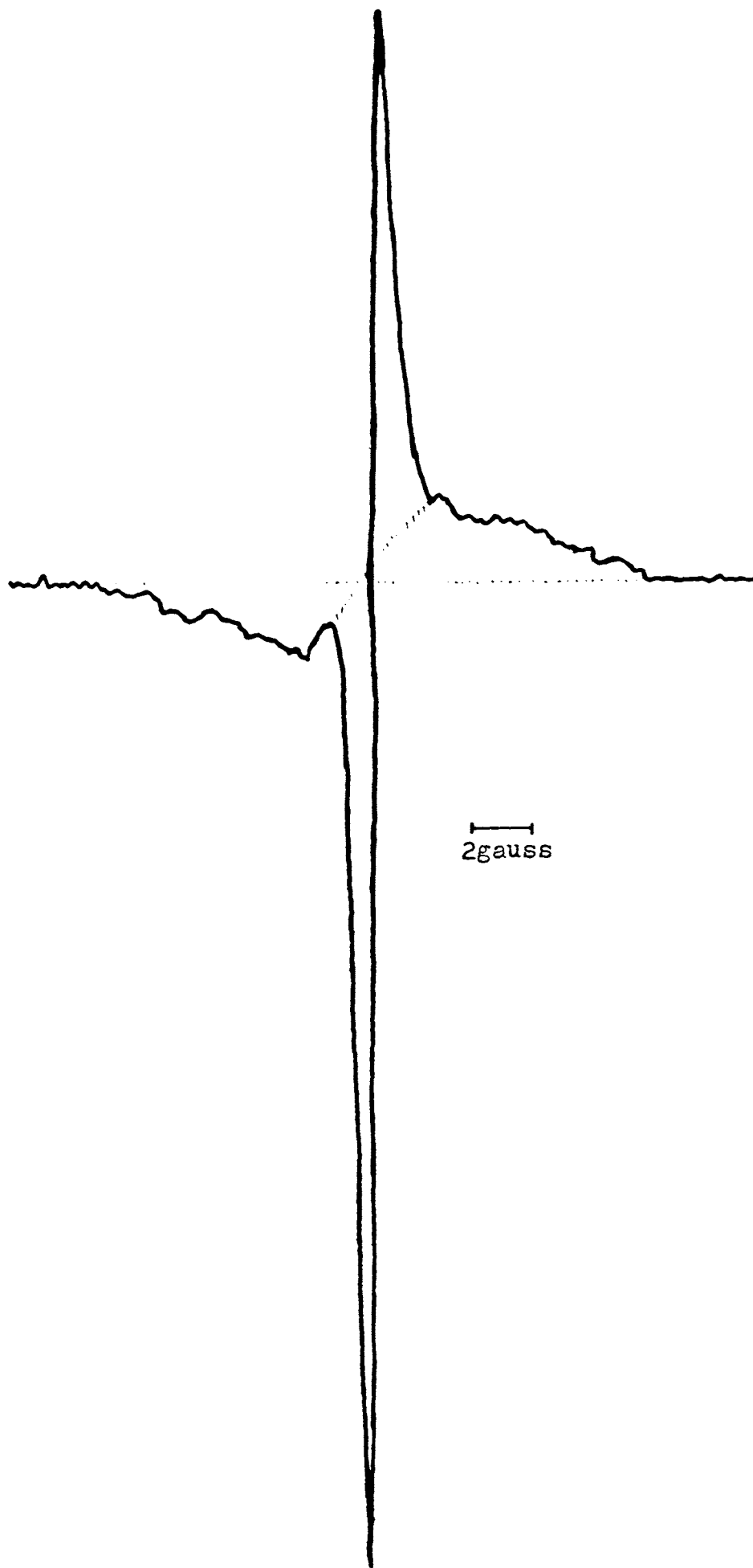Fig. 8.6 : Tracing of proton resonance signal from rice

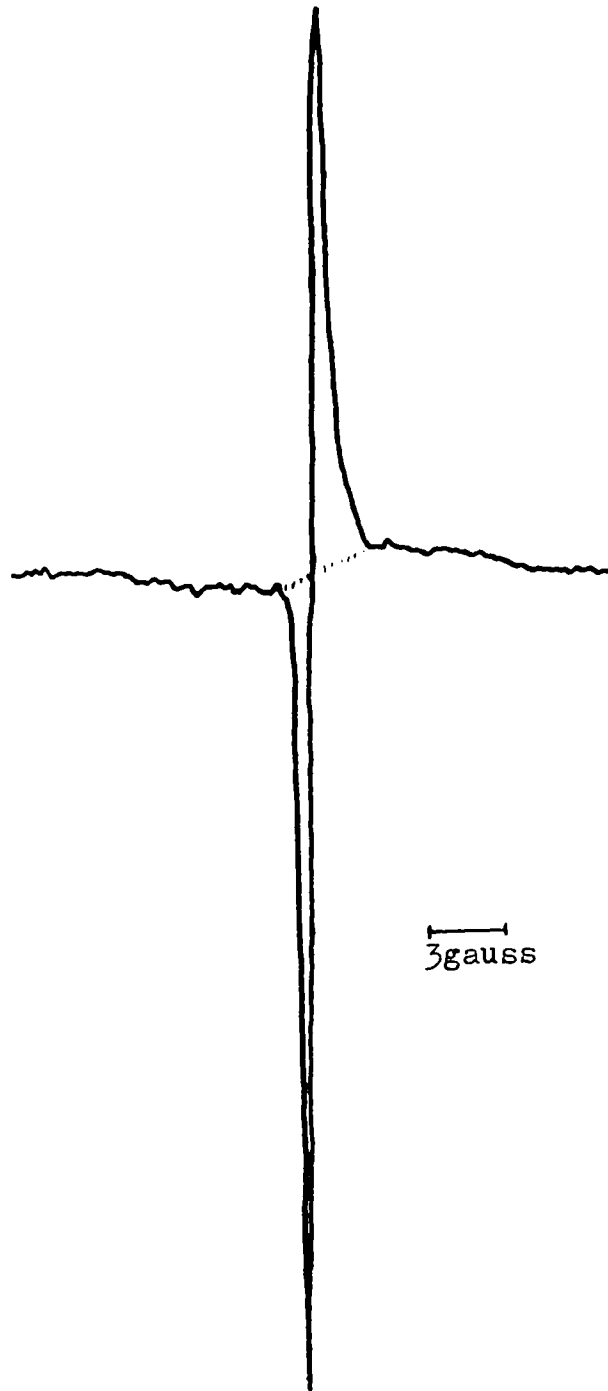Fig. 8.7 : Tracing of proton NMR signal from wheat

3gauss

Fig. 8.8 : Tracing of proton resonance signal from pepper

Since the absorption due to protons in the non-aqueous constituents of the above mentioned samples are substantially constant over the narrow frequency region occupied by the `water signal', the intensity of the latter can be used for a quantitative measure of water content. The fairly strong `water line' from pepper indicates that the NMR method of moisture analysis can be adopted for the convenient and accurate monitoring of the extent of drying required for pepper and other spices before being exported.

The proton resonance signal from dried coconut (`copra') sample has also been recorded, out of curiosity. A very sharp resonance signal was obtained, due from the coconut oil content. No `solid line' was observed, indicating the abscence of adequate hydrogen in non-aqueous form. The tracing of the signal is shown in Fig. 8.9. It appears that the peak-to-peak strength of the resonance signal from copra can be utilised as a true measure of the oil content in a copra sample of a given volume. An initial calibration will enable the determination of the oil content to be done very accurately. This method will enable coconut oil producers to accurately grade copra of different batches in terms of the oil content in them.

8.6 : Discussion

The various investigations mentioned in this chapter proves that the experimental set up fabricated for the present thesis work function as an excellent wideline NMR sepctrometer for investigating solids as well as liquid samples. Besides being able to record the broad proton lines from standard solid samples, it has also been possible to give a satisfactory explanation for the anomalous features observed in the proton resonance signal from ammonium chromate. The studies carried out have shown that the NMR technique could be applied for the dynamic estimation of molecules absorbed by zeolites as well as for the accurate estimation of oil content in `copra'.
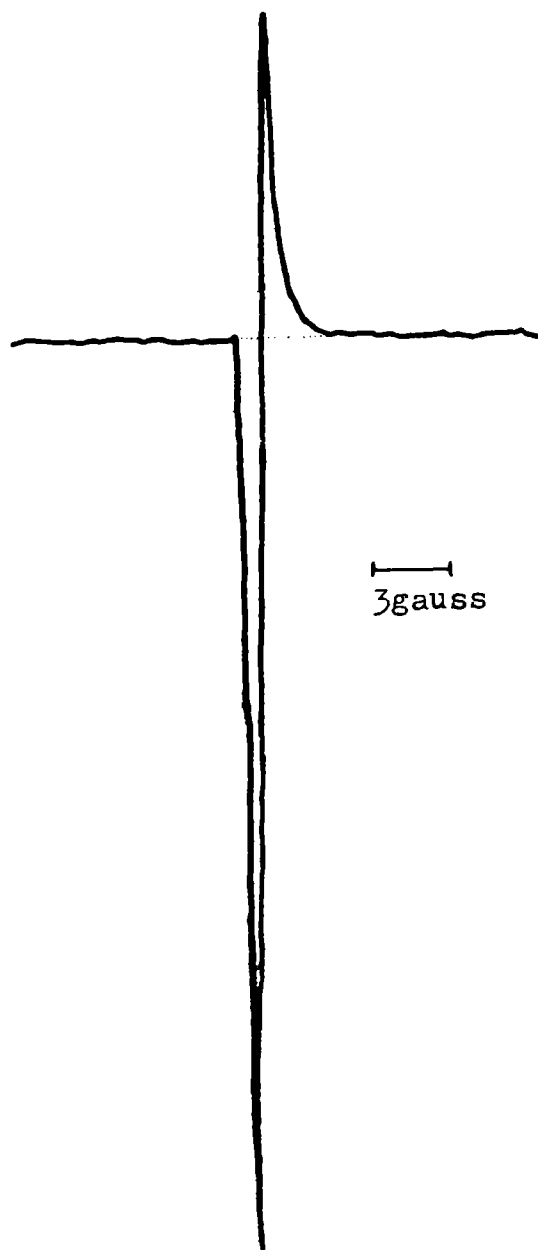
Fig. 8.9 : Tracing of proton NMR signal from 'copra'

REFERENCES

[1]   R.E.Richards and T.Schaefer; Trans Faraday Soc. (GB), 57 (1961) 210

[2]   D.I. Bujor; Z.Krist; 105 A (1944) 364

[3]   Ralph W.G. Wyckoff; Crystal Structures-Volume 3 (USA; InterScience Publishers:1965)

[4]   F.Bralisford; Physical Principles of Magnetism (Great Britain; D.Van Nostrand Company Ltd: 1966)

[5]   F.A.Cotton and G. Wilkinson; Advanced Inorganic Chemistry (USA; Wiley: 1972)

[6]   Russell Paterson; An introduction to Ion exchange (Great Britain; Heyden & Son:1970)

[7]   J.A.Pople, W.G.Schneider and H.J.Bernstein; High-resolution Nuclear Magnetic Resonance (USA; Mc Graw-Hill:1959)

[8]   T.M.Shaw and R.H.Elsken; J.Chem.Phys; 18(1950) 1113

[9]   T.M.Shaw and R.H.Elsken; J.Appl.Phys; 26(1955)313